Spring 2014

DEVELOPING A HARDWARE PLATFORM FOR A LOW-POWER, LOW-COST, SIZE-CONSTRAINED BIOMECHANICAL TELEMETRY SYSTEM

Aditya Balasubramanian
Purdue University

Graduate School ETD Form 9
(Revised 12/07)

PURDUE UNIVERSITY
GRADUATE SCHOOL
Thesis/Dissertation Acceptance

This is to certify that the thesis/dissertation prepared

By Aditya Balasubramanian

Entitled
Developing a Hardware Platform for a Low-power, Low-cost, Size-constrained Biomechanical Telemetry System

For the degree of Master of Science in Electrical and Computer Engineering

Is approved by the final examining committee:

THOMAS M. TALAVAGE, Co-Chair
Chair

ERIC A. NAUMAN, Co-Chair

SAURABH BAGCHI

To the best of my knowledge and as understood by the student in the *Research Integrity and Copyright Disclaimer (Graduate School Form 20)*, this thesis/dissertation adheres to the provisions of Purdue University's "Policy on Integrity in Research" and the use of copyrighted material.

Approved by Major Professor(s): THOMAS M. TALAVAGE, Co-Chair

Approved by: M. R. Melloch 04/14/2014
Head of the Graduate Program Date

DEVELOPING A HARDWARE PLATFORM FOR A LOW-POWER, LOW-COST, SIZE-CONSTRAINED BIOMECHANICAL TELEMETRY SYSTEM

A Thesis

Submitted to the Faculty

of

Purdue University

by

Aditya Balasubramanian

In Partial Fulfillment of the

Requirements for the Degree

of

Master of Science in Electrical and Computer Engineering

May 2014

Purdue University

West Lafayette, Indiana

This thesis is dedicated to my family, whose unconditional love and support has guided me towards my accomplishments.

ACKNOWLEDGEMENTS

I would like to express my sincere thanks to the members of my advisory committee – Tom Talavage, Eric Nauman and Saurabh Bagchi – for their time and effort in reviewing this work.

I would like to thank my advisor, Tom Talavage, for his excellent guidance, providing me with a first-rate research environment and letting me build things. I am also grateful for my most excellent lab mates, Brandon Blaine Gardner and Jeffery Ray King III, who helped make this project successful and fun. I am also grateful for the amazing members of the PNG – particularly Diana, who helped keep the peace, and Trey, who kept the caffeine flowing. Special thanks go to Amanda, for constantly reminding me that grammar is good.

TABLE OF CONTENTS

Page

Page

Page

LIST OF TABLES

LIST OF FIGURES

Figure Page

Appendix Figure Page

Appendix Figure Page

ABSTRACT

Balasubramanian, Aditya M.S.E.C.E., Purdue University, May 2014. Developing an Embedded System Solution for High-Speed, High-Capacity Data Logging for a Size-Constrained, Low-Power, Biomechanical Telemetry System and Investigating Components for Optimal Performance. Major Professor: Thomas M. Talavage.

As sport-related traumatic brain injuries face increasing attention from the media and the general public, the need to be able to detect brain injury quickly, inexpensively and accurately is more important than ever. Commercially-available event-based systems exist that claim to achieve this goal; however, they collect little to no continuous-time data and primarily indicate when a pre-determined acceleration threshold has been exceeded under the unvalidated assumption that a potentially concussive blow has occurred. Recent findings by the Purdue Neurotrauma Group (PNG) have indicated that repeated exposure to both concussive and subconcussive blows can result in cumulative trauma disorder. To track cumulative trauma over time it is necessary to record all accelerations experienced by the head. The lack of effective commercially-available systems resulted in the PNG undertaking the development of a custom hardware platform that allows real-time telemetry. This project focuses on the analysis of various designs for an effective hardware platform intended specifically for use in contact-sport settings. The analysis investigates both commercially available systems and previous hardware platform design efforts by the PNG. Essential design criteria which influenced current platform design are discussed, including special hardware features and preliminary device benchmarks. The work is concluded with the most optimal hardware platform design achieved to date, and recommendations for expansion of the developed platform.

1. INTRODUCTION

1.1 Motivation

In recent years mild Traumatic Brain Injury (mTBI), particularly in sports, has gained considerable attention from the media and the general public – so much so that organizations like the National Football League (NFL) and Pop Warner[1] have been forced to respond with initiatives such as the Pop Warner-NFL "Heads Up Football" program [2] and the funding of research projects investigating the true long-term effects of TBIs [3]. In the United States alone, up to 3.8 million sports-related TBIs are reported each year, with annual costs due to medical costs and lost productivity estimated to be $60 billion [4].

Traumatic brain injury (TBI) is typically described as the permanent or temporary injury of the brain tissue, resulting from an external mechanical force. TBI can result in deficits in cognitive, behavioral, emotional and physical function, both in the short and long-term. Often times, these changes are not immediately apparent [4]. Mild traumatic brain injury (mTBI) is typically defined as an injury to the head resulting from translational and rotational components of acceleration forces that result in transient confusion, memory dysfunction and loss of consciousness lasting less than 30 minutes. While mTBI symptoms are generally easily observed after an insult to the brain, the exact level of injury is often difficult to determine. MTBI symptoms and effects typically resolve within two weeks, but the long-term consequences of both singular and multiple mTBI events are largely unknown.

One of the most common forms of mTBI is concussion, which can be characterized by additional symptoms including headache, dizziness, rapidly changing pupil size and

[1] Pop Warner, or Pop Warner Little Scholars is a not-for-profit organization that provides over 425,000 children between the ages of 5 and 16 with youth football, cheer and dance programs [1].

fatigue – all of which can be used to support diagnosis of an mTBI [5]. There has been extensive coverage by both academia and the media on the negative effects of concussions on long-term neurological health and incidence of neurodegenerative diseases such as Alzheimer's. The Purdue Neurotrauma Group (PNG), along with others have gathered evidence that long-term, permanent neurological damage is not solely based on the number of concussions sustained by an individual over the course of their lifetime – it is more likely to be caused by the cumulative effects of repetitive sub-concussive events [6], [7]. It has been posited that sub-concussive hits inducing damage at a rate faster than the body is capable of recovering from may be a cause of long-term deficits. The prevention of accumulation of injury and delivery of appropriate care can be made more effective by the consideration of an individual's history of exposure to head-acceleration events.

The PNG has theorized that the prevention and early detection of brain injury, particularly in sports, can be substantially improved through active monitoring of athletes using real-time telemetry systems to record information on the rotational and translational accelerations experienced by athletes' heads. This, combined with the extensive PNG database relating acceleration event exposures to neuroimaging-related biomarkers[2] to altered neurophysiology, can be used to devise predictive-model based intervention strategies. In order to be able to accurately record a history of head acceleration events, there is need for a low-cost, low-power, size-constrained hardware platform that is capable of accurately and consistently recording head acceleration events experienced by athletes in contact sports.

1.2 Background

Commercially available telemetry systems have been observed by the PNG, Jadischke [8] and Allison [9] to rely on oversimplified kinematic models. Additionally, all such systems rely on an event-based recording system[3]. Instead of providing a continuous stream

[2] Neuroimaging-related biomarkers utilized by the PNG include but are not limited to neurocognitive testing (ImPACT^{TM}), functional MRI, MR spectroscopy and diffusion tensor imaging (DTI) [6]

[3] Further discussion on the kinematic modelling and even-based system limitations will be conducted in Chapter 3

of data that can be monitored in real-time, only singular events above a predetermined acceleration threshold are deemed significant and consequently recorded. This is largely due to past assumptions that claim that large magnitude 'concussive' blows are the sole cause of mTBI [10], [11]. A five year study by the PNG, however, has demonstrated a lack of correlation between the magnitude of the allegedly 'causative' blow and the subsequent clinical diagnosis of brain injury severity. This lack of correlation is further substantiated by the fact that during this study, the PNG monitored athletes with multiple blows exceeding 185G, with no resulting clinically diagnosed mTBI. In the 10 blows preceding the 8 concussions recorded in this study, none of the blows exceed 120G. This substantiates the theory that it is not only the classic 'concussive' blows, but also the subconcussive blows accumulated over time that play a significant role in the development of mTBI in athletes [7].

Based on the preceding arguments, it is clear that in order to effectively build predictive models for impact-based brain injury, it is essential to record all accelerations experienced by the head. Commercial systems' failure to continuously record all events, concussive and subconcussive, leading to an observed injury is not only based on the classic 'singular event' based model, but continues to reinforce improper attribution of true causative events of mTBI. This point can be further illustrated by the 'random incidence paradox' [12], [13] – which posits that sub-concussive hits are not likely to be observed as the cause of brain injury. A player with a fixed, unknown accumulated damage threshold between 1 and 100 units is considered. If this player experiences, in random order, 50 blows producing 1 unit of damage, 3 blows producing 10 units of damage and 1 blow producing 20 units of damage, the threshold is 50% likely to be crossed be one of the 4 blows producing 10 or more units of damage, even though these blows make up only 7.4% of the collision event history. The exponential distribution of the magnitude of blows observed in athletes' results in the tendency for larger blows to push athletes over the 'concussion threshold' [14] – but with no clear relationship emerging between the magnitude of the most recent blow and the subsequent severity of the brain injury.

1.3 Objectives

While the overall goal of the PNG is to combine head acceleration event history and the previously discussed biomarker database to achieve the overall goal of building predictive models that will allow the accurately and timely prediction of brain injury resulting from participation in contact sports, the research and development presented in this project will focus on the development of a custom hardware platform to be utilized in contact sports as a real-time telemetry system.

This work will:

1. Perform a detailed analysis on both hardware design and limitations of commercially available telemetry systems
2. Detail previous hardware platform development efforts by the PNG, exploring design criteria, limitations and lessons learned
3. Detail hardware platform design efforts put forth by the author
4. Characterize the most optimal hardware platform design achieved to date
5. Outline future platform expansion capabilities and deployment

2. COMMERCIAL SOLUTIONS: AN ANALYSIS

This chapter will discuss in detail the various commercially available systems and devices that are marketed as head impact telemetry or monitoring systems. For each device/system, the device's theory of operation, hardware description and component specifications will be discussed. Where applicable, a thorough analysis of the packaging and costs associated with each device is conducted. The accuracy limitations of each device conclude the analysis.

Before diving into the discussion of each device, is it necessary to briefly outline the kinematic modelling approaches typically employed by most of these devices. Much of the research conducted in the field of traumatic brain injury often relies on measures such as the Head Injury Criterion (HIC) or Gadd Severity Index (GSI). These measures aim to 'index' the impact experienced by the head using weighted integrals of acceleration-time profiles obtained from sensors [15].

Measures such as the HIC and GSI have inherent limitations – for example, the HIC and GSI measures rely exclusively on linear acceleration measurements. This is clearly not the case for contact sport athletes – simply watching a football game will showcase the cornucopia of hits experienced by players – both linear and rotational in nature.

2.1 The Head Impact Telemetry System™ by Simbex LLC

2.1.1 Device history and theory of operation

The Head Impact Telemetry (HIT) System™ by Simbex is marketed as "the first and only commercially available system that can measure head accelerations (impacts) in real-time during [football] games and practices" [16]. In 2003, Riddell [17] integrated the HIT System with their line-up of helmets, and announced the Riddell Sideline Response System

(SRS). Primarily targeted at youth football leagues and high school football teams the system consists of three major components: (1) individual sensor ‘pods’ that are attached to individual players’ helmets between existing padding (seen in Figure 2.2), (2) a base station (seen in Figure 2.1) that wirelessly receives information regarding significant head impacts from each sensor ‘pod’, displaying relevant information on a laptop screen and (3) a proprietary algorithm , the Head Impact Telemetry Severity Profile (HIT-SP) developed by Simbex to enable the association of a single impact with a clinically diagnosed concussion.

In typical use, 20-30 pods are deployed at once, either during practice or game time, and each pod is tied to a specific player for the whole season. At the beginning of a recording session, each pod turns on and establishes a unique connection to the base-station over the 915MHz ISM radio band.

Once connections have been successfully established, the base station laptop displays a list of connected players, device health parameters associated with each pod. Based on sensor data collected during an impact that includes linear and rotational acceleration, a hit is deemed ‘significant’ using the proprietary HIT-SP^{TM} algorithm. The significant hits are displayed in ‘real-time’ as they occur, along with the associated hit vectors on pseudo-free-body force diagram. All significant hits are stored in a database on the base station laptop that can be exported and analyzed separately at a later time. In the event of a connection loss, each pod can store a limited number of hits on the device till a connection is reestablished – during normal operation however, no impact data is kept on the device. At the end of a recording session, the pods are generally left in the helmets to be cleaned and wiped down and automatically power off after a period of inactivity. Any pods reported to have low battery life by the base station will have their batteries swapped out at this point.

Figure 2.1. Riddell SRS base station unit

Figure 2.2. Riddell helmet fitted with a HIT system pod (white band with red, circular markings).

2.1.2 Hardware description and specifications

Each HIT System pod consists of a molded foam core with space for printed circuit boards (PCBs) that is sealed with a thick layer of plastic. An exposed connector and Velcro

strap allows the battery to be replaced as needed. The pod is activated at the beginning of each session by detecting the proximity of a player's head to the device using electrodes within the pod connected to a Quantum Research Group QT310 capacitance sensing IC. The HIT System pod gathers the information necessary to calculate rotational and linear acceleration vectors from six spring-loaded, single-axis non-orthogonal accelerometers. The sensors used are the ADXL193 linear accelerometers [18], which are high-g (±250G), low current (1.5mA) sensors capable of a default sample rate of 400Hz. Primarily developed for automotive applications, these sensors represent the first generation of high-g analog accelerometers.

The six sensors are sampled by an ultra-low power TI MSP430F148 [19] microcontroller, which performs the necessary calculations and determines whether a detected impact is significant enough to be flagged at the base station. The microcontroller is paired with Microchip 24FC512 EEPROM, which presumably stores the proprietary algorithms utilized in the HIT-SP^{TM} calculations. If an impact is determined to be significant, the details of the impact are transmitted wirelessly using a Semtech XE1203F [20] transceiver to the base station where it can reviewed by the appropriate athletic staff. The base station also provides athletic staff the option to receive notifications via a pager when certain hit thresholds are exceeded.

The HIT System^{TM} has been in use for 11 years [21] – and development on the system likely began a few years before that. As a result, much of the hardware in the device is outdated – particularly the sensor technology used. Cheaper, smaller and more accurate tri-axial accelerometers and high-sensitivity digital gyroscopes are now easily available.

2.1.3 Power consumption analysis

The device is powered using custom 1000mAh Ni-MH battery packs supplied by Riddell. Analysis of the battery packs reveal that the battery pack itself is a standard Ni-MH battery pack, typically found in cordless telephones and radio-controlled toys, with a non-standard Molex [22], [23] connector crimped to the terminals. Connected between the terminals of the battery pack is a 4.5V Zener diode, used to provide overvoltage protection.

The device is rated to last approximately 15 hours or so, which is commensurate with the calculations performed in Table 2.1.

In practice however, due to both the device design and the degradation of characteristics of Ni-MH batteries [24], a battery life of 6-8 hours of total use has been observed by the PNG. The power solution implemented further highlights the obsolescence of the HIT System: battery technology has improved substantially since 2003. Lithium-polymer batteries offer better stability, are readily available, affordable and capable of high-duty cycle use without degradation.

Table 2.1. Power consumption estimates for the HIT System™

Major component	Current consumption (mA)		Operating Voltage (V)	Power Consumption (mW)
	Typical	Maximum		
Texas Instruments MSP430F148	0.42	0.56	3.30	1.39
Semtech XE1203F (Transmit mode)	62.00	75.00	3.30	204.60
Microchip 24FC512 (Write mode)	5.00	5.00	5.50	27.50
Quantum QT310	0.60	1.50	5.00	3.00
Analog Devices ADXL193 (x6)	1.50	2.00	5.00	45.00
	Total Power Consumption:			281.49
	Voltage supplied by battery (V):			3.70
	Current drawn from battery (mA):			76.08
	Battery life expected (hours):			**13.14**

2.1.4 Cost analysis

The Simbex HIT System™ is only available for purchase through research agreements with high schools, school districts and colleges. In a Simbex press release [25], the device is touted as utilizing low-cost components. In reality, however, high schools and colleges have to pay between $1,500 - $2,000 *per helmet* [26], [27]. This puts the HIT System™ out of the reach of many high schools and colleges, simply because they cannot afford to spend $45,000 - $60,000 outfitting a team of 30 players. The system is not available for individual consumer purchase, as they would be required to purchase the base station to be able to use the device at all.

highlights the costs of the major components present in the HIT System™ pods, along with estimates on the cost of miscellaneous passive components present and probably PCB fabrication costs. The table does not include cost estimates for the base-station, which is simply a laptop with a proprietary software package developed by Simbex and a USB-enabled 915MHz antenna.

Table 2.2. Major components costs in the HIT System™

Major component	Cost
Texas Instruments MSP430F148	$4.87
Semtech XE1203F (Transmit mode)	$4.90
Microchip 24FC512 (Write mode)	$1.41
Quantum QT310	$2.82
Analog Devices ADXL193 (x6)	$48.12
Misc. passive components	$5.00
PCB fabrication costs (estimated)	$10.00
Total electronic costs:	**$77.12**

While it is impossible to speculate on the research costs incurred or the profit margins desired by Simbex in the development of the HIT System™,

conservatively estimates the component cost of each HIT System™ pod to be $77.12. The prices listed are current market prices, and while component costs were higher several years ago when the device was first developed, it is extremely unlikely they were more than 50% higher than today's prices. This worst-case scenario would put the major component cost total at approximately $115.

2.1.5 Packaging analysis

Figure 2.3 shows the top view of a typical HIT System™ pod. Each pod consists of the device electronics situated in a molded foam core wrapped encased in a form-fitting plastic sheath., with additional Velcro squares on the exterior of the device used to attach it to a helmet. The packaging is bulky, and can only be used in football helmets – no other contact sport can benefit from the system. Each circular extrusion from the device contains a spring-loaded ADXL193 mounted on a small PCB and shrink-wrapped for protection. Each single-axis accelerometer is connected to the main PCB via wires that are soldered directly to the boards. The main PCB, containing the microcontroller and wireless transceiver, is located on the left side of the device in a rectangular foam cut-out. The battery pack is placed on the right side of the device, and a Velcro strap is used to secure it in place. Figure 2.4 shows a cutaway view of the device and in the center, two additional PCBs are visible. The PCB on the left contains the QT310 capacitive sensing circuit and the PCB on the right contains a real-time clock circuit and a button cell. The electrodes for the capacitive sensing circuit are embedded in the foam under the two central accelerometer extrusions.

Upon initial inspection, the organization and assembly of the internal electronics appears to be relatively straightforward, but further disassembly shows that this is clearly not the case. The device consists of 11 individual PCBs, each wired to the main PCB using permanent soldered connections. Not only does this make it nearly impossible to service the $2000 device in the event of a malfunction, it also makes assembly an inefficient, tedious and expensive process. Separate wire groups exist for each of the 11 PCBs which

results in many wires running up and down the device unnecessarily. Each PCB is also coated in a thin film of silicone to help reduce corrosion effects from sweat and humidity exposure. The internal hardware of the system is inefficiently designed, cumbersome to assemble and nearly impossible to service.

Figure 2.3. Typical HIT System™ pod

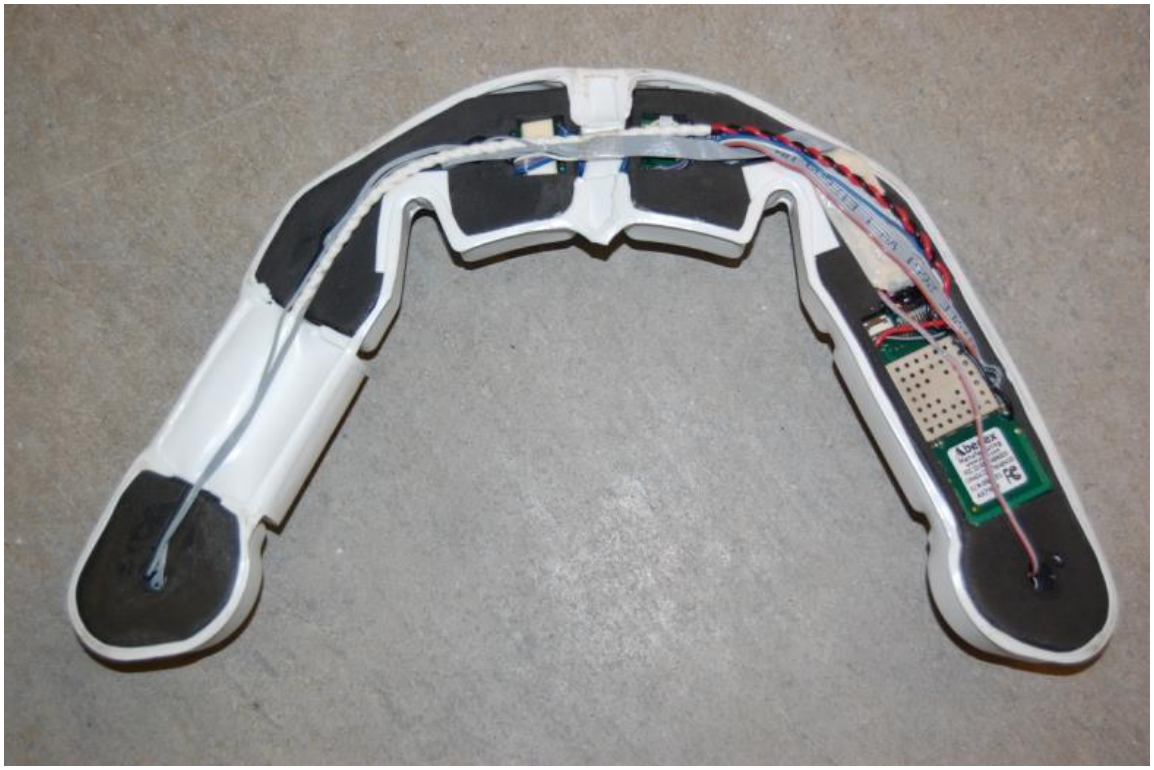

Figure 2.4. HIT System pod cutaway

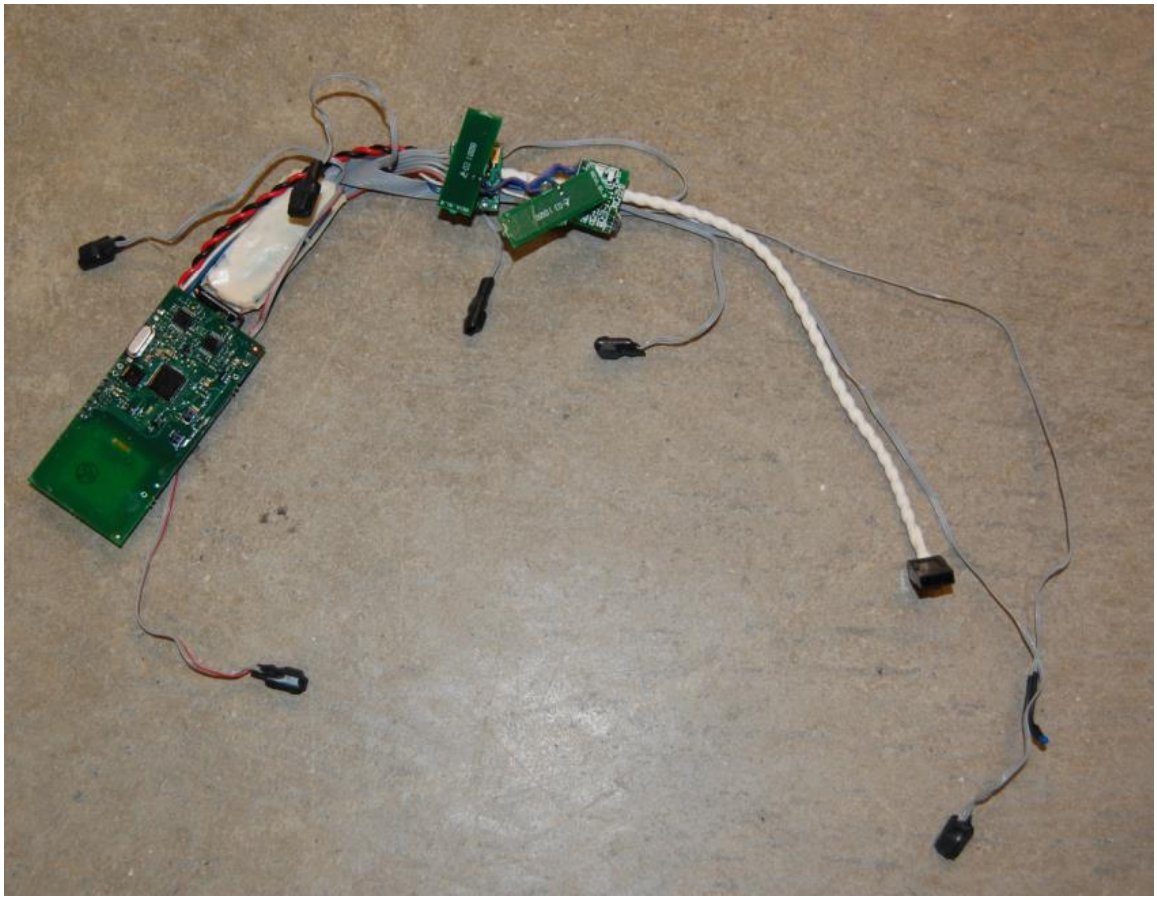

Figure 2.5. Internal electronics from HIT System™

2.1.6 Accuracy limitations

The HIT System has been used as part of both on-field head impact assessments and long-term mTBI research [6] in youth and collegiate football since 2003 [21]. The HIT System™ suffers from major drawbacks in terms of the accuracy of the kinematic modelling approaches used by Simbex to determine head injury information.

The device is purportedly able to calculate both rotational and linear accelerations, but because it utilizes only single-axis accelerometers, rotational information is inferred. This inference has resulted in inaccuracies in the rotational acceleration calculations. The rotational accelerations calculated are never allowed to exceed a fixed multiple of the calculated linear accelerations, resulting in the omission of purely rotational events [28], [9].

Multiple studies have been conducted studying the HIT System and the accuracy of the data generated by it. Testing by Jadischke et al. [8] comparing telemetry data from the HIT System with that generated by a Hybrid III dummy[4] showed that the majority of impacts recorded by the HIT System had an error greater than 15%. Jadischke also notes that the HIT System exhibited an root-mean squared error of 148% in detecting facemask impacts, which have been shown to represent nearly 60% of impacts experienced by a player during play [29].

Allison et al. [9] conducted similar tests using an ice-hockey version of the HIT System™ – which uses accelerometers tangential to the surface of the helmet, as opposed to the normally-oriented accelerometers in the football system. Their findings showed that the processing algorithms for the HIT System not only reported multiple hits inaccurately, but the system also removed 19% of all impacts. Allison et al. also independently corroborated findings by Nauman et al. [28] regarding the inaccuracy in calculation of rotational accelerations due to extrapolation from linear accelerometer readings.

The PNG has also observed limitations regarding the event-based model utilized by the HIT System – particularly in the case of multiple hits in rapid succession. By comparing both video footage collected and impact data generated by the HIT System during gameplay, multiple examples were found where the athlete sustained multiple blows from multiple directions that HIT System did not flag. Whether this is a failure record, or rejection of the blows based on the processing algorithms used is not certain.

The HIT System has been a key tool in many long-term mTBI investigations for many years. However, the numerous hardware and kinematic modelling flaws it suffers from greatly limit its effectiveness as a telemetry system, and its sustainability as a hardware platform.

[4] The Hybrid III dummy is an anthropometric representation of a human head, and is the gold standard employed by both automotive and federal entities when assessing head impact responses, particularly with respects to vehicular safety.

2.2 Brain Sentry by Brain Sentry LLC

2.2.1 Device history and theory of operation

Released in 2013, Brain Sentry (BS) is a standalone device that is marketed as a safe, affordable, low-maintenance system that accurately measures 'appropriate impact forces'. The device (Figure 2.6) is mounted onto an athlete's helmet using double-sided tape, and the sensor is activated using a paper clip. A sequence of flashing lights indicates that the device is fully operational. The device itself requires no user-intervention throughout a football season – the batteries are rated to last an entire season – and the end of the season, the device can be shipped back to Brain Sentry LLC, where it will be recycled and a new sensor sent back out to the player.

During gameplay, the only method of communication the Brain Sentry has with the athletic staff are the two on-board LEDs (red and green). If the device experiences a hit greater than 30G, the green LED will flash, and if the device experiences a hit greater than 80G, the red LED will flash once every 3 seconds [30]. If another 80G impact is recorded within a year, the red LED will flash twice every 3 seconds. If a third impact is detected, the red LED will flash thrice, and so on. The device was designed to detect the top 2% of the hardest hits in the game [31]. It is up to the athletic staff on the sidelines to keep a watchful eye on all the devices on the field at any given time. Once a member of the athletic staff notices a player with the red LED triggered, the player is to be assessed using the team's concussion assessment protocol (typically the SCAT3[5] or ImPACT[6] tools). The flashing red notification can be reset using a paper clip. All alerts are stored in the device memory until the battery dies or power is lost.

[5] SCAT3, or Sport Concussion Assessment Tool 3, is a standardized computer based tool used in evaluating injured athletes aged 13 and older for concussions.

[6] ImPACT, or Immediate Post-Concussion Assessment and Cognitive Test is a computerized concussion evaluation tool used to make return-to-play decisions.

Figure 2.6. The Brain Sentry device

2.2.2 Hardware description and specifications

The brain sentry device consists of a hard plastic casing (Figure 2.6) with a recessed reset button, small green LED and large red LED on the front fascia. The device can be ordered with custom colored labels to match team colors if so desired. The device is completely sealed and water proof. Electronically, the device is very simple. The device uses a STMicroelectronics H3LIS331DL [32] (±100G/±200G/±400G) digital SPI accelerometer. The accelerometer has a sleep-to-wakeup feature, which allows it to 'wake-up' the microcontroller, an ultra-low power Texas Instruments MSP430G2553 [33], when a certain acceleration threshold is detected. When the device is subjected to an impact, the accelerometer 'wakes-up' the microcontroller using an interrupt-based routine. The microcontroller then communicates with the accelerometer, and based on the magnitude of the impact, and number of impacts to date, the microcontroller triggers the red LED an appropriate number of times. If the impact is large enough, it is also stored on the device's EEPROM (Microchip 25AA128). Once this operation is complete, the microcontroller goes back into 'sleep' mode.

Figure 2.7 Brain Sentry PCB

2.2.3 Power consumption analysis

The Brain Sentry exhibits a relatively sophisticated power management system – running off two CR1225 coin cells it can monitor impacts for a whole season or more depending on the frequency of impacts. The power consumption estimates for Brain Sentry shown in Table 2.3 show that the device is capable of running for 4.5 years – provided it is in standby mode.

Table 2.3. Power consumption estimates for Brain Sentry

Major component	Current consumption (mA)		Operating Voltage (V)	Power Consumption (mW)
	Typical	Maximum		
Texas Instruments MSP430G2553	0.01	0.23	3.00	0.03
ST Microelectronics H3LIS331DL	0.01	0.30	3.00	0.03
Microchip 25AA128	0.01	5.00	3.00	0.02
	Total Power Consumption:			0.08
	Voltage supplied by battery (V):			3.00
	Current drawn from battery (mA):			0.03
	Battery life expected (hours):			40000
	Battery life expected (years):			**4.57**

Four and a half years is a long time – so to better characterize the real world power consumption characteristics of the Brain Sentry, additional laboratory analysis was conducted. The true power consumption of the components and LEDs were analyzed in real-time under various scenarios using an 11.13Ω current sensing resistor and an oscilloscope (Figure 2.8).

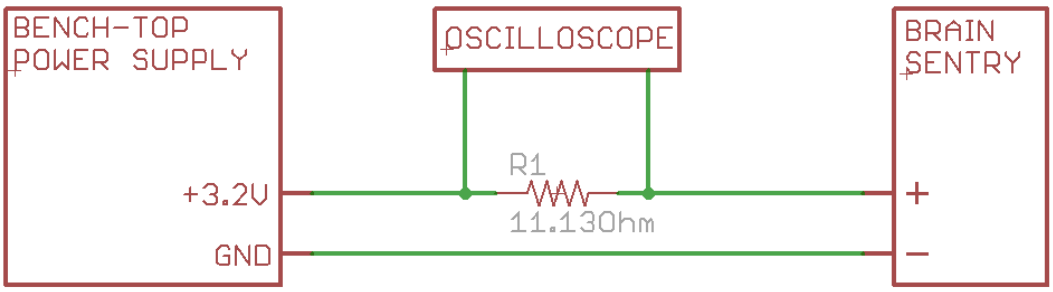

Figure 2.8. Power consumption measurement circuit

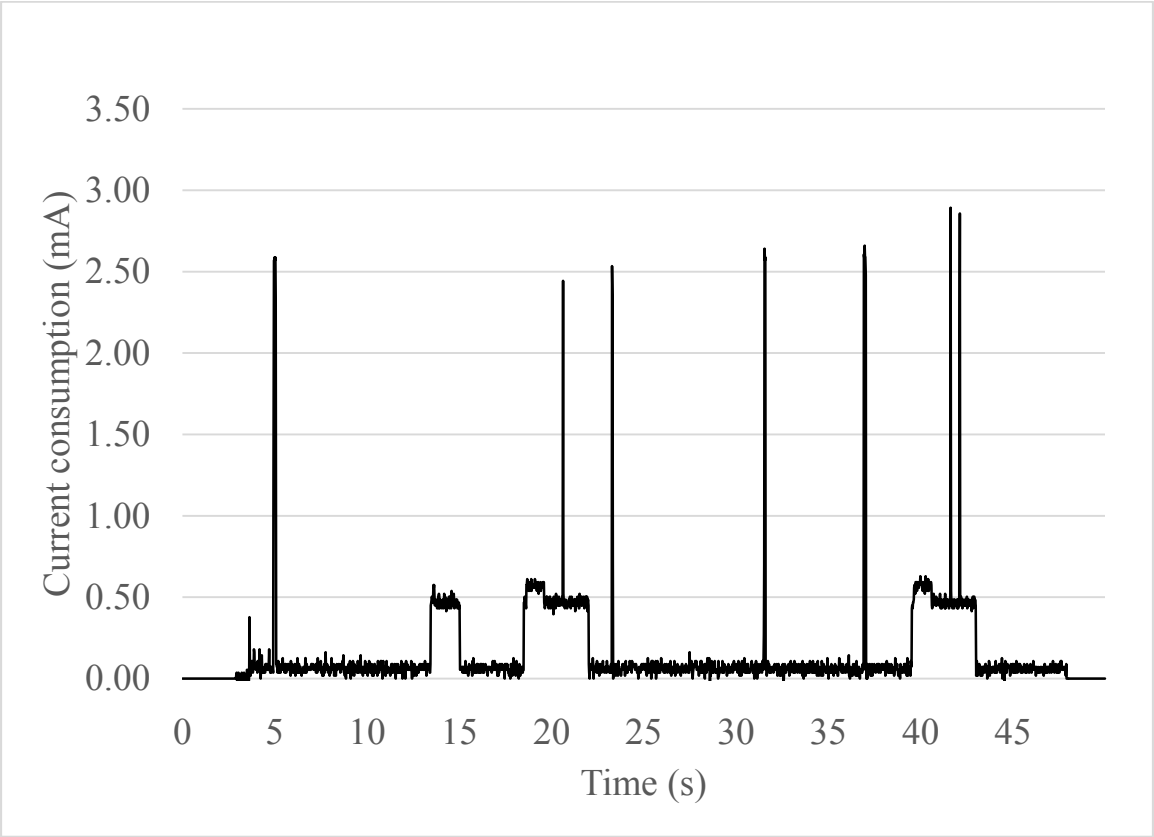

Figure 2.9. Current consumption vs. time of Brain Sentry device

As can be expected, the flashing green and red LEDs contributed significantly to the power consumption of the device, most notably during power on and whenever a red light warning flashes. In Figure 2.9 we see that at 5 seconds, when the device was powered on, current consumption spiked to approximately 2.5mA. The short plateau of 0.5mA seen at 14s indicates that a hit occurred and is being analyzed for approximately 1 second. At 18

seconds, another hit occurred, and the first sharp spike to 2.5mA indicates the device writing the information to EEPROM. The following spikes to 2.5mA and above indicate the red LED flashing. At 40 seconds, multiple hits of equal magnitude occurred but only 1 impact registered, resulting in the red LED now flashing twice every 3 seconds. The ramifications of this behavior will be further discussed in Section2.2.6.2.2.6 below.

2.2.4 Cost analysis

At $65.00, the Brain Sentry is one of the more affordable options discussed in this report. This puts it well within the range of most high schools and colleges. Also, since an elaborate support system is not required for the device, it is accessible to the recreational consumer as well. Again, it is impossible to speculate on the costs of research and development behind the Brain Sentry, but cost analysis estimates put the manufacturing cost of the device at $18.20.

Table 2.4. Major component costs in the Brain Sentry

Major component	Cost
Texas Instruments MSP430G2553	$1.01
ST Microelectronics H3LIS331DL	$6.37
Microchip 25AA128	$0.82
Misc. passive components	$5.00
PCB fabrication costs (estimated)	$5.00
Total electronic costs:	**$18.20**

2.2.5 Packaging analysis

The package design for the Brain Sentry is relatively simple – it consists of the PCB mounted inside a frosted plastic casing, which is sealed shut. The device interior is not user-accessible, so if and when the device requires new batteries, it must be sent back to Brain Sentry for servicing. The device is available in a multitude of colors, including custom team colors should the consumer so desire.

2.2.6 Accuracy limitations

The Brain Sentry is designed to activate with impacts of 30G or higher, and to record impacts at 80G and higher. As noted in section 2.2.3, the Brain Sentry device appears to be incapable of distinguishing multiple hits that occur in rapid succession – the device ignores all accelerometer data while processing a hit, so any hits that occur immediately after a large impact are lost. This flaw renders the Brain Sentry effectively useless, as it will dramatically underestimate critical hit counts whenever they occur in rapid succession, and correspondingly force the athletic staff to underestimate the urgency of administering concussion assessments. The device is mounted on the exterior of the helmet, it is measuring the acceleration experienced by the players' helmets, not their heads – this can lead to inaccurate readings, particularly if helmet fitment is not good. Additionally, the device has no way of detecting rotational accelerations due to the lack of an onboard gyroscope.

2.3 Shockbox by Impakt Protective

2.3.1 Device history and theory of operation

Launched in October 2011, the Shockbox is a long range wireless sensor that connects to a smartphone via Bluetooth to display impact information. Aimed primarily hockey players (a football version is available), the device is placed along the sagittal plane of a helmet with the aid of adhesive or industrial Velcro strips. The device is initially charged using a standard micro-USB connector, and is turned on using a recessed push-button. Before the device can be used to monitor head impacts, it must first be paired via Bluetooth

with either an iOS or Android device with the Shockbox app installed – and up to 100 devices can be paired. Once the device is paired, the user has the ability to tie player metadata such as name, age, emergency contact information, team information together with the impact history recorded. The app also allows the user to be notified in real-time if any hits occur that exceed a user-defined threshold.

When a critical hit is detected, the app notifies the user with of the player name, time, and approximate magnitude and direction of the hit. The user is then presented with the option to assess the player in question, by running through a basic SCAT and a balance test, or discard the hit in case of a known false positive. The app also includes an option to enter information from a clinical assessment after the basic concussion assessment. Additionally, all collected data can be exported via email. A sample of exported data can be found in Appendix B.

Figure 2.10. The Shockbox device mounted on a hockey helmet

2.3.2 Hardware description and specifications

Due to the construction of the Shockbox, it was nearly impossible to tear down the device in a useful manner. This is due to the unique construction method employed by Impakt Protective, which will be discussed in greater detail in Section 2.3.3. The device can be approximated by the diagram in Figure 2.11.

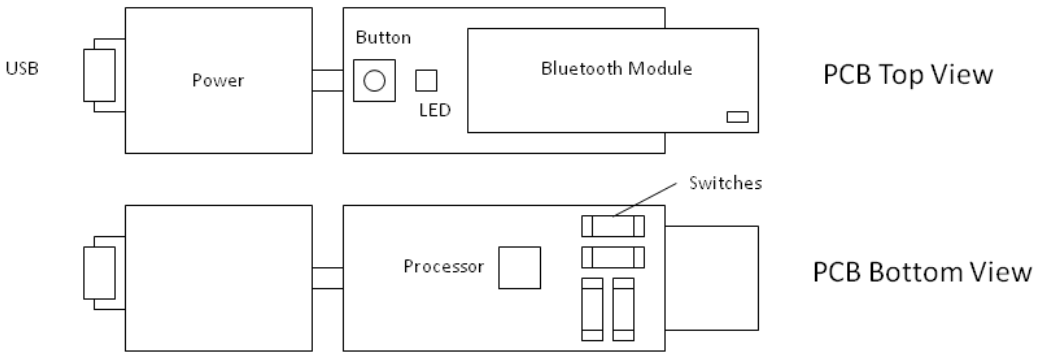

Figure 2.11. The Shockbox PCB layout

The device consists of a micro-USB connector, connected to an unidentifiable lithium-polymer charging IC and battery. The device senses impacts through the use of binary electromechanical force switches [34]. Signals from the switches are processed by a microprocessor and sent to a Bluegiga WT11i Bluetooth Class 1 module which transmits the impact information wirelessly to a smartphone.

2.3.3 Power consumption, cost and packaging analysis

The device is rated for approximately 500 hours of use between charges. The low power consumption of the binary electromechanical force switches coupled with the extremely low current draw of the Bluegiga Bluetooth module in standby mode (50μA) [35] allows the device to prolong battery life. When the Bluetooth module enters transmit mode, however, it can consume up to 180mA of current – therefore the more a player gets hit, the shorter the device battery life will be.

The Shockbox retails for $149.99. Aimed at both recreational consumers and athletic team staff the device is simple and user-friendly enough to appeal to both demographics. The only component included in the Shockbox of significant cost is the Bluegiga Bluetooth module, which costs $21.11. Estimating device packaging and assembly costs at approximately $10.00 per unit, this puts the manufacturing cost of the device at $31.11. The companion app is a free download from both the iTunes Store and the Google Play Store.

The Shockbox packaging is rather unique. The PCB itself is manufactured out of polyamide based flexible printed circuit board material (FPCB). It appears that the FPCB is then placed at the bottom of a mold, and a rubber compound is poured on top of it. Essentially fused to the FPCB, this forms the exterior casing of the device. As shown in Figure 2.12, the device is broken up into segments which allow it to flex with the curvature of the helmet when mounted. The segments are connected with additional FPCB material that is exposed. During laboratory testing, it was observed that repeated attachment and removal of the device from a helmet caused the exposed FPCB to degrade rapidly, eventually affecting the device performance and ultimately leading to device failure.

Figure 2.12. The Shockbox device

2.3.4 Accuracy limitations

The biggest limitation of the Shockbox comes from the use of binary electromechanical force switches. In the whitepaper published by Impakt Protective [34], the disadvantages of accelerometers are highlighted – yet none of the discussed disadvantages of accelerometers has been relevant in recent years. The binary force switches have their own set of limitations – they are only able to sense when a fixed acceleration threshold has been exceeded, and are unable to detect the actual magnitude of acceleration, forcing the device to classify all impacts detected as either ‘mild’, ‘moderate’, or ‘severe’. The device does not have any onboard memory or EEPROM, so if impacts are detected when the device is out of range of the paired phone/tablet, the impact is lost.

2.4 Reebok Checklight by MC10

2.4.1 Device history and theory of operation

Announced in January 2013, the Reebok Checklight was developed by mc10, in collaboration with Reebok. The device features a unique form-factor – the player is required to wear a breathable fabric skullcap, and the Checklight device slips into a pocket stitched into the device.

The device is turned on by holding the 'on' capactive button for a few seconds, upon which the device will flash a green LED intermittently to indicate it is on and 'listening' for impacts. The device uses a set of three LEDs, red, yellow and green, to indicate the impact count and hit severity detected. The hit severity is assessed through the use of a 'proprietary algorithm similar to the calculation of the Head Injury Criterion (HIC)'. The device conveys information to the user in two ways: (1) when in use under a helmet and (2) while the device is being charged.

When the player is wearing the device under their helmet, if a moderate hit is detected, the yellow LED begins to flash. If a more severe hit is detected, the red LED begins to flash. The green LED will flash once for every 100 less severe impacts detected. A yellow or red LED notification indicates that the device recommends the player undergo concussion assessment. The only way to dismiss or reset these notifications is to power cycle the device.

When the device is being charged, a more detailed impact count can be viewed using the LEDs. By inserting the charging cable and immediately removing it, the device LEDs will flash in sequence to indicate the number of less severe, moderate and more severe impacts sustained by the device. Each green LED flash indicates 100 less severe impact, each yellow LED flash indicates 1 moderate impact, and each red LED flash indicates 1 more severe impact. Total impact counts are only displayed in the charging mode.

2.4.2 Hardware description and specifications

The Reebok Checklight is based on a PIC 24FJ64 microcontroller, which takes rotational accleration readings from an ST Microelectronics L3G4200D MEMS tri-axial digital gyroscope ($\pm 2000°s^{-1}$), and linear accleration readings from a Bosch BMA250

(±16g) MEMS tri-axial digital accelerometer, and stores the data in the microcontroller flash memory (assumed, since no external EEPROM is present on the device). The device is powered via a 80mAh battery at 3.7V, and a Linear Technologies LTC4080 combination battery charger/buck converter IC is used for power management. The device requires recharging after approximately 6 hours of use, and takes about 4 hours to reach a full charge.

Figure 2.13. Reebok Checklight and accompanying skull cap

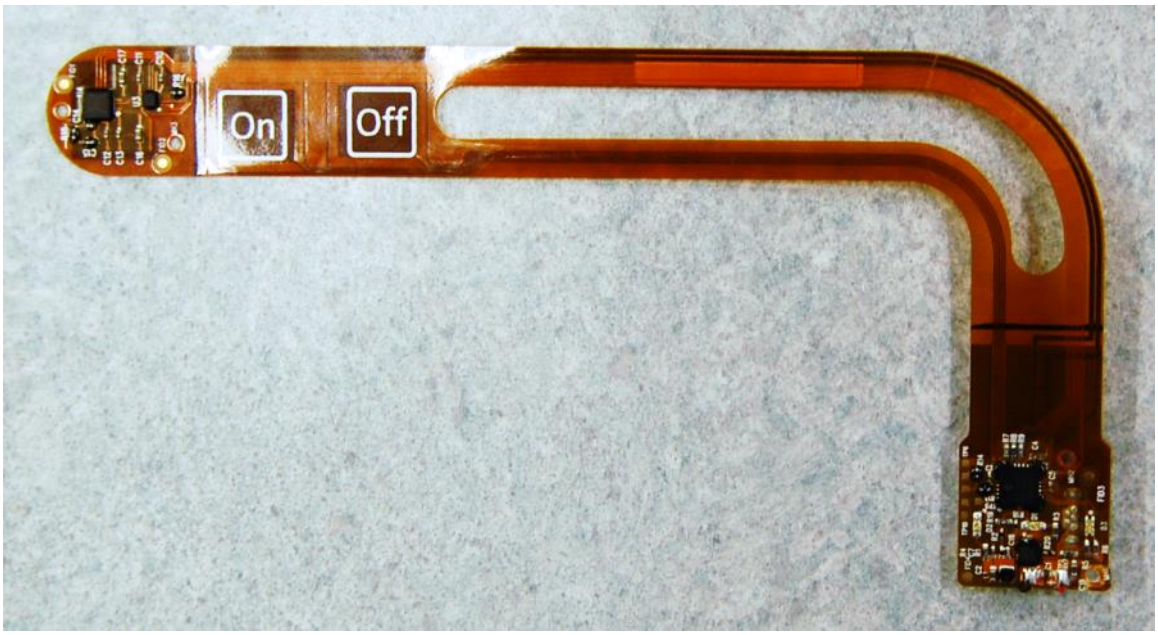

Figure 2.14. Reebok Checklight PCB

2.4.3 Packaging and cost analysis

The Reebok Checklight boasts what is perhaps the most creative packaging of the devices presented in this chapter. All the components are soldered onto a polyamide based flexible PCB. This allows the device to fit better when inside the skullcap, as the flexion allows the device to conform better to the curvature of the head. Both the sensor section and the microcontroller section have stiffening material, in addition to epoxy reinforcement, to prevent the PCB from bending excessively, which could cause the components to shear off.

The Reebok Checklight retails for $149.99. A breakdown of the component costs can be seen below in Table 2.5. The device is aimed at both recreational and athletic team staff. The device is simple and low maintenance enough to make it appealing to the target demographics.

Table 2.5. Major component costs for the Reebok Checklight

Major component	Cost
Microchip PIC24FJ64	$3.89
Bosch BMA250	$2.78
ST Microelectronics LG34200D	$3.20
Linear Tech. LTC4080	$2.24
80mAh Li-Po battery pack	$5.99
Misc. passive components	$5.00
PCB fabrication costs (estimated)	$10.00
Total electronic costs:	**$33.10**

2.4.4 Accuracy limitations

The most glaring limitation of the Reebok Checklight is perhaps the extremely low range accelerometer used – football related impacts are regularly in excess of 30g, and have been known to exceed even 200g. The device claims to use a proprietary version of the HIC algorithm, but the HIC was established as a means to measure automotive related impacts – where linear acceleration is the primary acceleration experienced. While the

exact implementation of HIC measures used by the Reebok Checklight cannot be determined, it is extremely likely that that are not truly indicative of mild, moderate or severe impacts. Indeed, in laboratory testing, a simple flick of the device with a finger caused it to flash red, but dropping the device repeatedly from varying heights barely registered.

3. INITIAL DEVELOPMENT EFFORTS

In the summer of 2012, the PNG initiated full-time development of a custom hardware for continuous real-time telemetry. Up to this point, the PNG had been relying extensively on the HIT System™ as its primary method of tracking head acceleration events. As outlined previously, the HIT System has many limitations – the most relevant of which being its inability to continuously record all acceleration events in real-time.

To collect the data necessary to construct predictive models for brain injury, the PNG required a hardware platform with the following device characteristics:

1. Must be wearable and fit comfortably under a helmet, preferably behind the ears (BTE)
2. Easily deployed across multiple players and teams
3. Records all head acceleration data in real-time with no data omission
4. Robust packaging
5. Low power consumption/long battery life
6. High flash-storage capacity

Low device cost was of importance to the project, but this initial development was intended to illustrate proof-of-concept first, before cost-reduction and manufacturing optimizations measures were introduced. While the author contributed during initial stages of the project, the final hardware development was the result of work done by Paul Rosenberger – resulting in the device codenamed BTEv01.

3.1 Hardware specifications

The BTEv01 device is based on the Atmel ATxmega256A3BU [36] microcontroller, due to the microcontroller's ultra-low power capabilities – between 1.1mA – 10mA depending on processor load. The microcontroller is also capable of multiple 'standby'

modes during which it consumes less than 1μA of current. It is a fully featured 8/16-bit microcontroller with on-board ADC, SPI, USB and capacitive touch sensing peripherals. The capacitive sense module was crucial, as BTEv01 intended to emulate the HITS System in the way the device is turned on – by using capacitive sense electrodes.

In order to detect any and all head acceleration events, a minimum specification was established such that the device required a minimum of 2 accelerometers and 1 gyroscope. Ultimately the device was designed to utilize 3 accelerometers and 2 gyroscopes. This was done to simultaneously introduce data redundancy into the systems and study variability between the individual sensors. The accelerometer chosen was the Analog Devices iMEMS^{TM} ADXL377 - a small (3mm x 3mm), low-power (0.3mA) tri-axial linear analog accelerometer. At the time of device development, this was one of the only high-G range (±200g) accelerometers available on the market. The gyroscope selected was the Invensense dual-axis IDG500, as it had a high rotational sensitivity (±500°s^{-1}) and low power consumption (7mA) and a small package size (4mm x 5 mm).

The unique real-time monitoring goals of the PNG, combined with the 5 on-board sensors, resulted in an immense amount of data generated per unit time. Therefore the BTEv01 device required considerably larger flash memory storage solutions compared to commercially available systems. Flash memory on-board the microcontroller and external EEPROM ICs cannot provide the memory capacity and density required for the storage of multiple hours of continuous telemetry data. Many high-capacity flash storage solutions were explored, but ultimately a NAND flash memory module, the MT29F16G08CBACA manufactured by Micron, was selected. The module boasts low current consumption (10mA during read/write cycles), up to 32Gb (4GB) of storage and compatibility with the Open NAND Flash Interface (ONFI) protocol. The ONFI protocol was developed to simplify NAND Flash integration into electronic products – so the selection of a NAND flash module with support for the protocol was expected to reduce total development time of the device. Sampling the sensors at 2kHz [37] allowed a theoretical maximum of 15 hours of data to be stored on a 16Gb (2GB) NAND flash IC.

Power was delivered to the device via a 400mAh lithium-polymer battery and a Maxim MAX1874 charge management IC that allows device charging and system loading simultaneously.

3.2 Printed Circuit Board design

In order to place the 3 accelerometers and 2 gyroscopes effectively around the head, 3 separate PCBs were designed. The main PCB contained the microcontroller, flash storage, capacitive sensing electrodes, 1 accelerometer, 1 gyroscope and battery and power management circuitry. The right-side PCB (situated behind the right ear when used) contains capacitive sensing electrodes, the second gyroscope and an accelerometer. The left-side PCB contains the third accelerometer, additional capacitive sensing electrodes and an AD7151 capacitance converter. The AD7151 was used over the capacitance converter on-board the microcontroller, as the on-board converter exhibited erratic behavior, and was unable to be calibrated correctly.

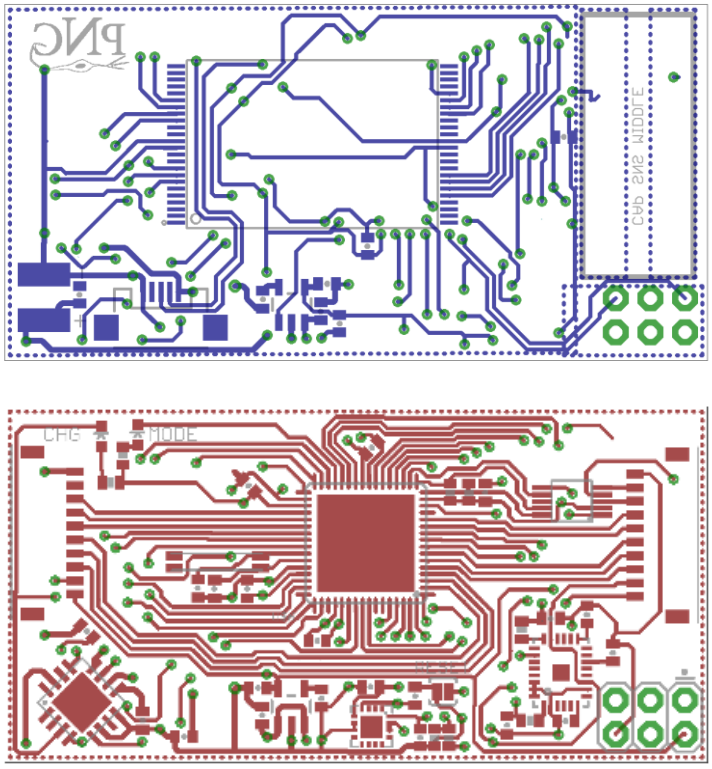

Figure 3.1. Bottom and top copper layers for the BTEv01 middle PCB

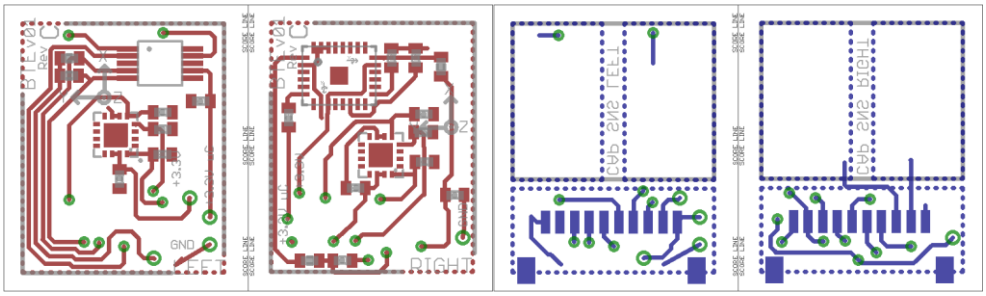

Figure 3.2. Top and bottom copper layers for the BTEv01 side PCBs

3.3 Performance limitations

Design and development of the device was conducted between January and June of 2012. In July 2012, components and PCBs for the device were ordered in bulk quantities. Thorough testing of the device began only after the components for the device were ordered en masse, revealing a number of critical flaws and failure points. The NAND flash memory module experience major read/write issues – the implemented interface between the NAND flash memory and the microcontroller was extremely low-level. This meant that the microcontroller was constantly performing 'house-keeping' operations for the NAND flash memory, maintaining the file structure and keeping track of the sectors and pages used. Additionally, every NAND flash memory module come with a pre-loaded table of good and bad sectors (variability introduced during the silicon wafer manufacturing stage). This table could be easily corrupted by the microcontroller if the correct initialization sequence was not performed, rendering the NAND flash memory module useless.

The microcontroller originally selected for its ultra-low power features, proved extremely difficult to work with – the development environment was restrictive and the available hardware development tools were expensive. During testing, the device would randomly power on/off, or reset itself in the middle of an operation, independent of the on/off switch. While the root cause of this fault was never determined, it is likely that a malfunction or design flaw in the capacitive sensing circuit was at fault. The capacitive sensing electrodes are located directly below the wiring harness connectors between boards, so it is theorized that electromagnetic interference (EMI) from the harness, which carried both analog and high-speed digital signals, may have caused the capacitive sensing electrodes to detect a false positive, causing the random power cycle behavior observed.

In order to confirm that accurate readings were measured by the device's accelerometers and gyroscopes, the device was subjected to tests on a drop tower at the Human Injury Research and Regenerative Technologies (HIRRT) Laboratory at Purdue University. Consistent readings were nearly impossible to obtain for accuracy comparison, because the device continued to suffer from random reset issues. After bypassing the capacitive sensing electrodes, the reset issue was temporarily alleviated, but as soon as drop testing began, the issue reappeared. Prior to a drop, the device was turned on and the heartbeat LED present on the device indicated all systems were ready. After the device was dropped, the heartbeat LED was still functioning, but no data was recorded by the device. Similar behavior was not observed during smaller impact tests – evidence which supports the theory that large impacts caused the device to malfunction. It is believed that due to the large, rectangular design of both the main PCB and the NAND flash memory module, the PCB experiences electrically disruptive flexion during large impacts, causing the device to malfunction and resulting in data not being recorded.

3.4 Packaging Limitations

The packaging for BTEv01 was fabricated using a 3-D printer. It consists of a single-piece polymer band that sits on the ears and wraps around the back of the head (Figure 3.4). While the goal was to have the device constructed in such a way that it could sit comfortably underneath a helmet, it is clear from Figure 3.3 that the desired fitment cannot be achieved.

The aspect ratio of the middle PCB proved too high, and did not align with the curvature of the head or the polymer band, resulting in additional flexion of the PCB during use. As seen in Figure 3.5, each of the 10 JST wires in the harness is required to be hand-crimped – which is both time-consuming and prone to error during the crimping process. In practice, the crimped wires easily came loose and the connectors deformed under moderate mechanical stress, making the harness unreliable and introducing another point of failure for the device. A closer look at Figure 3.5 also reveals that the PCBs mounted on the band protrude significantly. Not only is this uncomfortable and unsafe for athletes as it can scratch them during play, it also introduces yet another point of mechanical stress. The

packaging is also completely exposed – the polymer band does not have a covering or casing of any sort. For field testing, the device was wrapped in electrical tape to provide some protection, but the device is still extremely susceptible to corrosion and water damage from the high-temperature, high-humidity environment that is an active athlete's head.

Figure 3.3. BTEv01 being fitted on a Jefferson High School student

Figure 3.4. Multi-angle view of BTEv01 packaging

Figure 3.5. View of connectors and wiring harness

3.5 Lessons learned

Many of the shortcomings of BTEv01 were valuable lessons learned – particularly in terms of device optimization for manufacturing. Minimizing the number of through-hole components and components on the bottom-side of the PCBs, as well as using a pre-made wiring harness will reduce the manufacturing time required for each device dramatically. To improve the packaging, a more iterative process should be adopted – where the packaging and device are designed simultaneously, instead of sequentially. This prevents design decisions governing the electronics side affecting the packaging adversely and vice versa.

All of the lessons learned were used in constructing a new set of design criteria for the next generation of BTE devices. The design criteria and approaches used will be discussed in the following chapter.

4. DESIGN CRITERIA, APPROACHES AND METHODS

This chapter serves to discuss the hardware development efforts put forth by the PNG, specifically the author, during the May 2013 – March 2014 period. Based on the lessons learned from both commercial devices and the previous efforts of the PNG, a thorough revision and discussion of the design criteria required will be presented. The numerous design approaches applied to these criteria and each iterative stage of the system design will be detailed, along with special hardware features developed to achieve the desired goal of a low-power, low-cost, size-constrained real-time biomechanical telemetry system.

4.1 Design criteria

With the overarching goals of the PNG in mind, it is possible to establish a set of design criteria that will help minimize unnecessary design decisions, and maximize device functionality and effectiveness. While the desired characteristics are largely unchanged from the PNGs first efforts, the detailed discussion of both commercial systems and previous efforts by the PNG have allowed the team to clearly define the specifics behind each design criteria.

4.1.1 Criterion 1: The device must be wearable under a helmet

As concluded in Chapter 3, building one-size-fits all devices than can be worn by athletes in both helmeted and non-helmeted sports resulted in design compromises that ultimately led to the device being impractical in both settings. The PNG primarily focuses research efforts on football players, so the decision was made to pursue a form-factor that would be both comfortable and practical for football players to have under their helmets. If a device is to be wearable under a helmet, its packaging must be extremely robust, as the

inside of an athlete's helmet is an extremely inhospitable environment. Temperatures can exceed 40°C regularly, and the environment is typically saturated with sweat. Therefore the device needs to be corrosion resistant.

Safety regulations regulating football helmet design are governed by an organization called the NOCSAE[7]. Most helmets used by football players today have been certified by NOCSAE, but if any modifications are made to a helmet, such as the addition of a wearable device, the helmet and device must be recertified by the NOCSAE. Most, if not all youth and high school football leagues mandate the use of helmets that have been NOCSAE certified.

By constraining the size of the device to be small as possible, maximum flexibility in developing packaging and placing the device inside a helmet is achieved.

4.1.2 Criterion 2: The device must be accessible, user-friendly and easily deployed across multiple players and teams

A particularly valuable lesson learned from commercial systems is that they either cater to the individual user (Shockbox, Reebok Checklight), or require an elaborate system to be set up by the athletic staff (HIT System) before the devices are useful. The PNG aims to build a device that is capable of catering to both demographics. This increases the value proposition of the device, as it is no long exclusively a research tool or exclusively a consumer device – it is both. While the short term goal of the PNG is to conduct research to build predictive models using the devices to collect data, the end game is to validate these predictive models and load them back onto the devices. This approach not only reduces the total development time needed to bring the device to market but also reduces the total non-recurring engineering (NRE) costs associated with the device development.

In the case of team-based deployment, the devices will be primarily administered by athletic staff. Individual users' devices will be likely handled by either the athlete themselves, or their respective guardians. By making the device user-friendly – easy to use

[7] The National Operating Committee on Standards for Athletic Equipment is a non-profit organization focused on providing standards and certification for the safety of athletic equipment.

and maintain – the device is more likely to be used correctly and consistently, improving the efficacy of the device. If the device is used by athletic staff or a research team, they will be managing 20-30 devices at any given time, so the devices must be easy to administer en masse and individually as well.

4.1.3 Criterion 3: The device must be able to record all data with no omissions or discrepancies

The predictive models that the PNG will develop as a result of the data collected by the device will rely heavily on a complete dataset – which requires that every head acceleration event that an athlete experience must be recorded. The ability to record all the necessary data without interruption will require robust electromechanical design. Due to the large amount of data generated by multiple sensors recording continuously in real-time, the device will also require the ability to store hours of telemetry data on-board. The device must also have battery-life sufficient to match its ability to record data: the device needs to be designed to consume as little power as possible and maximize battery life.

4.1.4 Criterion 4: The device must be as low-cost as possible

In order to minimize cost to the PNG and the end-users of the device, the device is designed to be as low cost as possible. Many commercial systems are priced out of the reach of individual users and would be too expensive for most youth and high school football teams to adopt. The PNG believes that the real-value proposition of the devices and research being performed lies in the predictive-models being developed, therefore the sales of hardware is not regarded as an opportunity for profit. The target price for each device is $100. By developing a low-cost device, it becomes more accessible to users, and is more likely to be widely adopted and will correspondingly generate more data for the PNG to develop predictive models with.

4.1.5 Criterion 5: The device must be easily assembled and manufactured

Lessons learned from the efforts behind BTEv01 have highlighted the importance of designing a device to not only function correctly, but to be easily assembled during the

prototype stages and manufactured in large quantities as well. This drives the total cost of development down and reduces hardware revision times required.

4.1.6 Summary

The 5 design criterion outlined above may be summarized as follows:

1. The device must be wearable under a helmet
2. The device must be accessible, user-friendly and easily deployed across multiple players and teams
3. The device must be able to record all data with no omissions or discrepancies
4. The device must be as low-cost as possible
5. The device must be easily assembled and manufactured

4.2 Design approaches and methods

The design approaches and methods used to fulfill the design criteria previously detailed include following topics:

1. Proposed hardware roadmap and timeline
2. Component selection rationale
3. Unique design features
4. Lessons learned from iterative hardware development

4.2.1 Proposed hardware roadmap

The majority of the hardware development was slated to take place over the summer of 2013. To gain a better understanding of the device development cycle and outline hardware revision expectations, a development roadmap was created – which included turnaround times, design priorities, anticipated issues and expected costs. The proposed roadmap can be viewed in Appendix A.

The first device developed was a full featured test bed. The test bed, dubbed BBTE_FIX_V01, was a large scale device with extensive that allowed rapid prototyping and debugging of all major device components, including but not limited to the microcontroller, flash memory storage and sensors. Once all the major hardware and software kinks were worked out, the roadmap progresses to the first major miniaturization push in the form of BTE_MICRO_TEST. The purpose of this board was two-fold: (1) to practically determine how small the device could be made and (2) to evaluate the quality of a new printed circuit board house the author was negotiating with.

BTE_MICRO_V01 was the first revision of the device to include side boards. The side boards are intended to place accelerometers behind the ears (BTE) for better sensor data acquisition. Hardware revisions BTE_MICRO_V02 through BTE_MICRO_V02.7 primarily consisted of incremental hardware improvements primarily consisting of improving PCB layout optimization, reducing component counts and providing feedback on external packaging development efforts, and incorporating the unique design features developed and discussed in Section 4.2.3.

Device development was initially expected to last the duration of the summer of 2013, with an alpha test deployment of 20-30 devices expected to take place in July/August. Unfortunately, due to catastrophic setbacks with regards to the flash memory and packaging development, device development slowed down dramatically in August 2013. To rectify the issues that caused the setbacks, dramatic steps were taken to revise the hardware architecture of the board, both in terms of component changes and form-factor redesigns. Device development regained momentum in January 2014 after changes were proposed to rectify the issues with the packaging and memory issues, resulting in the BTE_HITS family of devices discussed in Chapter 5.

4.2.2 Component selection rationale

The section serves to discuss the rationale behind the various components used in the hardware design of the device. All components discussed represent those present in the latest revision of the device, unless otherwise noted and costs discussed represent bulk quantity pricing, unless otherwise noted.

4.2.2.1 The Accelerometer

Based on data collected by the PNG over many years of studying football players using the HIT System, athletes regularly experience impacts in excess of ±80G, up to ±150G. Additionally, the resonant frequency of the head is known to be approximately 900Hz [38] and the average impact has been observed to last between 5-10ms [37], so to accurately capture any ringing effects resulting from impacts without violating the Nyquist rate, a sampling frequency of approximately 2000Hz is required. At the time of component selection, one of the only accelerometers that fulfilled these specifications was the Analog Devices ADXL377, a tri-axial high-g (±200G) analog MEMS accelerometer [39]. The sensor is contained within a small 3mm x 3mm package and consumes a maximum of 0.3mA of current during use. It also features user-adjustable bandwidth based on the responsiveness required. The sensor is also considerably cheaper than many of its competitors, at $5.82 per sensor.

4.2.2.2 The Gyroscope

The gyroscope selected was the Invensense MPU-6000. The sensor contains a tri-axial digital SPI gyroscope, with programmable sensitivity up to 2000°s^{-1}, which sufficient to capture rotational acceleration events, which last longer than typical linear acceleration events. The sensors also contains a low-g (±16G) tri-axial accelerometer that can be used to sense normal-motion, which is potentially useful in filtering out non-critical impacts as predictive models are developed.

4.2.2.3 Flash storage

The drawbacks of using the NAND flash memory modules for high-capacity storage were outlined the previous chapter, highlighting the need for a new solution. The micro SD flash storage standard chosen after extensive research. The micro SD memory card was the only solution that had adequate storage density, small form-factor and low-cost. Due to the limitations imposed by the SD Card association, the protocol is only open to 2GB cards or smaller and expensive licensing agreements are required to use cards larger than 2GB. To circumvent the expensive licensing costs that would inevitably have to be passed on to the end users, the decision was made to develop a custom SPI based protocol for the micro SD card that would allow high-speed communication. The implementation of the micro SD protocol proved far more complicated than originally expected. The unexpected complexity of implementing this custom protocol resulted in one of the major setbacks in the device development [40].

4.2.2.4 The Microcontroller

Based on the needs of the multiple sensors and the high-capacity flash storage, the Texas Instruments (TI) MSP430F5659 microcontroller was selected. Hardware revisions BBTE_FIX_V01 through BTE_MICRO_V2.7 were based on the MSP430F5529, but the F5529 lacked the hardware to sample multiple sensors while handling the custom micro SD protocol simultaneously.

The MSP430 line of microcontrollers from TI is known providing full featured 32-bit microcontrollers in an ultra-low power consumption device. In addition to the comprehensive list of on-board peripherals, the F5659 was selected specifically due to its

internal Direct Memory Access (DMA) controller that allows data transfer from one address to another with CPU intervention. Advantages of the DMA also include the ability to increase peripheral module throughput, and reduction of power consumption by alleviating some of the load on the CPU [41].

4.2.2.5 Voltage regulation and battery management

Due to the low-power and size requirements of the device, a small, efficient power regulator was needed to regulate the battery voltage down to the required 3.0V. In an attempt to reduce power consumption, the device was designed to run off 3.0V, so off-the-shelf 3.3V switching regulators were not suitable. Ultimately, the TI LM367X adjustable switching regulator was chosen, which is capable of providing up to 350mA of current at 3.0V. The BTE_MICRO_TEST through BTE_MICRO_V2.7 devices utilized a 1.5mm x 1.0mm Ball Grid Array (BGA) package in an effort to save space. The BGA package introduced a host of problems, expanded upon in Section 4.2.4.3, resulting in the switch to a SOT-23 package (Figure 4.8) of the same device in all subsequent iterations.

The device can be powered using either a 400mAh or a 1000mAh 3.7V lithium-polymer (Li-Po) battery. Initial prototypes required the battery to be removed and charged using a special charger, but in the interest of usability, it was decided to include an on-board charging circuit – allowing the device to be charged en mass using a custom charging station, or individually via a standard USB cable. The charging IC used was the MAX1874 – chosen for its ability to allow the device to function normally while the batter is being charging, which will enable researches and individual users to download information off the device while it is being charged.

4.2.2.6 PCB design

Design complexity and cost analyses were performed to determine the ideal PCB substrate and technology to be used in the design process – resulting in the selection of 2-layer FR4 0.062” PCB substrate. The cost of developing prototypes on 4-layer boards, or on polyamide based flexible PCB substrate was simply too high to remain sustainable for long term development. Further negotiations were carried out with various board houses in

order to drive cost of 2-layer FR4 PCB fabrication down. All boards were manufactured using Pentalogix's US Quickturn PCB service.

4.2.3 Unique design features

This section outlines some of the unique features incorporated into the device design that allow the device to better fulfill the criteria stated in Section 4.1. The features discussed were primarily incorporated during the BTE_MICRO series development stage.

4.2.3.1 Footprint based ZIF programming interface

One of the challenges faced in designing a size-constrained device is programming the microcontroller once the components are placed on the PCB. In-circuit programmers often use large, bulky connectors, which in turn require the addition of receptacles on the target device. The receptacles not only add cost, but take up valuable board real-estate. The BTE series of devices utilize the JTAG protocol for in-circuit programming and debugging. A typical implementation of a 14-pin JTAG circuit is seen in Figure 4.1, along with the connector and receptacles used.

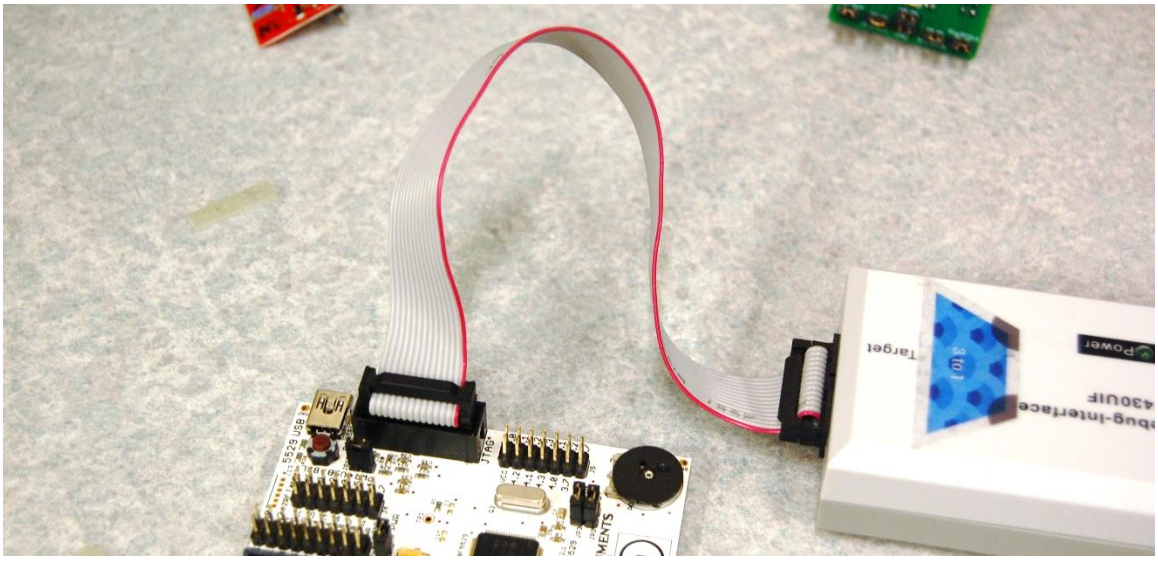

Figure 4.1. Typical 14-pin JTAG circuit implementation.

Several alternatives were explored, including creating a custom connector using pogo pins and a PCB, but this was deemed to be too costly and time consuming – particularly

given the author's limited mechanical expertise. The Tag-Connect™ solution was chosen, to provide a footprint-based zero insertion force (ZIF) programming and debugging interface. The Tag-Connect does not require a mating connector on the PCB, resulting in zero cost per board in terms of programming circuitry. The Tag-Connect also occupies a significantly smaller footprint than the standard MSP430 JTAG connector, reducing the use of valuable PCB real-estate. The 14-pin Tag-Connect cable is also polarized, so it can only be inserted in the correct way. The cable uses high reliability gold plated pogo pins which ensure a secure connection each time, and also reduces repetitive mechanical stress on the PCB.

4.2.3.2 Debug bridge

During complex hardware design, it is often necessary to include breakout pins and LEDs for debugging – something that is very common in large commercial development boards. The rapid development of the BTE family of devices presented a unique challenge, however. The simultaneous development of software and hardware meant that the hardware was being shrunk faster than the software could be finalized, so a solution was needed that would preserve the advanced debugging capabilities of a larger development board while taking up as little space on the PCB as possible.

A novel solution was proposed by Jeffery King III, and executed by the author. The Tag-Connect cable mentioned in the previous section uses 14 pins to mate with a PCB, but only 7 of these pins are actually used as part of the JTAG programming circuit. The remaining 7 pins were not connected to anything so they were rerouted on the main PCB, and connected to the signals required for debugging. With all 14 pins now routed to the Tag-Connect, an additional in-line debugging bridge PCB was designed that would serve as a pass through for the JTAG connections on to the TI MSP430 in-circuit debugger, while containing breakout pins and LEDs for the 7 additional signals. The purple Tag-Connect cable, connected to the in-line debugging PCB can be seen in Figure 4.2.

4.2.3.3 Solid state design (hall-effect sensor)

In order to allow users to turn the device on and off, a switch was needed, but electromechanical switches typically require ports or slots cut out of the packaging. Given

the hostile environment the device will be operating in, any holes in the packaging are opportunities for sweat and humidity to seep in and damage the device. The solution devised was the use of a Hall effect sensor. When exposed to an orthogonal magnetic field, the Hall effect sensor outputs an active low signal which can then be used drive switching MOSFETs. The circuit used is pictured below in Figure 4.3.

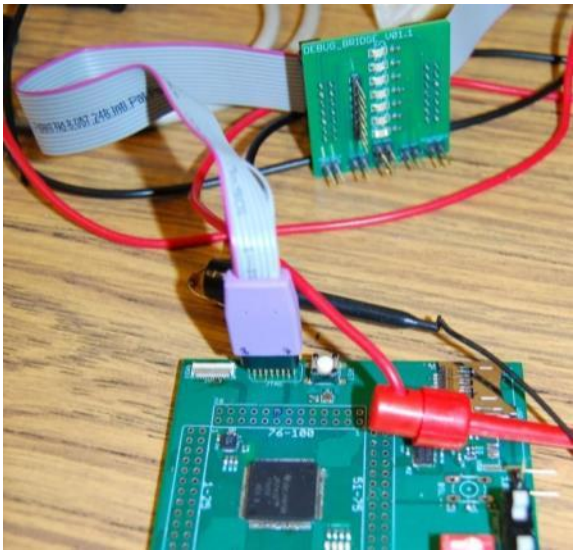

Figure 4.2. Tag-Connect cable with in-line debugging PCB

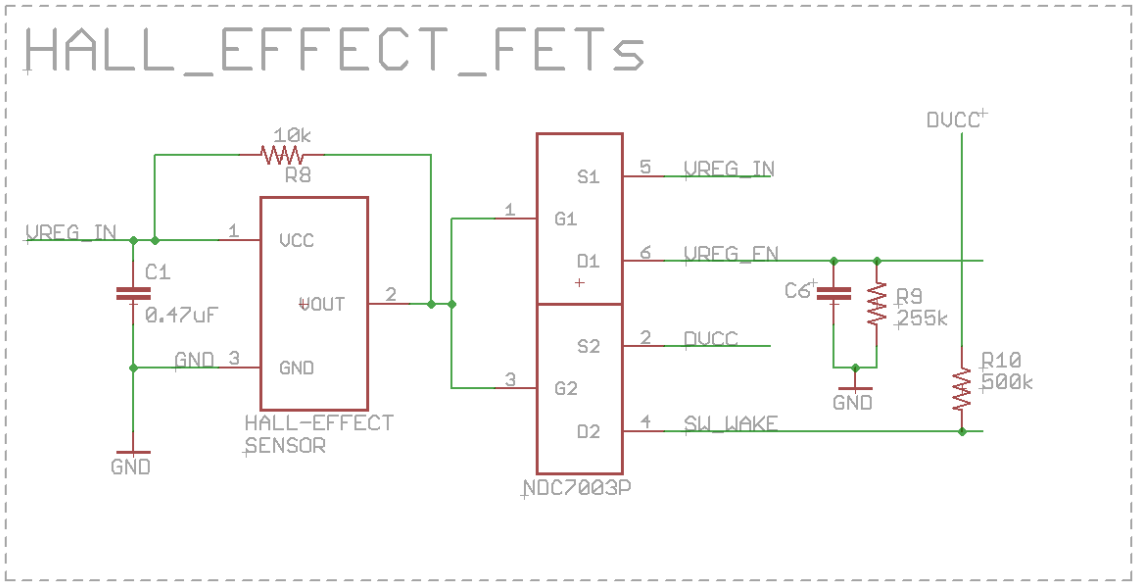

Figure 4.3. Circuit used to implement the Hall effect sensor.

The Hall effect sensor [42] is powered directly from the battery (VREG_IN), with a pull up resistor (R8) and a decoupling capacitor (C1). When exposed to an orthogonal magnetic field, the output of the Hall effect sensor (VOUT) is pulled low. This pulls the two gates (G1 and G2) on the dual-PFET [43] low, which opens the channel between the source and drain (S1,D1 and S2, D2) causing VREG_EN (voltage regulator enable pin) to be pulled high to the battery voltage (VREG_IN) and SW_WAKE to be pulled high to DVCC (3.0V). When a magnet is swiped over the Hall effect sensor, the VREG_EN pin and SW_WAKE pins are pulled high long enough to power on the microcontroller and have it wake up via an interrupt on the SW_WAKE pin. Once the microcontroller is running, it drives the VREG_EN pin high, ensuring the voltage regulator stays on after the magnet is removed.

To power down the device, the magnet is simply held over the Hall effect sensor for 2 seconds, and upon removal the microcontroller drives the VREG_EN pin low, thereby turning the device off. The 'instant-on, long-exposure' on/off sequence was chosen to make it difficult to accidentally turn the device off. Testing revealed that a 1 second turn off time resulted in erratic on/off behavior as users would tend to hold the magnet near the device for 1 second when turning it on, even though a simple swipe was required. Increasing the turn-off time beyond 3 seconds not only also resulted in erratic on/off behavior, but also led to impractical on/off sequence times when deploying 20-30 devices at a time.

4.2.4 Lessons learned from iterative hardware design

During the development of the BTE_MICRO family of devices, several major hardware design issues were encountered which hindered the functionality and reliability of the device. This section serves to discuss those issues, and the measures taken to alleviate them.

4.2.4.1 Board-to-board connectors

As shown in Figure 3.5, the board-to-board wiring harness used in BTEv01 was both unreliable and cumbersome to assemble, requiring hand crimping of each individual wire. A receptacle was needed in addition to the connector used, adding to the total cost of the

device. Initial versions of the BTE_MICRO device utilized directly soldered board-to-board wires, shown in Figure 4.4. This method proved to be extremely robust, with solid connections between boards achieved. It also provided the option of grouping wires into twisted pairs to reduce EMI effects and increase signal integrity. With both a gyroscope and accelerometer on a side board a total of 16 wires was required per sideboard. Soldering individual wires was extremely time-consuming and prone to human error. The permanent nature of soldering the wires directly also meant that if a device failed or required trouble-shooting, it was extremely difficult to swap out the side boards or debug the connections. Many of the alternative connectors considered required expensive crimping tools and that each wire be individually crimped – not a considerable improvement over soldering individual wires.

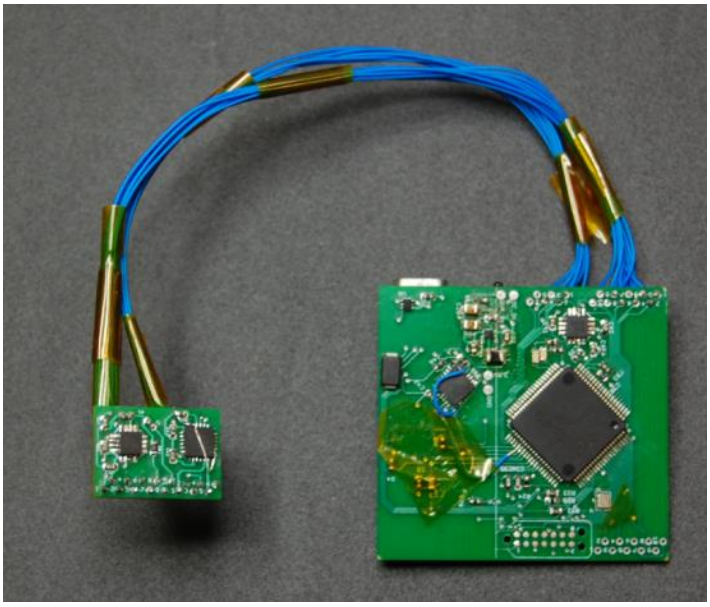

Figure 4.4. BTE_MICRO_V01 board-to-board connections

Subsequent versions of the BTE_MICRO device utilized 25 conductor polyamide based flexible flat cables (FFC) (Molex 15015-0425) coupled with 25 pin rotary backlock connectors (Omron XF3B-2545-31A). While only 16 and 10 conductors are required for the left and right sideboards respectively, the 25 conductor cables were the only option available. A cable length of 4” was selected to allow the sideboards to easily reach behind

the ears. The rotary backlock connectors (RBC) were simply soldered in during PCB assembly, and can be unlocked easily if the sideboards need to be replaced or removed for any reason. While the FPC and RBC components provided an extremely streamlined solution for creating board-to-board connections, they suffered from three fatal flaws: (1) the RBCs were not very robust, and often suffered heat damage during solder reflow (2) the RBCs had a limited number of insertion cycles after which the internal connections in the RBC would fall out and (3) the FPCs were susceptible to kinking. Bending the cables along the conductor axis caused no problems, but even moderate lateral bending produced kinks which affected the signal integrity, even causing shorts in some cases. The FPC and connector are pictured in Figure 4.5 and Figure 4.6.

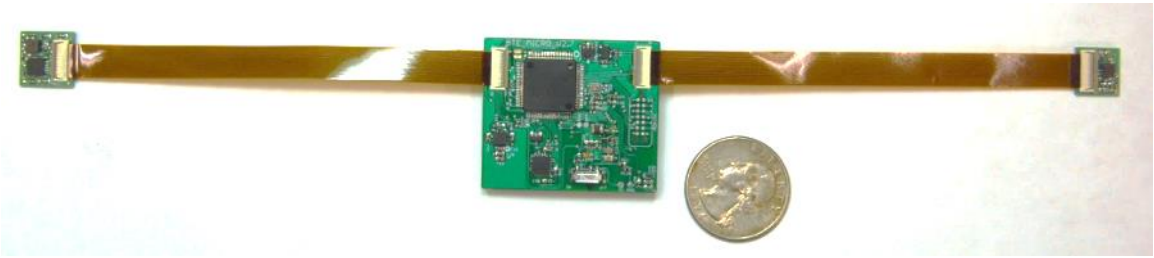

Figure 4.5. FPC and connector assembly

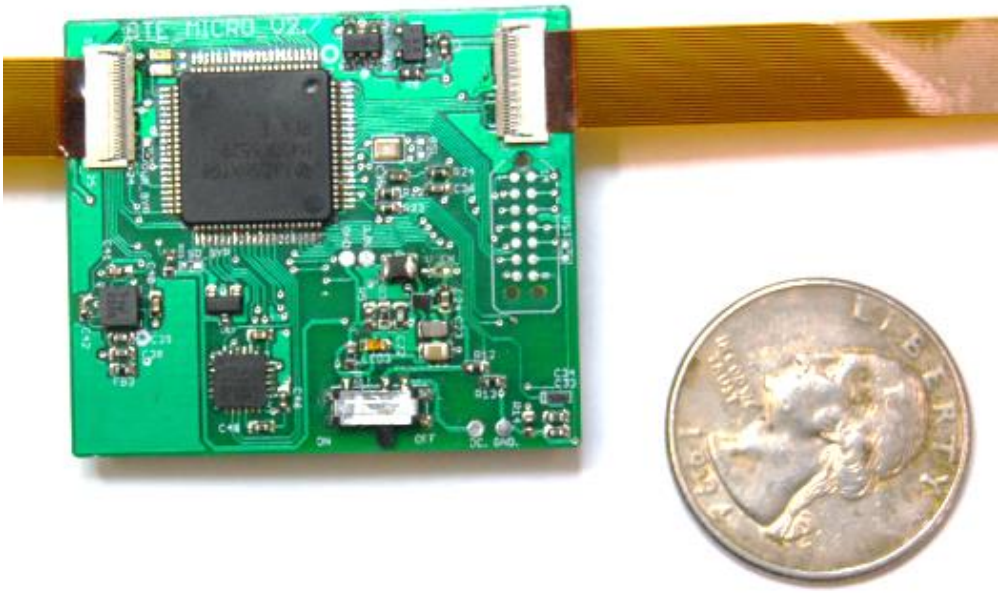

Figure 4.6. FPC and connector assembly – close up

4.2.4.2 Corrosion issues

Another major issue discovered was the susceptibility of the PCBs to corrosion. To save cost during the development and prototyping stage, a leaded solder mask finish was used. During initial drop-tower testing, the device was mounted externally on a helmet. The curvature of the helmet resulted in only a small portion of the PCB being in contact with the helmet. After several drop tests had be conducted, the device was disconnected and put in storage for a week. At the end of the week, the device began exhibiting erratic behavior, and eventually ceased to function at all. Close inspection of the board revealed that the area of the board that had been in contact with the helmet had suffered severe corrosion, to the point of components falling off and traces being severed.

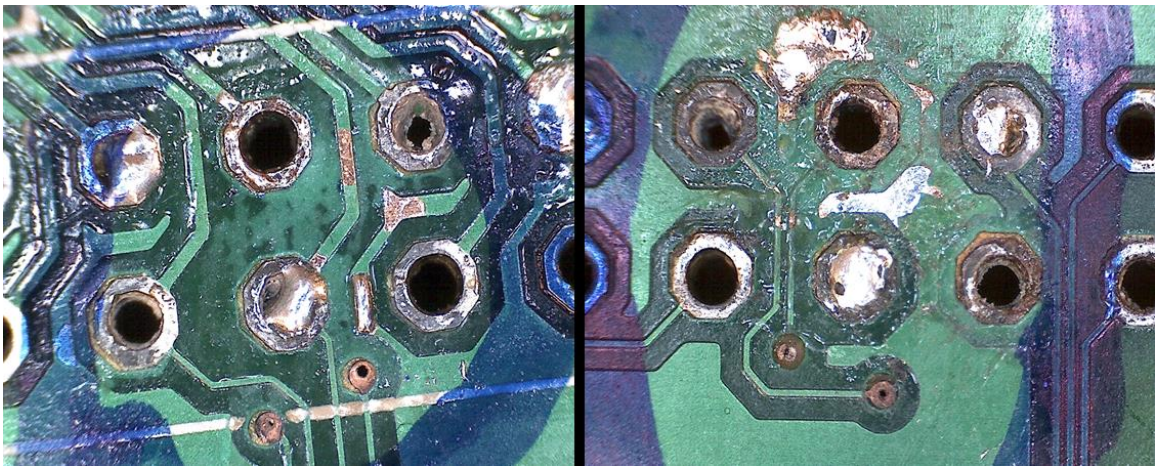

Figure 4.7. Microscope photograph showing corrosion

4.2.4.3 BGA switching regulator

In an effort to reduce the size of the device as much as possible, aggressive measures were taking to reduce component counts and use the smallest packages available for most components. Most efforts to miniaturize the design were successful, with one exception: the switching regulator circuit. The smallest package available for the LM3673 [44] switching regulator IC is a Ball Grid Array (BGA) package sized at 1.4mm x 1mm, with 0.25mm diameter bumps. The dimensions of the package posed several problems: (1) although they were within specification of the board house used, the quality of the footprint

fabricated varied significantly enough to affect the alignment of the IC with the PCB (2) with all the bumps located directly underneath the package, it was impossible to verify that they had been successfully soldered without the aid of an X-ray inspection tool and (3) the BGA package itself was a raw silicon wafer painted black on top, as such it is extremely brittle and susceptible to fracture during assembly and rework. This lead to much frustration when assembling the PCB, as there was little to no guarantee the power circuit would function correctly the first time. Many parts were wasted due to fracture or deformation from assembly and rework, adding additional time and cost to the development of the device.

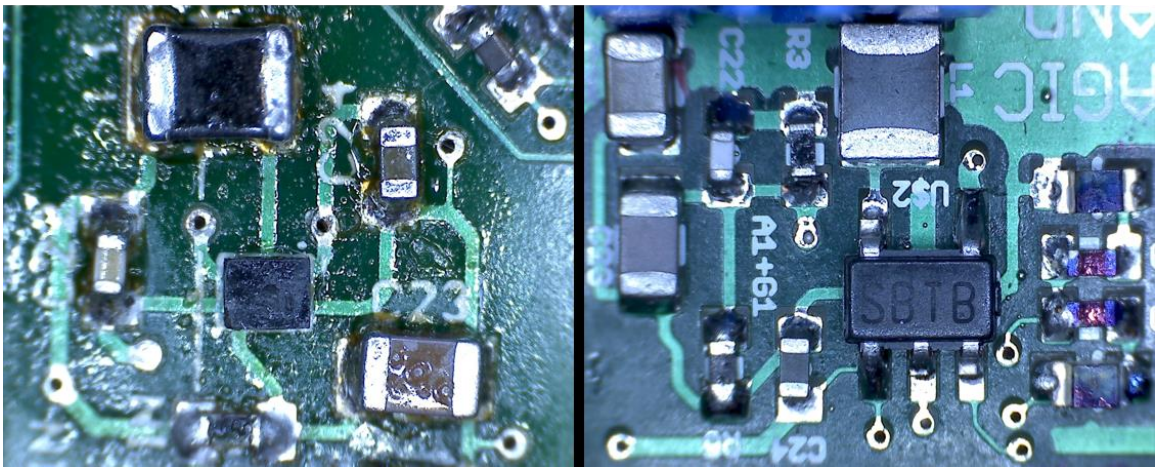

Figure 4.8. Comparison between BGA (left) and SOT packages (right)

4.2.4.4 Packaging limitations

A major setback of the BTE_MICRO family of devices was the lack of appropriate packaging. While the focus of the author did not include the mechanical design required for the packaging, it is a crucial part of the project warranting discussion. The packaging for the BTE_MICRO devices was to be fabricated using a rapid prototyper, in this case a MakerBot 3-D printer, and once the packaging concept was finalized, a mold would be created for large scale production. The idea was to encase the middle, left and right boards with a slim PLA[8] casing similar to that shown in Figure 4.9. In reality, however, the

[8] PLA, or polylactic acid, is a thermoplastic polyester commonly used as feedstock in extrusion-based 3-D printers.

packaging prototypes produced with the 3-D printer exhibited poor fit – partly due to the design of the packaging, and partly due to the resolution limitations of the 3-D printer. A hermetically sealed package was nearly impossible to generate using the printer, making the any molds generated from the 3-D printed prototypes useless.

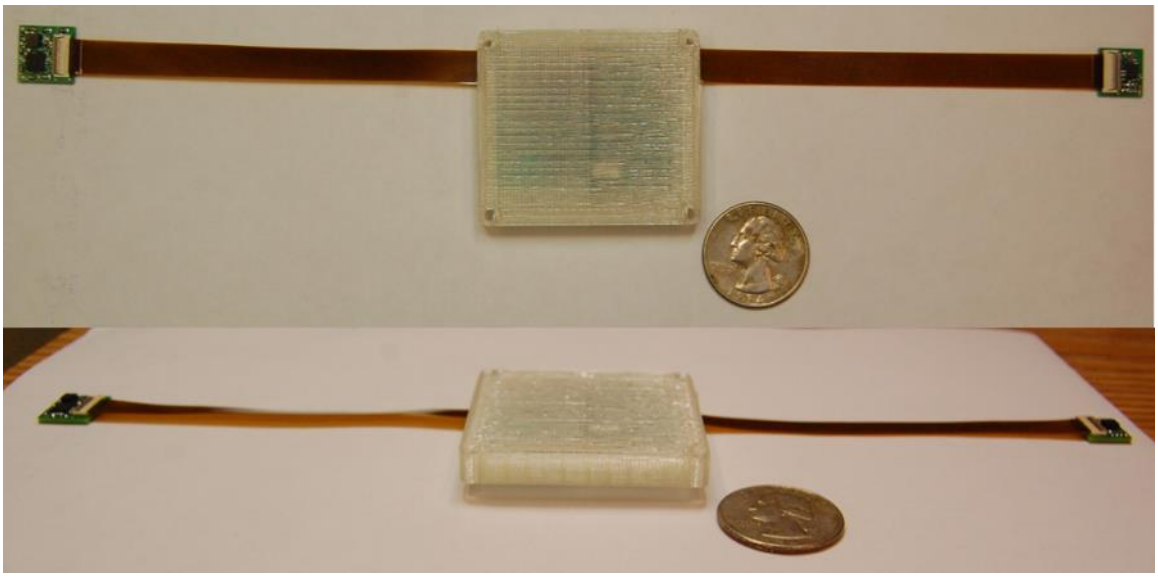

Figure 4.9. Prototype packaging for BTE_MICRO devices

5. PROPOSED HARDWARE SOLUTION

This chapter details the most advanced BTE device developed between January 2014 and March 2014: the BTE_HITS series of devices. The device's packaging redesign and theory of operation will be discussed in detail, as will the PCB layout. Also presented are power consumption and cost analyses. These are proceeded by design features included to facilitate future development and expansion of the platform.

5.1 Packaging redesign

As demonstrated in previous sections, the packaging design of the device has proved problematic repeatedly. In an effort to alleviate packaging development resource requirements, and ensure a speedy NOCSAE approval process, it was decided that the BTE_MICRO device series should be completely redesigned.

Many of the internal components remained the same, but the number of accelerometers was reduced from 3 to 2, and the number of gyroscopes from 2 to 1 – thus eliminating the need for a second sideboard and simplifying package requirements. While the original number of sensors was selected to provide redundant sensor readings on all axes, the reduced number of sensors still provides sufficient data on each axis for reliable data collection [37].

By mimicking the HIT System form factor, NOCSAE certification was guaranteed to be far less complex and time consuming than if completely original packaging had been developed. As the PNG plans to focus primarily on football players in the near future, the football helmet-only form factor of the HIT System presents no immediate disadvantages, and allows the BTE devices to be installed in any commercially available helmet without any major modifications. The existing HITS form factor can also be reduced in size by

almost 50%, since all previously developed BTE hardware is considerably smaller than any of the standard HITS electronics. A preliminary mock-up of BTE_HITS_V01 placed in HITS padding is shown in Figure 5.1. The HITS padding used represents only half of the original padding – the half housing the battery Velcro strap and 3 accelerometers has been removed. In order to maximize packaging flexibility, two versions of the BTE device were created:

(1) BTE_HITS_V02, which serves as a 'drop-in' replacement for the HIT system. This version is capable of using the same battery pack and charger as the HIT System and fits within the original HIT System padding.

(2) BTE_HITS_V03, which aims to improve slightly on the HIT System form factor. This version is completely contained within the right half of the HIT System padding. It is designed with on-board battery charging capability, and uses a 1000mAh Li-Po battery.

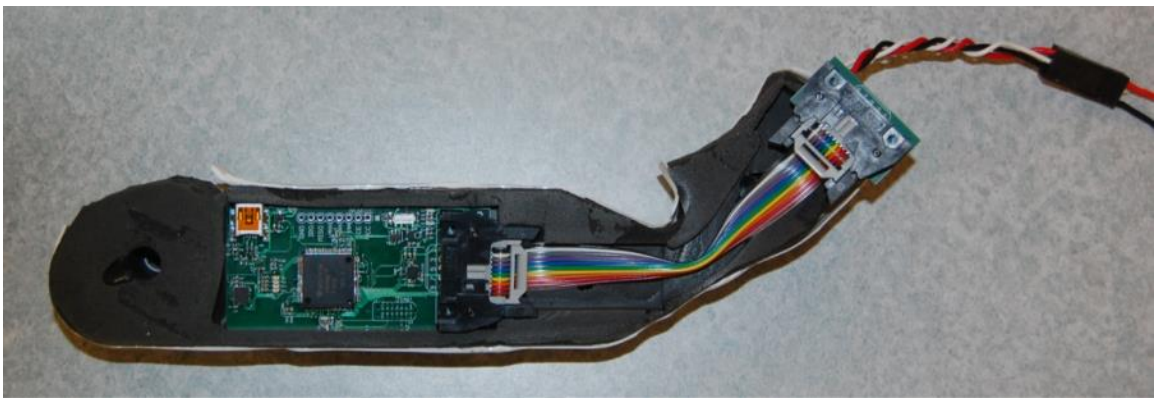

Figure 5.1. Preliminary mock-up with BTE_HITS_V01 and hits padding. Note the 'kinking' in the multicolored IDC ribbon cable

5.2 Board-to-board connector redesign

Another major design component that has resulted in numerous setbacks is the implementation of an effective board-to-board connector solution. Previous attempts using crimped connectors, wires soldered directly to the PCBs, and polyamide based flexible ribbon cables have been shown to be ineffective, impractical and unreliable. For the

BTE_HITS series redesign, "the simpler-is-better" approach was taken when evaluating connectors. The basic requirements for the connectors were specified as the following:

(1) The connectors must be simply constructed – excessive mechanical complexity should be avoided.

(2) The connectors must be easily assembled – extensive assembly time or skills should not be required.

(3) The connectors must be 'hot-swappable' – in the event of PCB or wiring damage or malfunction, the connectors and wiring must be easily replaceable.

(4) The connectors must be low-cost – in the case of the polyamide ribbon cable, the cable and connectors were some of the highest value items on the PCB, but provided little value in terms of the device functionality.

The best solution determined was the use of IDC[9] ribbon cables and standard 0.10" DIP connectors – this would drastically reduce the time spent assembling cable assemblies or soldering connectors on to PCBs. The board-to-board connectors seen in Figure 5.2 are the first iteration implementation of IDC ribbon cables and DIP connectors. Latching connectors were used to allow easy replacement of the ribbon cable assembly should it malfunction or become damaged. Note, however, that the latching connectors while extremely robust and secure, are large and bulky. They also contain several 'sharp' edges that could potentially act as stress points on any surrounding packaging which could compromise packaging integrity. The connectors were also large enough that they could be felt through the padding, potentially causing discomfort to athletes with the device in their helmets.

For BTE_HITS_V02, the board-to-board connectors were revised to incorporate both the ribbon cable connector and receptacle into a single 0.10" DIP part. As seen in Figure 5.3, this causes the loss of the ability to be able to swap out ribbon cable assemblies easily – however, it was discovered that the ribbon cable can be removed relatively easily with a

[9] IDC, or insulation displacement connectors are connectors that use sharpened blades or pins to pierce insulated wire to establish an electrical connection. It is often used as an alternative to expensive, time consuming crimping methods.

sharp blade and tweezers, without damaging the connector that is permanently soldered to the PCB.

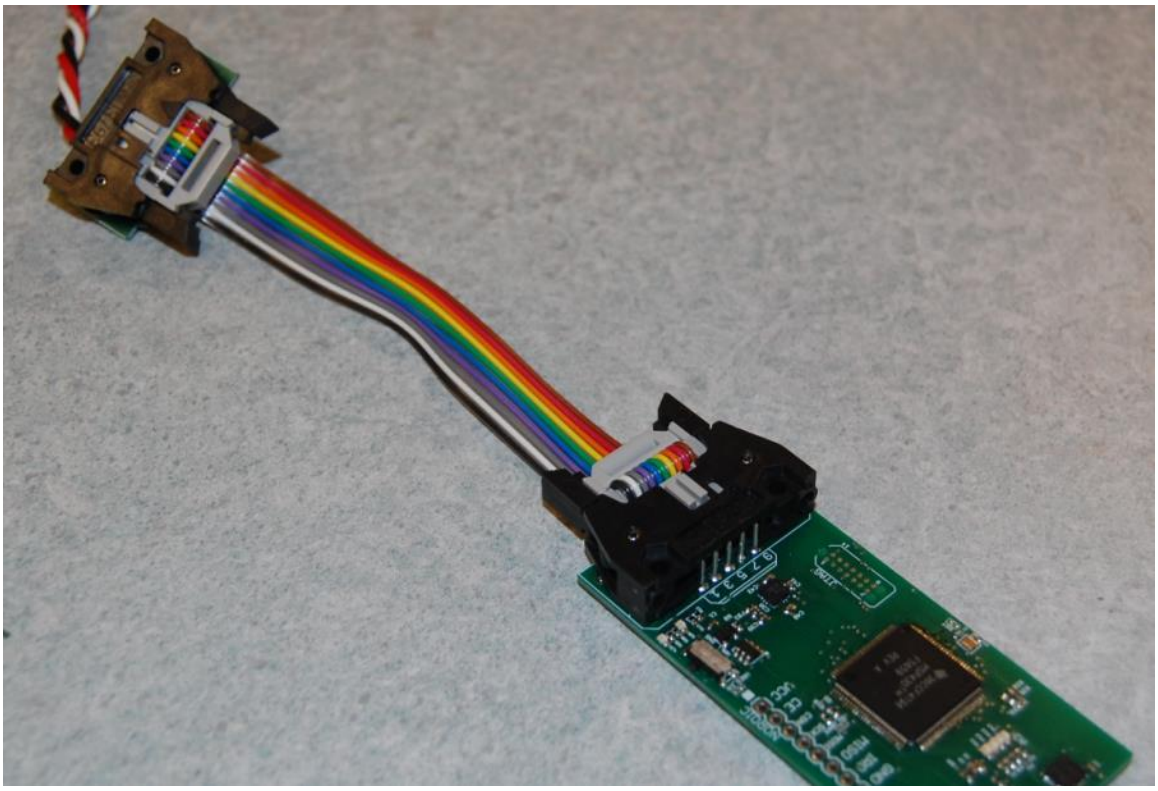

Figure 5.2. BTE_HITS_V01: First attempt at using IDC ribbon cable and latching connectors.

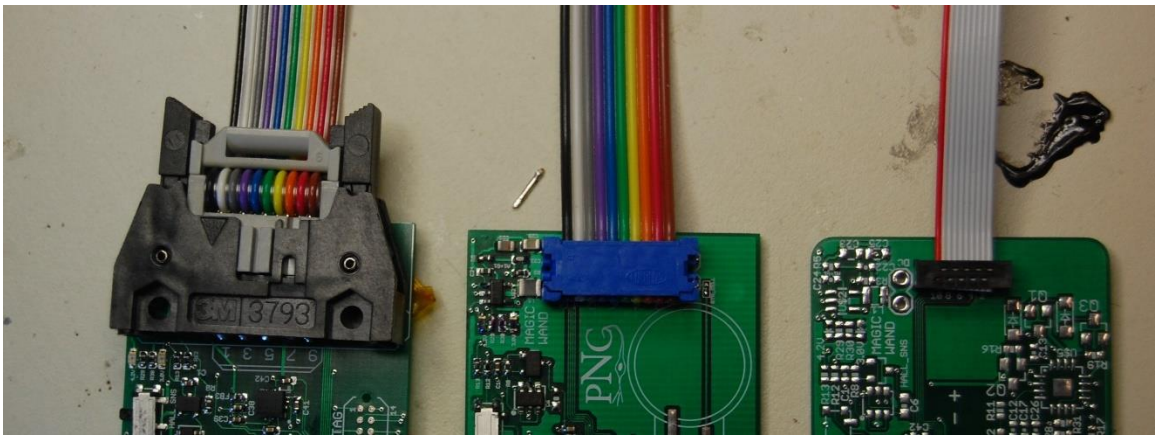

Figure 5.3. Evolution of board-to-board connectors. Left-to-right: BTE_HITS_V01, BTE_HITS_V02, BTE_HITS_V03.

The connector used in BTE_HITS_V02, while significantly smaller than that used in V01, was still bulky enough to be felt through the HITS padding – so a smaller solution was needed. The HIT System itself uses ultra-fine-pitch 0.05” DIP connectors, so research was conducted in implementing a similar solution. The HIT System’s board-to-board connectors can be seen in Figure 5.4. The connections are not very organized, and the ultra-fine-pitch connector consists of both a connector and a receptacle, and is coated in some sort of epoxy in an attempt to group the wires together.

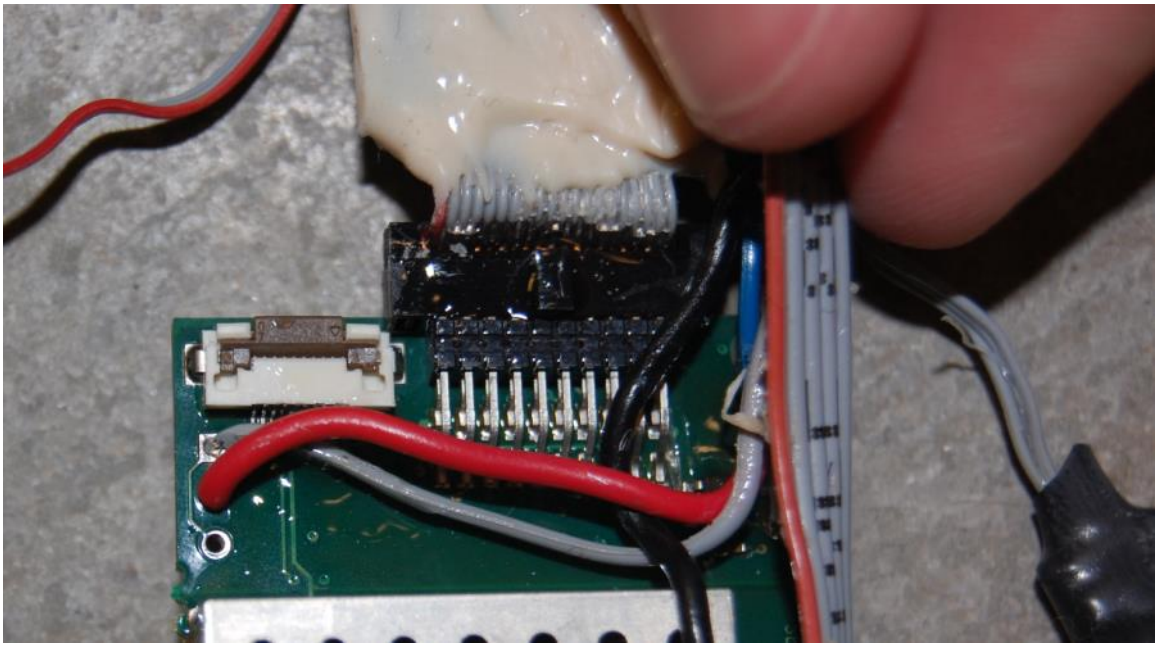

Figure 5.4. HIT System board-to-board connector solution

The BTE_HITS_V03 devices instead use an ultra-fine-pitch connector/receptacle combination similar to that used in BTE_HITS_V02, only smaller. The ultra-fine-pitch DIP connector used can be seen in Figure 5.3 along with the 0.025” pitch ribbon cable.

5.3 PCB redesign

In order to accommodate the packaging redesign, the PCB had to be completely redesigned. In a sense, this solved many of the PCB issues associated with the BTE_MICRO devices, since there was more room to work with within the HIT System

padding. The BTE_MICRO device was laid out to fit comfortably within the area of the HIT System main PCB, with the second accelerometer on a PCB the size of the capacitive sensing PCB of the HIT System.

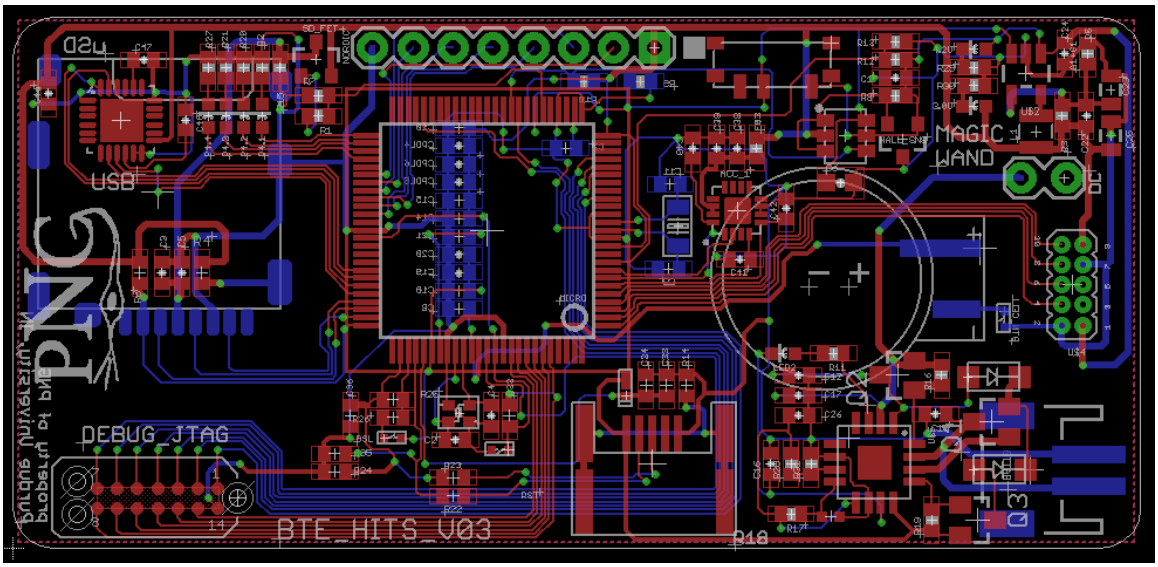

Figure 5.5. BTE_HITS_V03 – Main PCB

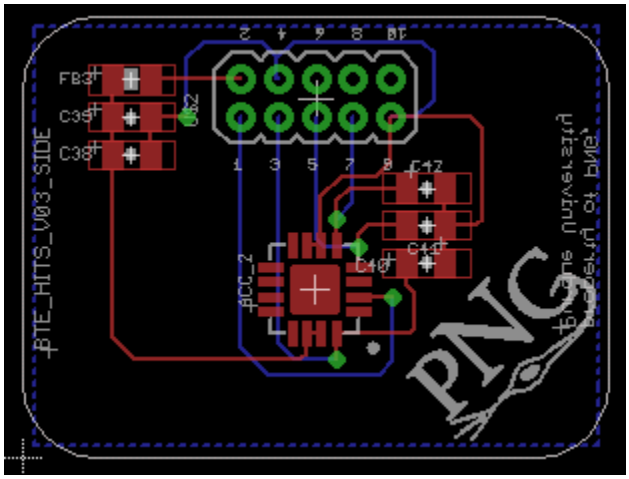

Figure 5.6. BTE_HITS_V03 – Side PCB

5.4 Device theory of operation

The BTE series of devices boasts vastly simpler operational concepts compared to the commercial devices detailed in Chapter 2. In order to achieve the goals of the PNG, in

building predictive models for brain injury, the device is initially required to record all sensor data generated over time. Thus, the device has a very simple operational model: record all data

The BTE_HITS_V03 device retains the solid-state on/off circuit of its predecessors – a simple wave of a magnetic wand over the Hall effect sensor powers the device on. Powered by a 1000mAh Li-Po battery (or Ni-Mh battery), the on-board voltage regulator converts the battery voltage to a regulated 3.0V, which powers all the sensors, the micro SD card and microcontroller. A heartbeat LED is programmed to blink for a tenth of a second, every second, to indicate when the device is on and recording data. The two accelerometers and one gyroscope are sampled at 2000Hz, and the data collected is packaged by the microcontroller and stored on a micro SD card. An 8 GB micro SD card is capable of storing up to 60 hours of continuous sensor data [40]. A 1000 mAh battery is expected to provide around 20 hours of continuous run time. A detailed power consumption analysis is performed in Section 5.5. If the device memory is running low, or the battery life is nearly depleted (less than 10% left), LEDs on-board the device will blink in specific sequences to indicate the relevant error code. BTE_HITS_V02 uses a removable battery pack, which can be charged using the standard charging station supplied as part of the HIT System. BTE_HITS_V03 has on-board charging circuitry, so it can be charged either using a direct DC connection at 1A, or via USB at 500mA.

The data recorded by the device can be downloaded by either removing the micro SD card and manually copying the files to a computer, or via USB in a similar fashion to USB 'thumb drives'.

5.5 Power consumption analysis

The majority of the components on the BTE_HITS devices are ultra-low power consumption – with the exception of the micro SD card. The micro SD card has been shown to consume up to 80mA of current during write cycles. Fortunately, the micro SD only requires 5ms to write 1 second of recorded sensor data [40] – thereby reducing the overall power consumption of the device.

Table 5.1. Estimated power consumption figures for BTE_HITS devices

Major component	Current consumption (mA)		Operating Voltage (V)	Power Consumption (mW)
	Typical	Maximum		
Texas Instruments MSP430F5659	5.00	10.00	3.00	15.00
Analog Devices ADXL377 (x2)	0.30	0.30	3.00	1.80
Invensense MPU-6000	3.60	5.00	3.00	10.80
Micro SD card (active write)	80.00	250.00	3.00	12.00
Micro SD card (standby)	2.00	2.00	3.00	0.30
Heartbeat LED (0.1s each second)	10.00	20.00	3.00	3.00
	Total Power Consumption:			42.90
	Voltage supplied by battery (V):			3.70
	Current drawn from battery (mA):			11.59
	Battery life expected (hours):			**86.25**

The power consumption analysis estimates in Table 5.1 are utilized a combination of theoretical and measured values. In reality, due to additional power consumption by passive elements, non-linear characteristics of the Li-Po/Ni-Mh battery packs and environmental variability will likely reduce the real-world battery life down to 60-70 hours. Long-term testing will be required to verify this. This battery life, while not as long as some of the commercial systems, allows for 1:1 data downloading and battery charging cycles – minimizing maintenance required for the devices. Furthermore, none of the

competing devices records data continuously – which dramatically reduces the average power consumption of competing devices.

5.6 Cost analysis

Table 5.2 outlines the major components required by the BTE_HITS devices. A component level breakdown of the device cost can be found in Appendix C.

Table 5.2. Summarized cost analysis for the BTE_HITS devices

Major component	Cost
Texas Instruments MSP430F5659	$6.18
Analog Devices ADXL377 (x2)	$11.62
Invensense MPU-6000	$5.08
8GB micro SD card	$5.38
Battery Pack	$11.95
Maxim MAX1874	$2.13
Misc Passive Components	$12.10
Total component costs:	$54.44
PCB Fabrication costs:	$10.00
Packaging costs:	$10.00
Total device cost:	**$74.44**

At approximately $75, the device components costs are significantly higher than many of the competing products' component costs – but the value of functionality in the BTE_HITS devices is also far greater than those of competing devices.

5.7 Preliminary sensor testing

In order to verify sensor data is being recorded by the device correctly, the device was testing using the HIRRT drop tower test rig. Both linear and rotational acceleration data

was collected and can be seen in the figures below. The main board accelerometer and the drop tower accelerometer both generated acceleration profiles similar to one another – both in magnitude and time. The minor discrepancies can be attributed to differences in the placement of the sensors – the drop tower places its accelerometer inside a dummy head. The side board showed considerably higher linear acceleration compared to the main board and the drop tower. This can be attributed to differences in placement as well as differences in accelerometer calibration. The performed tests further highlighted the need for a calibration routine for the accelerometers and gyroscopes, as manufacturer specifications and laboratory observations both indicate the presence of sensor drift over time.

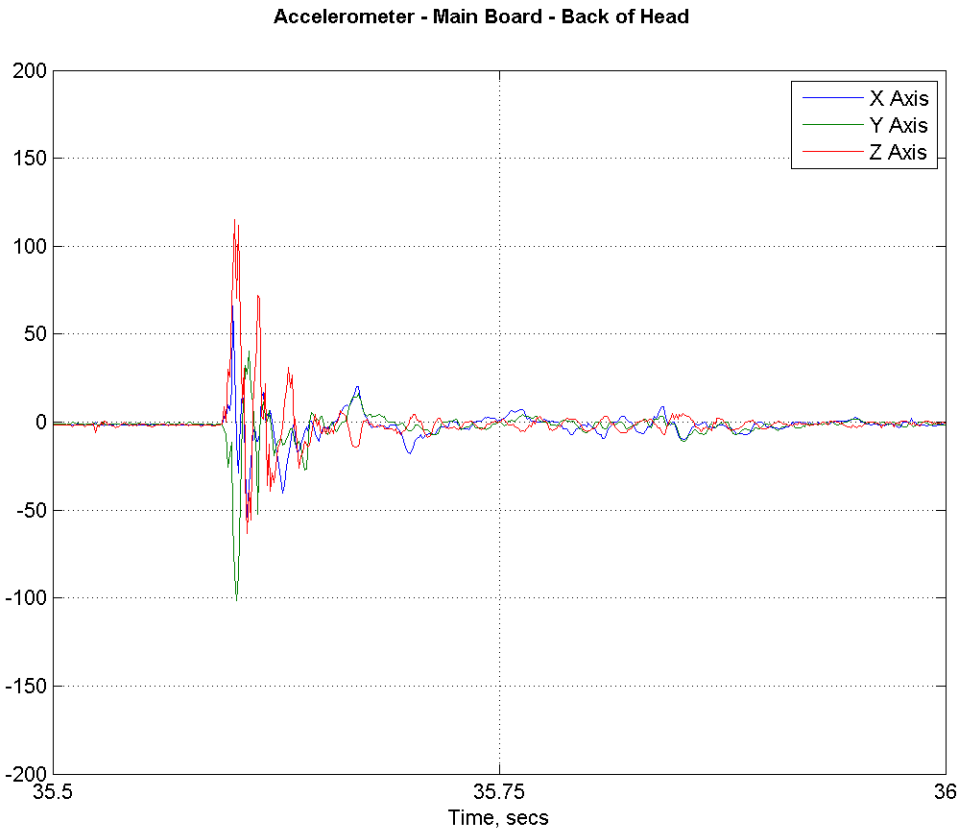

Figure 5.7. Accelerometer readout from Main Board

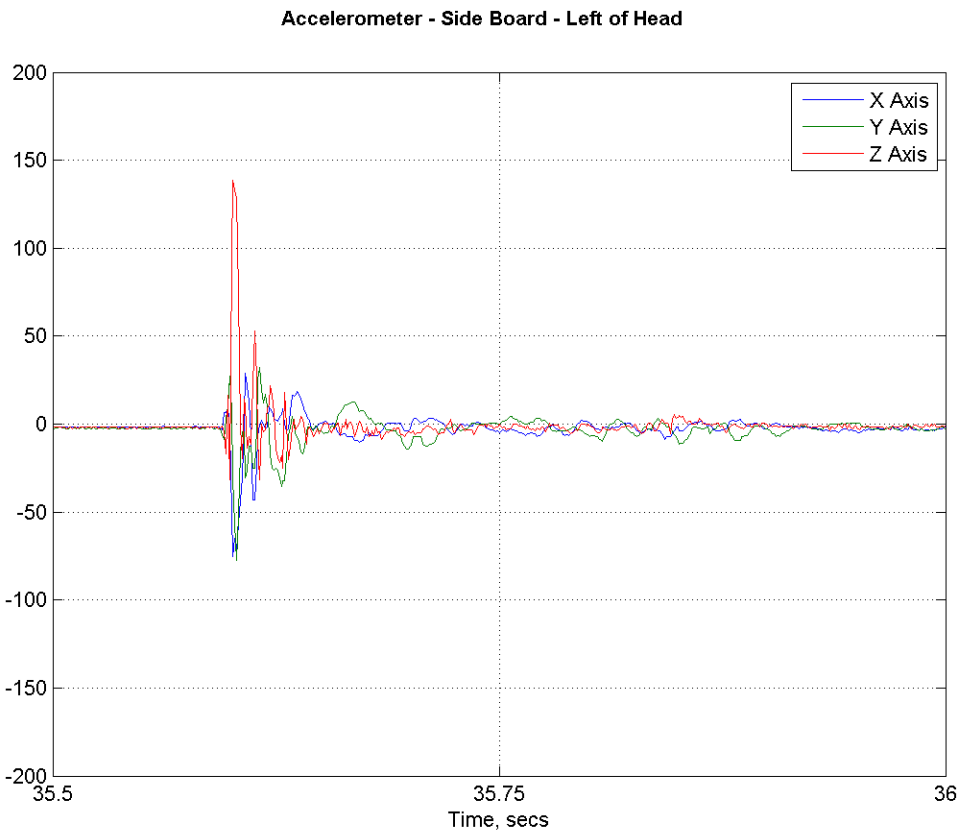

Figure 5.8. Accelerometer readout from side board

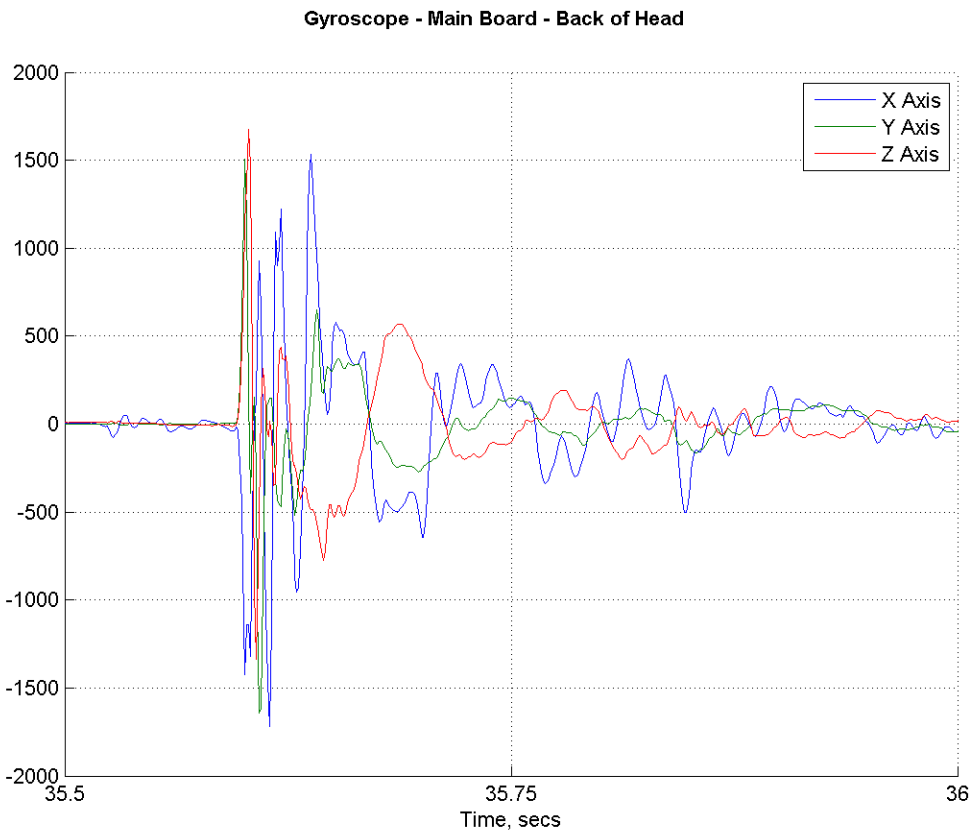

Figure 5.9. Gyroscope readout from Main Board

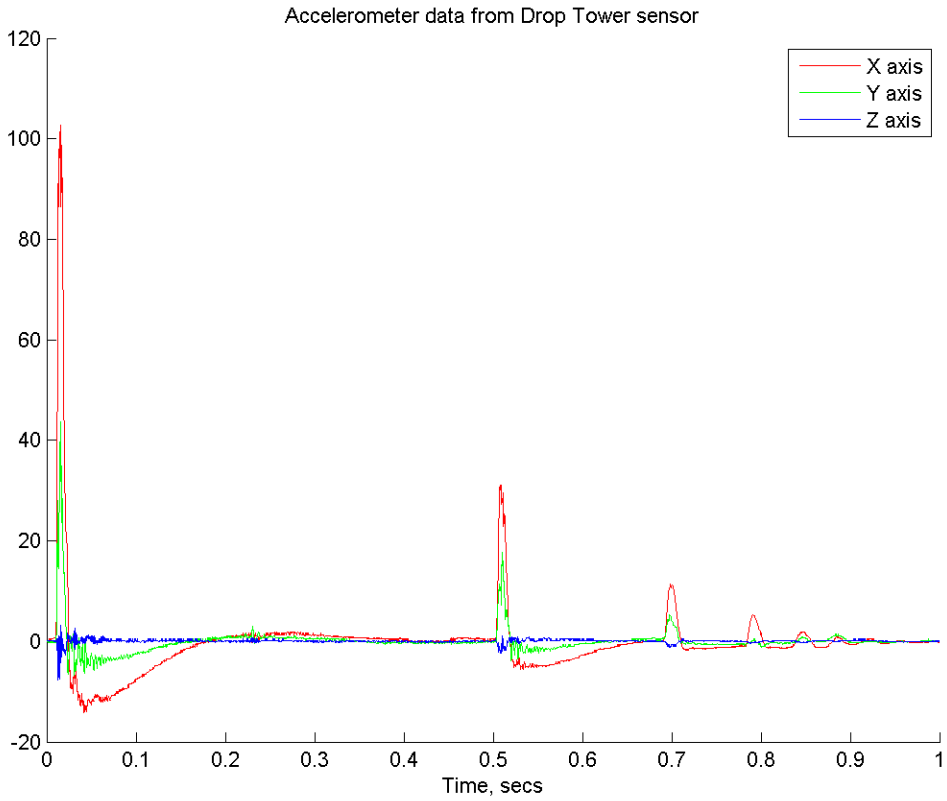

Figure 5.10. Accelerometer readout from drop tower sensor

5.8 Future platform expansion capabilities

Several design features were added to the BTE_HITS_V03 hardware design to ensure that development can continue and product functionality can continue to expand.

5.8.1 Programming footprint and debug bridge redesign

One of the drawbacks associated with the original programming footprint design is that the addition of 7 debugging signals in addition to the original 7 programming signals led to a complex PCB layout around the Tag-Connect programming footprint, due to the TI specified pin-out for the programming header, shown in Figure 5.11.

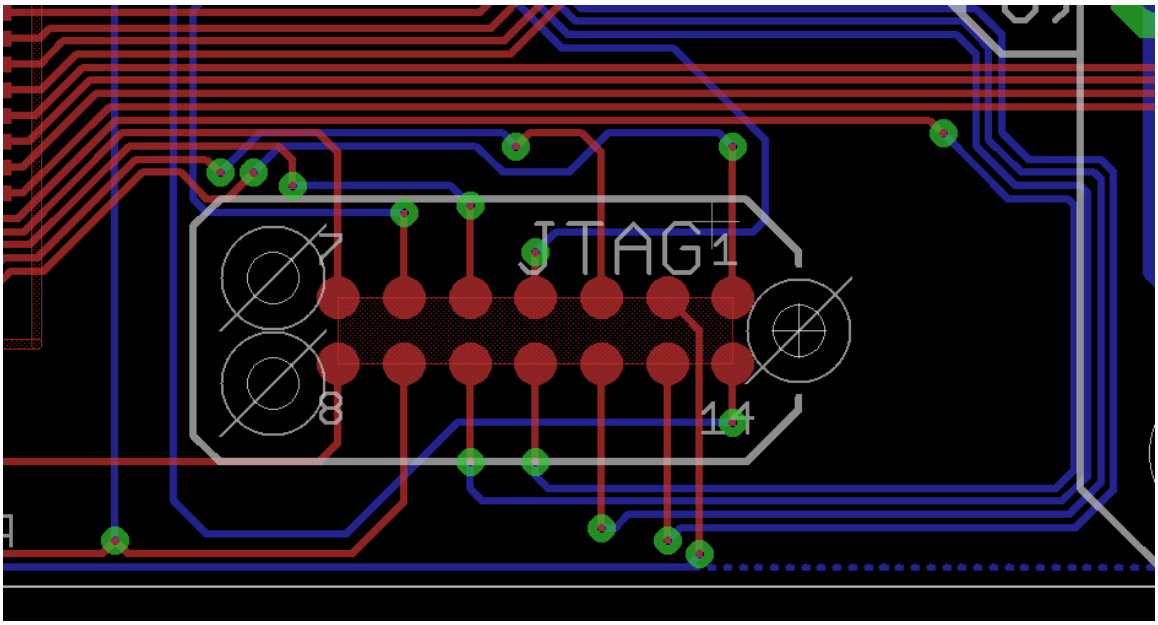

Figure 5.11. Old programming footprint PCB layout

In order to simplify the PCB layout for the BTE_HITS devices, and to increase flexibility in the placement of the Tag-Connect footprint, the pin assignment was completely reassigned. The specific pin reassignments can be found in Appendix D. The improved, cleaner layout can be seen in Figure 5.12. The new layout and pin assignment will make it much easier to alter the placement of the programming footprint in any future board redesigns.

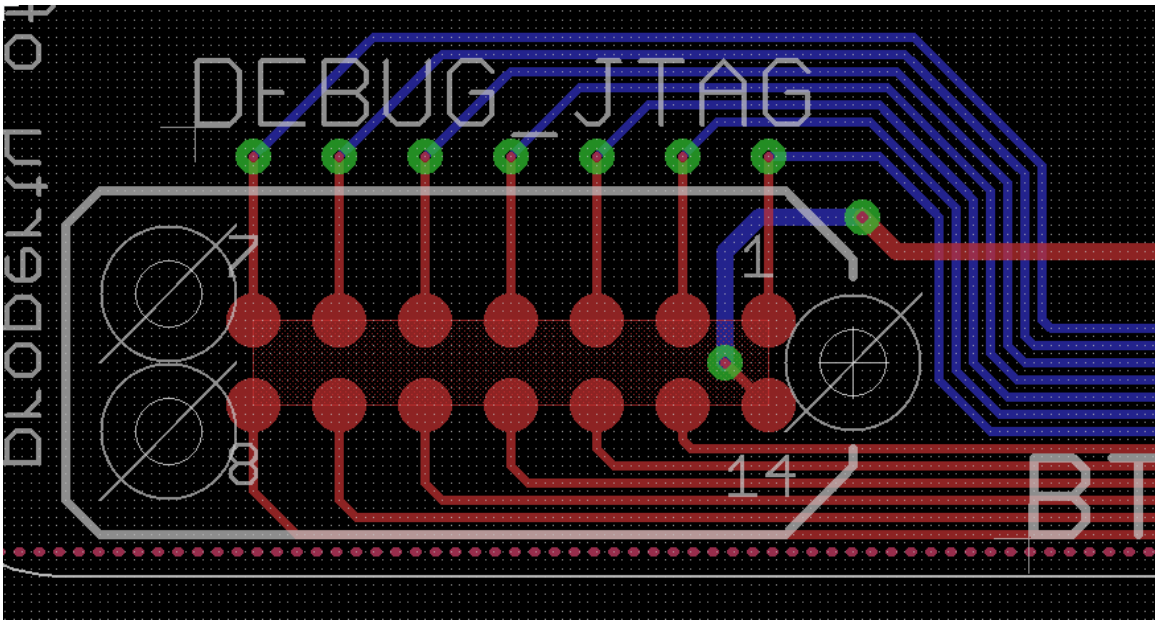

Figure 5.12. BTE_HITS programming footprint

In addition to revising the programming footprint on the main PCB, the connector on the debug bridge PCB was also revised to accommodate the new pin assignments. The debug bridge PCB was also redesigned to provide a more 'in-line' experience and to include the ability to function independently, without the in-circuit programmer attached. This allows the debug bridge to be used in the field to display error codes. This will prove to be useful during initial device deployment – device users can simply attach the debug bridge to the device to diagnose potential malfunctions or errors.

Figure 5.13. BTE_HITS debug bridge

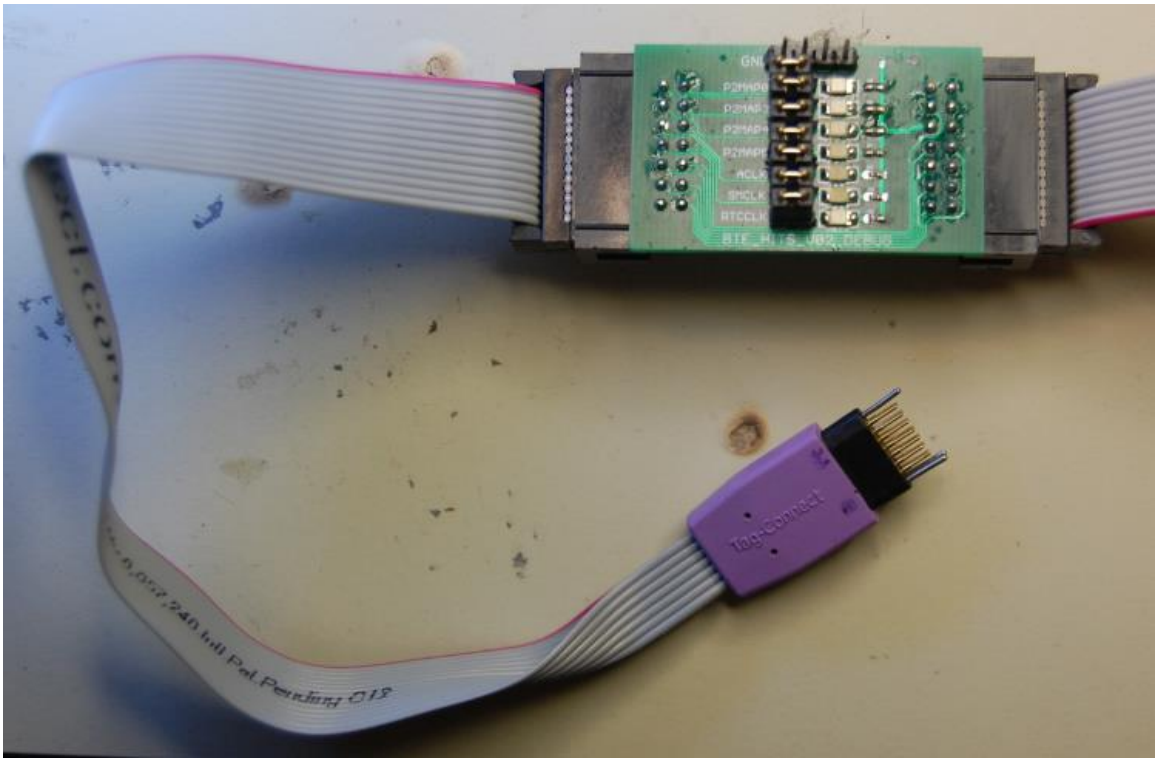

Figure 5.14. BTE_HITS debug bridge and Tag-Connect cable

5.8.2 Real-time clock circuit

Due to the large amounts of data generated by the sensors sampling data at 2000Hz and multiple devices deployed at once, it is imperative to devise a method of determining the temporal details of all the data collected, so that the data may be synchronized and interactions between players acceleration events can be studied in detail.

The most straight-forward solution to this is to add a time-stamp to each sample of sensor data collected. In order to preserve time-stamp consistency across multiple devices and activity sessions, the devices must be able to keep time even when they are powered off. This is typically achieved in embedded systems using a real-time clock (RTC) module or circuit. The TI MSP430F5659 microcontroller has an on-board RTC module, which requires an external power supply to keep the RTC module powered even when the device's battery is removed. A 3V 47mAh sealed button cell was selected, and based on the current consumption specifications for the RTC module, can maintain an accurate clock on the device for up to 7 years.

5.8.3 Wireless data transfer and analysis

A significant issue with the current line of BTE_HITS devices is that the data is stored on-board. While this offers many advantages in terms of device simplicity, low power consumption and reduced cost, it also means that the data collected cannot be reviewed till after-the-fact. This dramatically reduces the devices efficacy in both research and commercial settings. In a research setting, the ability to view the data generated by the sensors in real-time allows researchers to observe the players both visually and in terms of the sensor data – enabling researchers to correlate what they see with what the devices observe and ensure the relationship between the two is accurate. With consumers, particularly once the real-time predictive models are developed, it is imperative that any 'red-flags' determined by the predictive models be conveyed to the user as soon as possible, so that players may be removed from gameplay for assessment as soon as possible, and reducing the potential for further damage. It both settings, and particularly when a large number of devices are deployed simultaneously, it is also necessary to know parameters such as device status, battery life remaining and flash storage remaining. By using wireless transceivers, the devices will be able to transmit the necessary information to the sidelines for analysis by researchers and commercial users alike. In the interest of reducing overall research and development time, a 'bolt-on' wireless solution was designed, and the wireless development was divided into two stages: (1) adding basic device health monitoring (battery life, storage capacity) and (2) adding real-time sensor data streaming to the sidelines. Data streamed to the sidelines can then be analyzed by computers, which are more efficient at processing intensive tasks.

The 'bolt-on' wireless solution for the BTE_HITS devices comes in the form of a wireless 'breakout board' based on the Nordic nRF24L01+ transceiver. At the time of writing wireless development has begun its initial stages, but the BTE_HITS PCB has all the necessary connections required, as shown in Figure 5.15. The transceiver breakout board sits flush on top of the existing PCB, and minimal modifications to the packaging will be required to accommodate the transceiver board, as shown in Figure 5.16.

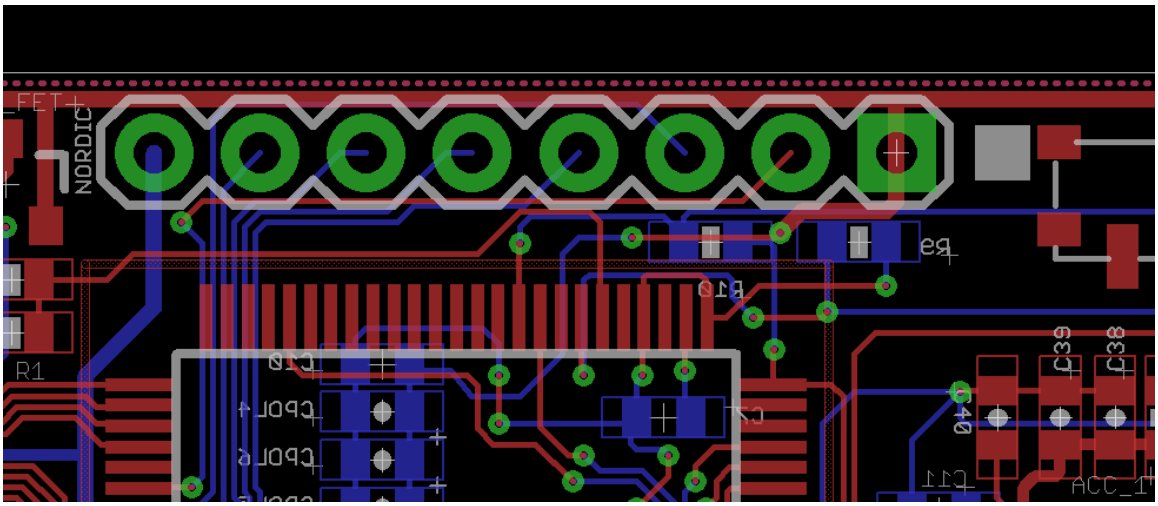

Figure 5.15. Nordic connections available for ‘bolt-on’ wireless solution

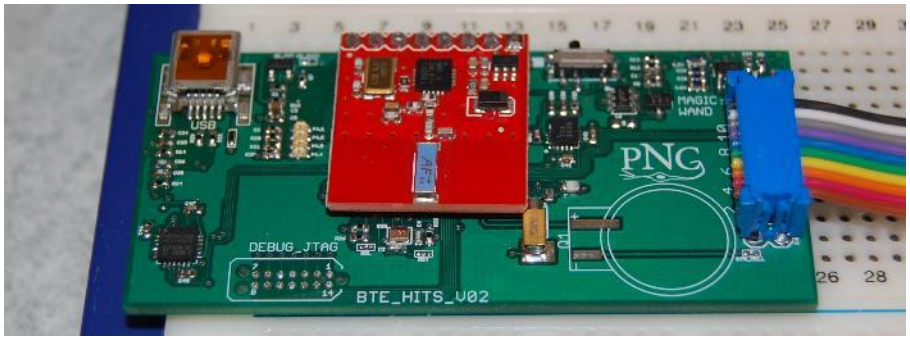

Figure 5.16. Nordic breakout board (red) attached to BTE_HITS_V02

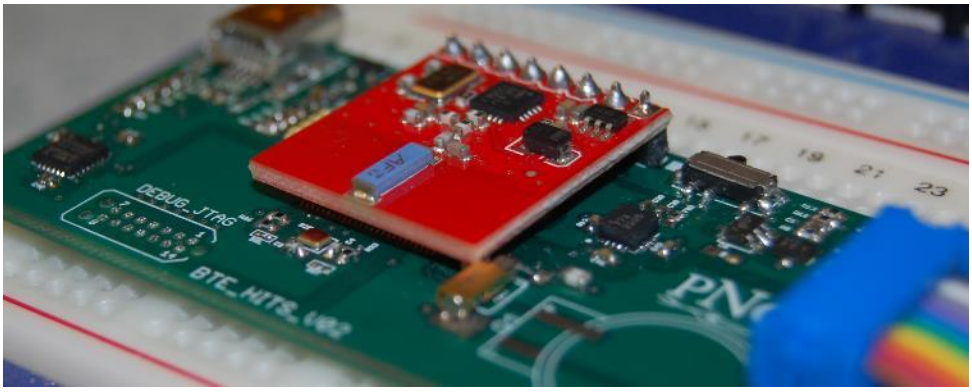

Figure 5.17. Nordic breakout (red) attached toBTE_HITS_V02

6. CONCLUSION

6.1 Summary

This document aimed to detail the specifications and operation of various commercial telemetry platforms typically used by contact sport athletes. Previous efforts by the PNG in developing such a platform was also discussed. Design criteria for the second major product development cycle were presented, followed by design approaches and methods used, along with lessons learned from those approaches. The document was concluded with a detailed discussion on the latest, low-cost, low-power platform developed, the BTE_HITS series of devices. Preliminary data generated from drop testing the devices were also presented.

6.2 Future work

Majority of the future work on the BTE platform will focus on adding wireless functionality as discussed in Chapter 5. Additional wireless development opportunities include adding interrupt-based wireless on/off functionality, real-time player localization, and high-throughput data streaming using mesh networks.

With additional development, the PCB design can be converted into a 4-layer design, which is expected to provide a 30-35% reduction in PCB size. The transition from FR4 fiberglass PCB substrate to polyamide based flexible PCBs will also allow for more flexibility in device packaging design.

Development efforts will also need to be channeled into developing a complete suite of support software for the device platform, both on mobile devices and personal computers. This will allow researchers and commercial users to analyze the large amounts of data generated by the devices more efficiently.

LIST OF REFERENCES

LIST OF REFERENCES

[1] "About Us." [Online]. Available: http://www.popwarner.com/About_Us.htm. [Accessed: 11-Mar-2014].

[2] "Pop Warner-NFL 'Heads Up Football' Partnership."[Online]. Available: http://www.popwarner.com/About_Us/Pop_Warner_News/nfl_heads_up_partnership_s1_p4300.htm. [Accessed: 11-Mar-2014].

[3] "NIH and NFL tackle concussion research." [Online]. Available: http://www.nih.gov/news/health/dec2013/ninds-16.htm. [Accessed: 11-Mar-2014].

[4] J. A. Langlois, W. Rutland-Brown, and M. M. Wald, "The epidemiology and impact of traumatic brain injury: a brief overview," *J. Head Trauma Rehabil.*, vol. 21, no. 5, pp. 375–378, Oct. 2006.

[5] J. L. Gerberding and S. Binder, "Report to Congress on Mild Traumatic Brain Injury in the United States: Steps to Prevent a Serious Public Health Problem." Centers for Disease Control and Prevention, 2003.

[6] T. M. Talavage, E. A. Nauman, E. L. Breedlove, U. Yoruk, A. E. Dye, K. E. Morigaki, H. Feuer, and L. J. Leverenz, "Functionally-Detected Cognitive Impairment in High School Football Players without Clinically-Diagnosed Concussion," *J. Neurotrauma*, vol. 31, no. 4, pp. 327–338, Feb. 2014.

[7] A. C. McKee, R. C. Cantu, C. J. Nowinski, E. T. Hedley-Whyte, B. E. Gavett, A. E. Budson, V. E. Santini, H.-S. Lee, C. A. Kubilus, and R. A. Stern, "Chronic traumatic encephalopathy in athletes: progressive tauopathy after repetitive head injury," *J. Neuropathol. Exp. Neurol.*, vol. 68, no. 7, pp. 709–735, Jul. 2009.

[8] R. Jadischke, D. C. Viano, N. Dau, A. I. King, and J. McCarthy, "On the accuracy of the Head Impact Telemetry (HIT) System used in football helmets," *J. Biomech.*, vol. 46, no. 13, pp. 2310–2315, Sep. 2013.

[9] M. A. Allison, Y. S. Kang, J. H. Bolte, M. R. Maltese, and K. B. Arbogast, "Validation of a Helmet-Based System to Measure Head Impact Biomechanics in Ice Hockey:," *Med. Sci. Sports Exerc.*, vol. 46, no. 1, pp. 115–123, Jan. 2014.

[10] M. A. McCaffrey, J. P. Mihalik, D. H. Crowell, E. W. Shields, and K. M. Guskiewicz, "Measurement of head impacts in collegiate football players: clinical measures of concussion after high- and low-magnitude impacts," *Neurosurgery*, vol. 61, no. 6, pp. 1236–1243; discussion 1243, Dec. 2007.

[11] K. M. Guskiewicz, J. P. Mihalik, V. Shankar, S. W. Marshall, D. H. Crowell, S. M. Oliaro, M. F. Ciocca, and D. N. Hooker, "Measurement of head impacts in collegiate football players: relationship between head impact biomechanics and acute clinical outcome after concussion," *Neurosurgery*, vol. 61, no. 6, pp. 1244–1252; discussion 1252–1253, Dec. 2007.

[12] T. M. Talavage, "Interview with Tom Talavage: Real-Time Telemetry-Based Modeling for Minimization of Head Injury Risk," 11-Feb-2014.

[13] O. C. Ibe, *Fundamentals of applied probability and random processes*. Burlington, MA; London: Elsevier Academic Press, 2005.

[14] E. L. Breedlove, M. Robinson, T. M. Talavage, K. E. Morigaki, U. Yoruk, K. O'Keefe, J. King, L. J. Leverenz, J. W. Gilger, and E. A. Nauman, "Biomechanical correlates of symptomatic and asymptomatic neurophysiological impairment in high school football," *J. Biomech.*, vol. 45, no. 7, pp. 1265–1272, Apr. 2012.

[15] R. M. Greenwald, J. T. Gwin, J. J. Chu, and J. J. Crisco, "Head Impact Severity Measures for Evaluating Mild Traumatic Brain Injury Risk Exposure," *Neurosurgery*, vol. 62, no. 4, pp. 789–798, Apr. 2008.

[16] "Simbex: HIT System." [Online]. Available: http://www.simbex.com/hit-system.html. [Accessed: 14-Mar-2014].

[17] "History - Riddell." [Online]. Available: http://www.riddell.com/history. [Accessed: 14-Mar-2014].

[18] "ADXL193 datasheet and product info | Single-Axis, High-g, iMEMS® Accelerometers | MEMS Inertial Sensors | Analog Devices." [Online]. Available: http://www.analog.com/en/mems-sensors/mems-inertial-sensors/adxl193/products/product.html. [Accessed: 14-Mar-2014].

[19] "MSP430 Ultra-Low Power 16-bit MCUs - 1 Series - MSP430F148 - TI.com." [Online]. Available: http://www.ti.com/product/msp430f148. [Accessed: 15-Mar-2014].

[20] Semtech Corporation, *XE1203F 433 MHz / 868 MHz / 915 MHz Low-Power, Integrated UHF Transceiver*. .

[21] J. R. Funk, S. M. Duma, S. J. Manoogian, and S. Rowson, "Biomechanical risk estimates for mild traumatic brain injury," *Annu. Proc. Assoc. Adv. Automot. Med. Assoc. Adv. Automot. Med.*, vol. 51, pp. 343–361, 2007.

[22] “43645-0300 Molex | Mouser,” *Mouser Electronics*. [Online]. Available: http://www.mouser.com/Search/ProductDetail.aspx?R=43645-0300virtualkey53810000virtualkey538-43645-0300. [Accessed: 15-Mar-2014].

[23] “43030-0007 Molex | Mouser,” *Mouser Electronics*. [Online]. Available: http://www.mouser.com/Search/ProductDetail.aspx?R=43030-0007virtualkey53810000virtualkey538-43030-0007. [Accessed: 15-Mar-2014].

[24] A. A. Mohamad, “Degradation in polymer Ni-MH battery,” *Ionics*, vol. 11, no. 3–4, pp. 294–300, May 2005.

[25] “Simbex Press Release.” [Online]. Available: http://www.simbex.com/about/pressReleases/20090319-LCAS.html. [Accessed: 15-Mar-2014].

[26] “Tracking HITS | Georgia Southern Magazine.” [Online]. Available: http://news.georgiasouthern.edu/magazine/2013/12/12/tracking-hits/. [Accessed: 15-Mar-2014].

[27] “OU: The Program -- Sensory overload,” *ESPN.com*. [Online]. Available: http://sports.espn.go.com/ncf/news/story?id=1919482. [Accessed: 15-Mar-2014].

[28] E. A. Nauman, “Rotational vs. Linear acceleration calculation limitations of the Simbex HIT System,” 12-Mar-2014.

[29] E. J. Pellman, D. C. Viano, A. M. Tucker, and I. R. Casson, “Concussion in Professional Football: Location and Direction of Helmet Impacts—Part 2,” *Neurosurgery*, vol. 53, no. 6, 2003.

[30] *Front Rowe: Week 5*. .

[31] “About,” *Impact Detectors. Accurate, Low Cost, Easy To Read - Brain Sentry*. .

[32] “H3LIS331DL MEMS motion sensor: low power high g 3-axis digital accelerometer - STMicroelectronics.” [Online]. Available: http://www.st.com/web/en/catalog/sense_power/FM89/FM89/SC444/PF253712. [Accessed: 15-Mar-2014].

[33] “MSP430 Ultra-Low Power 16-bit MCUs - Value Line - MSP430G2553 - TI.com.” [Online]. Available: http://www.ti.com/product/msp430g2553. [Accessed: 15-Mar-2014].

[34] S. Foreman and D. B. Crossman, “A Comparative Analysis for the Measurement of Head Accelerations in Ice Hockey Helmets using Non-Accelerometer Based Systems,” presented at the ASTM Concussion Mechanisms Symposium, 2013.

[35] BlueGiga, *WT11i_Datasheet.pdf*. .

[36] “ATxmega256A3BU.” [Online]. Available: http://www.atmel.com/devices/atxmega256a3bu.aspx. [Accessed: 16-Mar-2014].

[37] “Interview with Eric Nauman: On the Resonant Frequency of the Human Head.”

[38] Zakrajsek, Anne Dye, “Design of Micro- and Macro-scale Impact Mitigating Material Toward the Development of Helmet Padding Design Criteria,” Master’s, Purdue University, West Lafayette, Indiana, 2011.

[39] “ADXL377 datasheet and product info | 3-Axis High g Analog MEMS Accelerometer | MEMS Accelerometers | Analog Devices.” [Online]. Available: http://www.analog.com/en/mems-sensors/mems-accelerometers/adxl377/products/product.html. [Accessed: 17-Mar-2014].

[40] B. B. Gardner, “Developing an Embedded System Solution for High-speed, High-capacity Data Logging for a Size-constrained, Low-power, Biomechanical Telemetry System and Investigating Components for Optimal Performance,” Master’s, Purdue University, West Lafayette, Indiana, 2014.

[41] T. Instruments, *MSP430F665x, MSP430F645x, MSP430F565x, MSP430F535x Mixed Signal Microcontrollers*. .

[42] Toshiba Semiconductors, “TCS20DLR | Products | TOSHIBA Semiconductor & Storage Products Company.” [Online]. Available: http://www.semicon.toshiba.co.jp/info/lookup.jsp?pid=TCS20DLR&lang=en. [Accessed: 18-Mar-2014].

[43] Fairchild Semiconductor, “NDC7003P PDF Datasheet Dual P-Channel Enhancement Mode Field Effect Transistor.” [Online]. Available: http://www.fairchildsemi.com/pf/ND/NDC7003P.html. [Accessed: 18-Mar-2014].

[44] “Converter (Integrated Switch) - Step-Down (Buck) Converter - LM3673 - TI.com.” [Online]. Available: http://www.ti.com/product/lm3673. [Accessed: 18-Mar-2014].

APPENDICES

A. HARDWARE DESIGN ROADMAP

This appendix contains the proposed hardware design roadmap for the summer of 2013. Also included are the PCB schematic and layout for BBTE_FIX_V01, the initial large form-factor test platform. All schematics and layouts were generated using Cadsoft EAGLE 6.4.0 Professional unless otherwise noted. All schematic and layout files are versioned and stored in the PNG BTEv2 PCB repository.

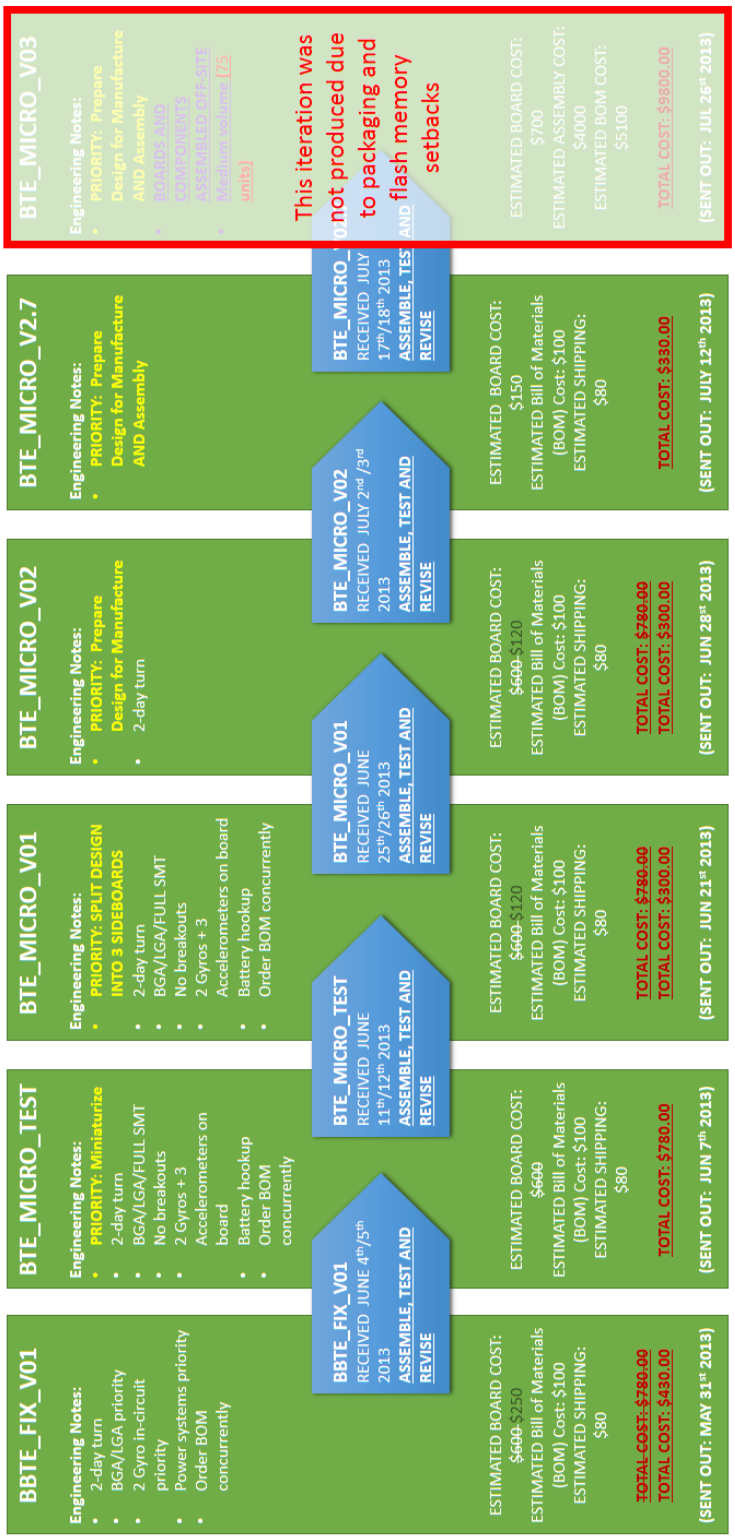

Figure A.1. Proposed hardware design roadmap

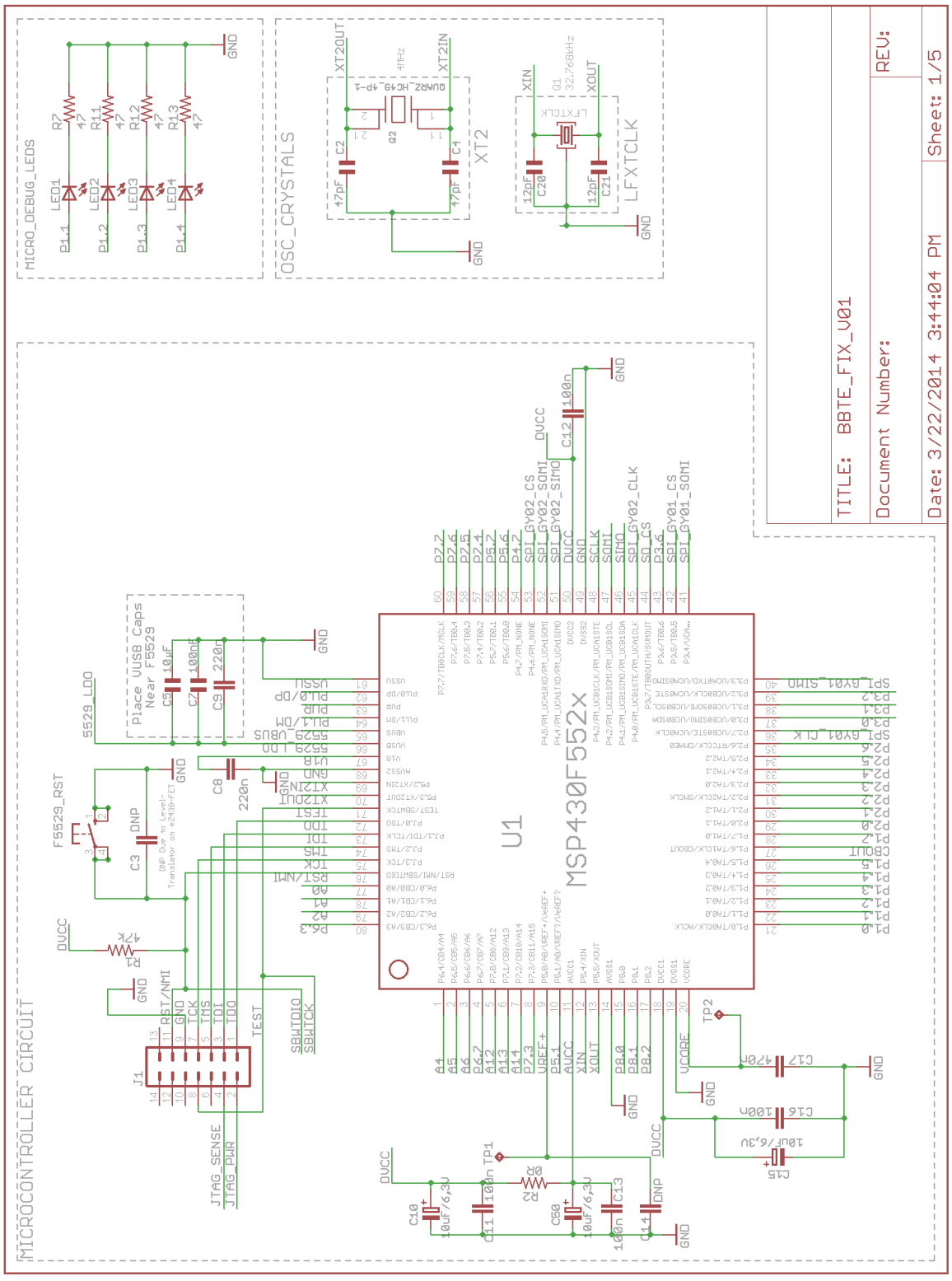

Figure A.2. Microcontroller schematic for BBTE_FIX_V01

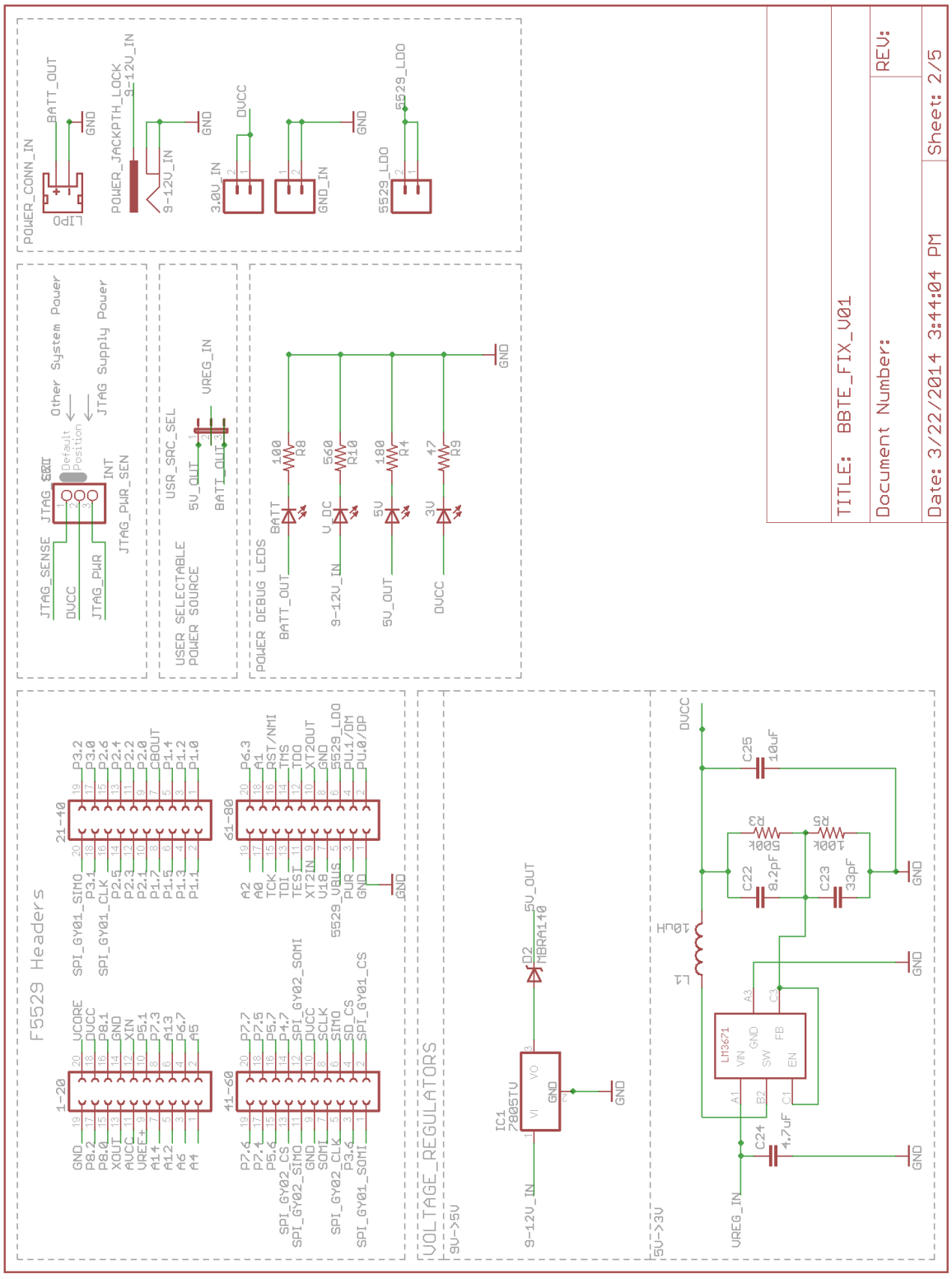

Figure A.3. Power circuit schematic for BBTE_FIX_V01

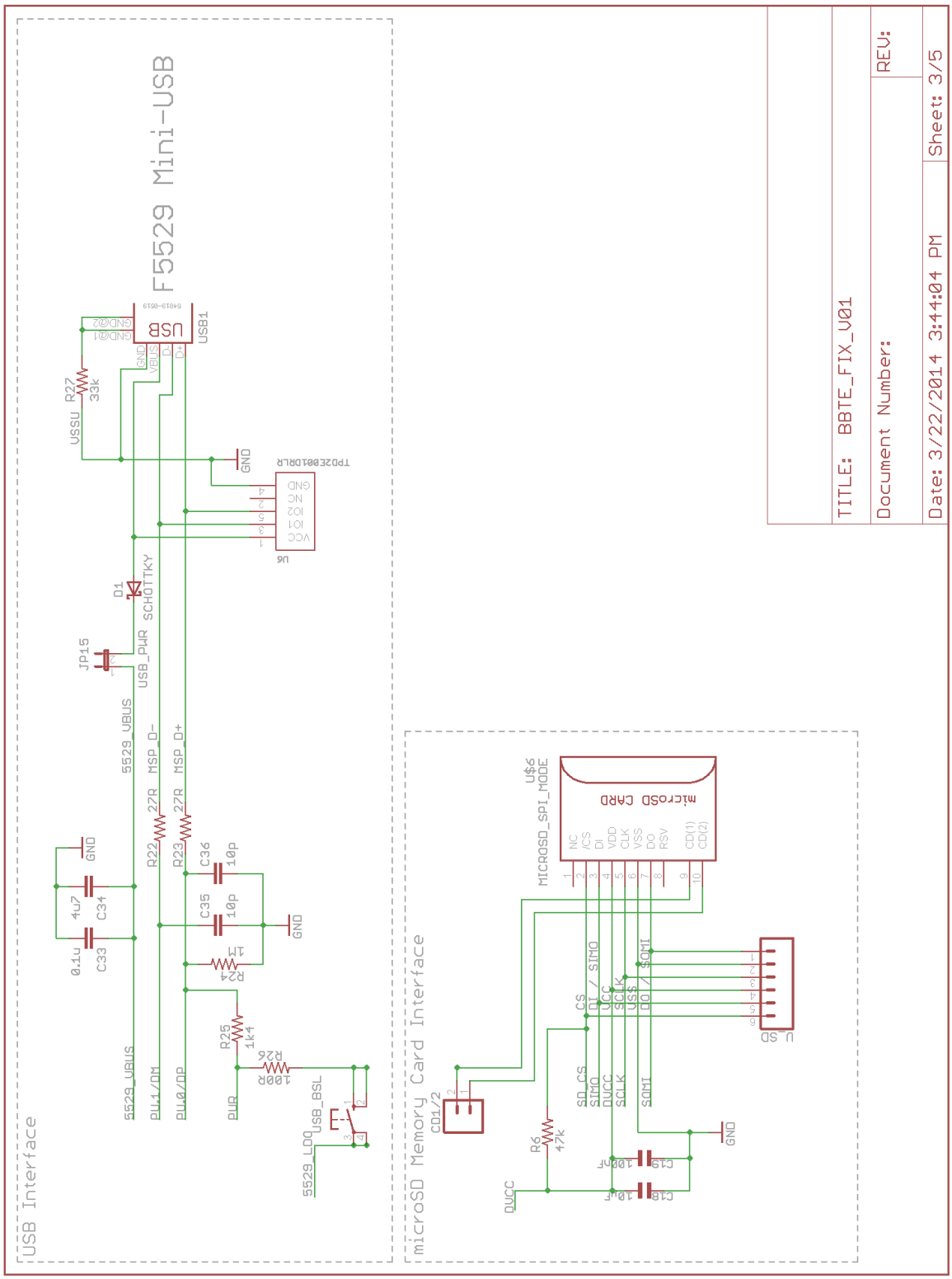

Figure A.4. USB and micro SD interface schematic for BBTE_FIX_V01

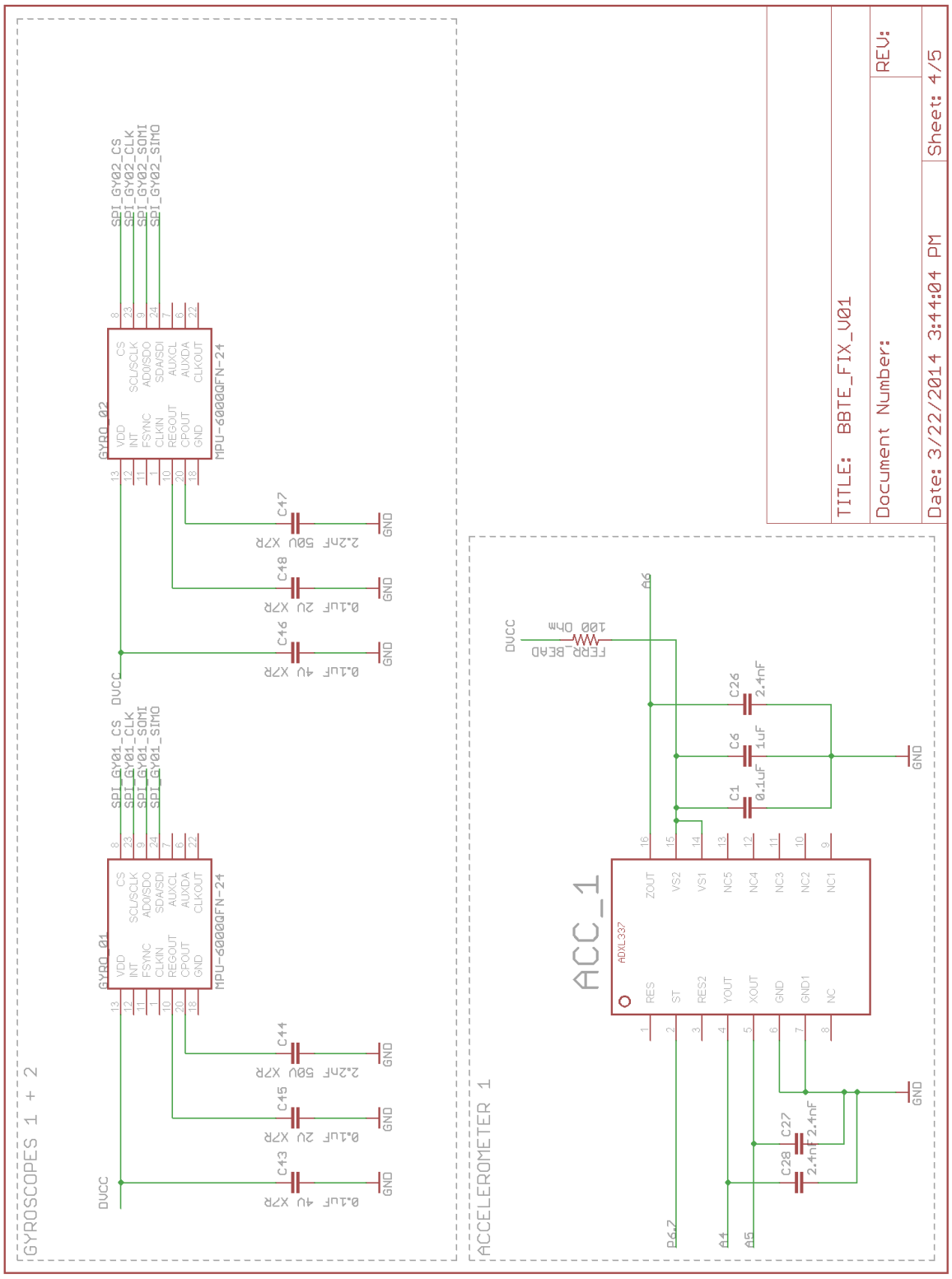

Figure A.5. Accelerometer and gyroscope schematic for BBTE_FIX_V01

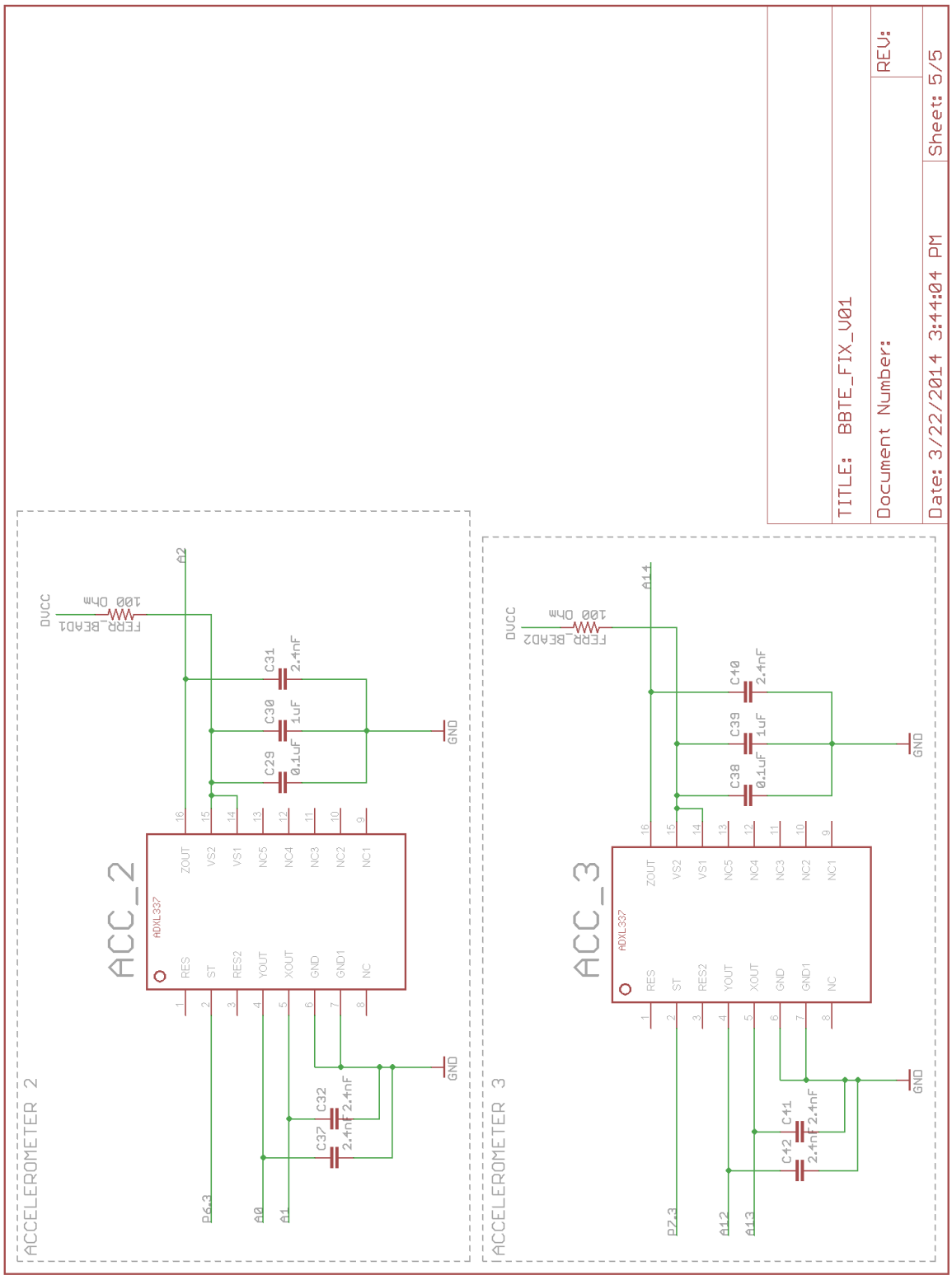

Figure A.6. Accelerometer schematic for BBTE_FIX_V01

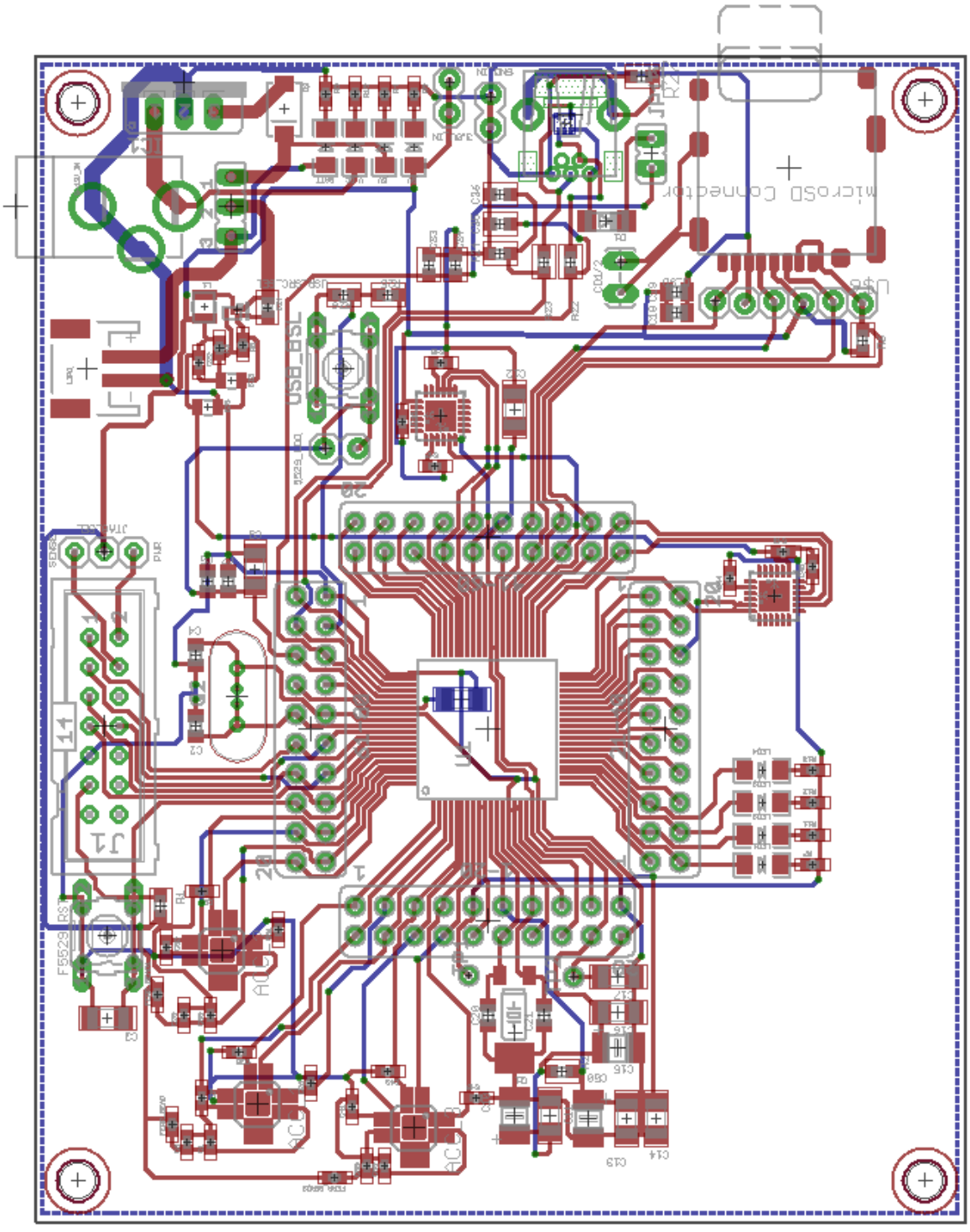

Figure A.7. BBTE_FIX_V01 PCB – top and bottom copper

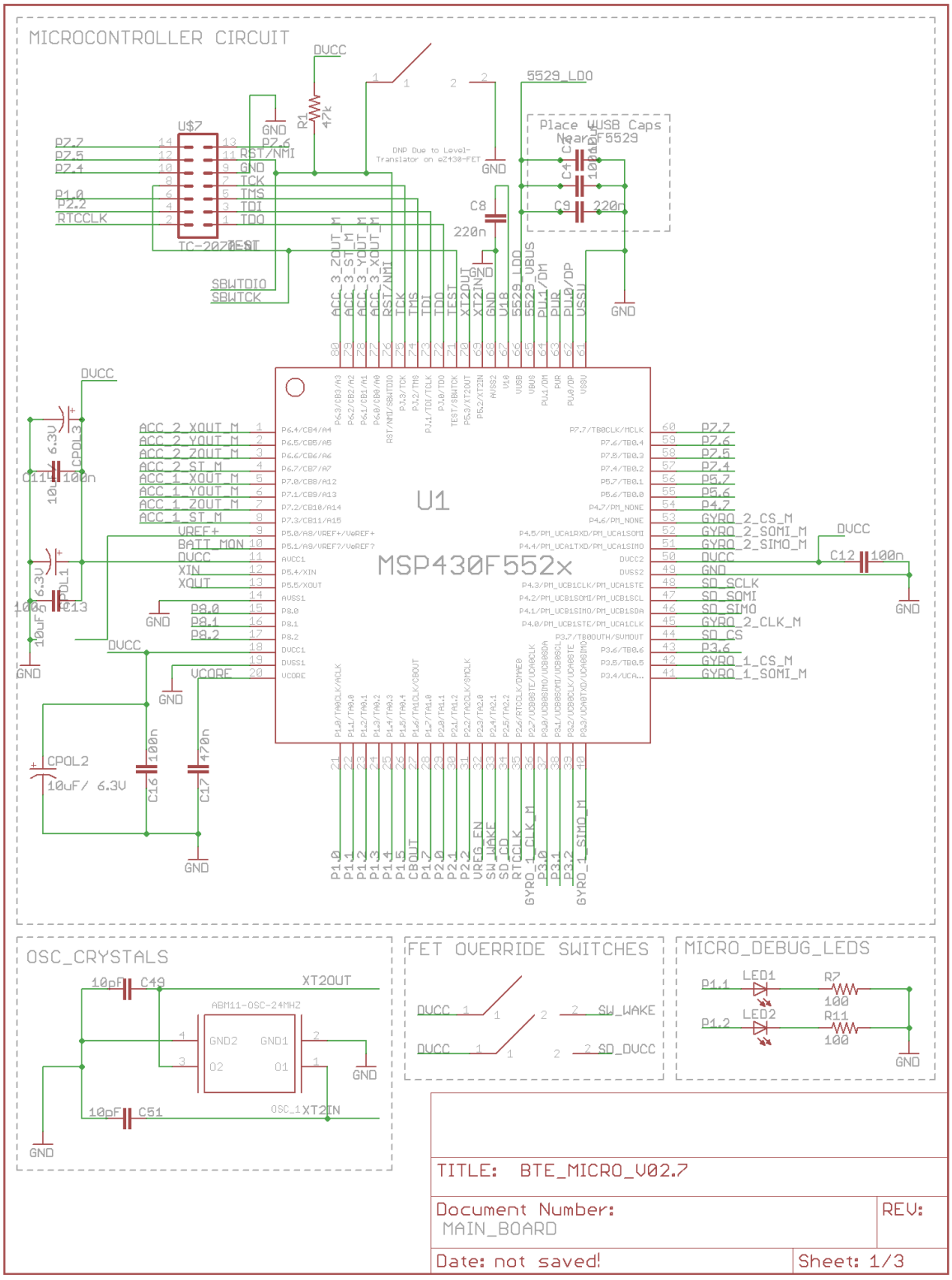

Figure A.8. BTE_MICRO_V2.7 Main PCB

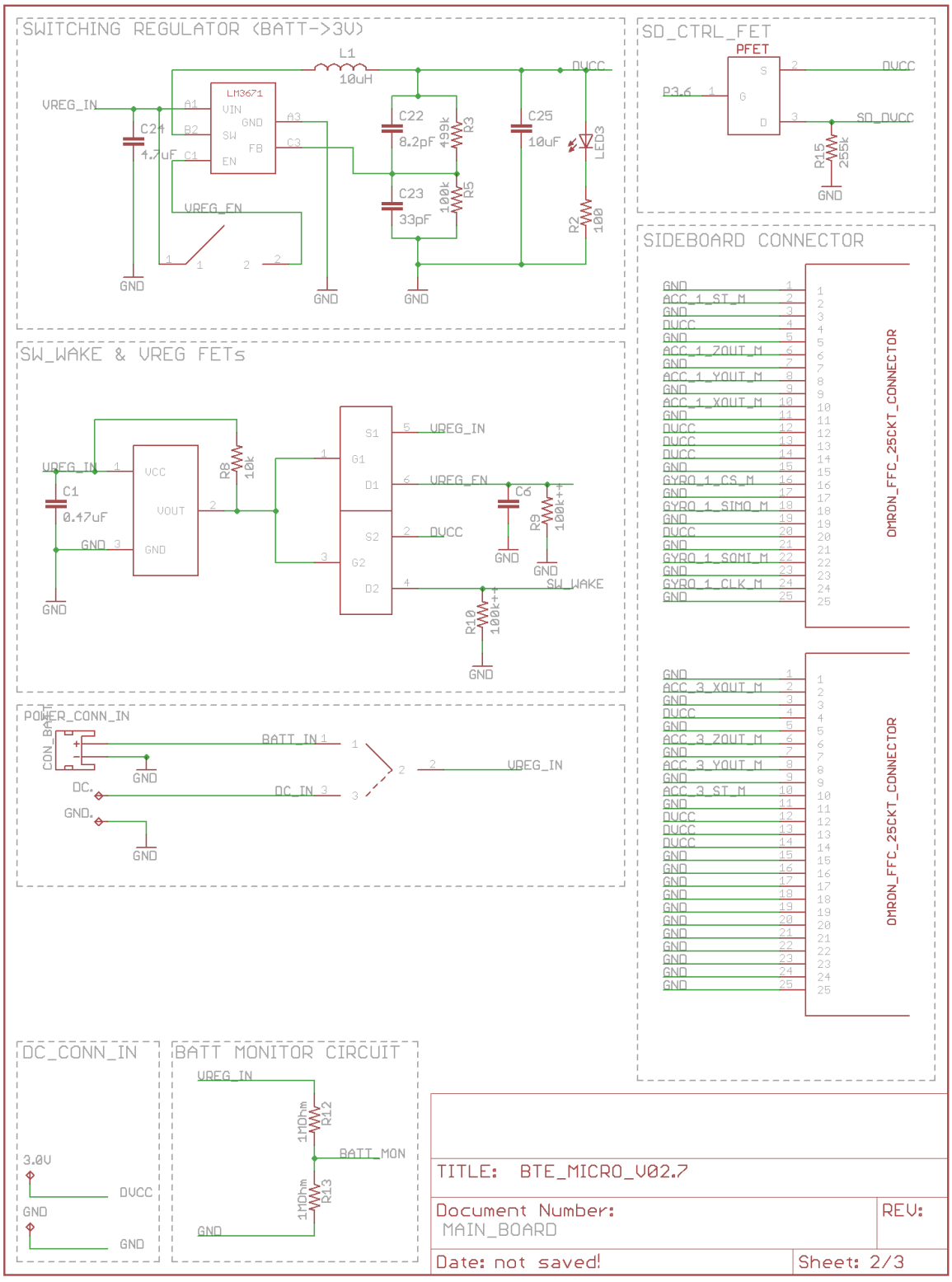

Figure A.9. BTE_MICRO_V2.7 Main PCB

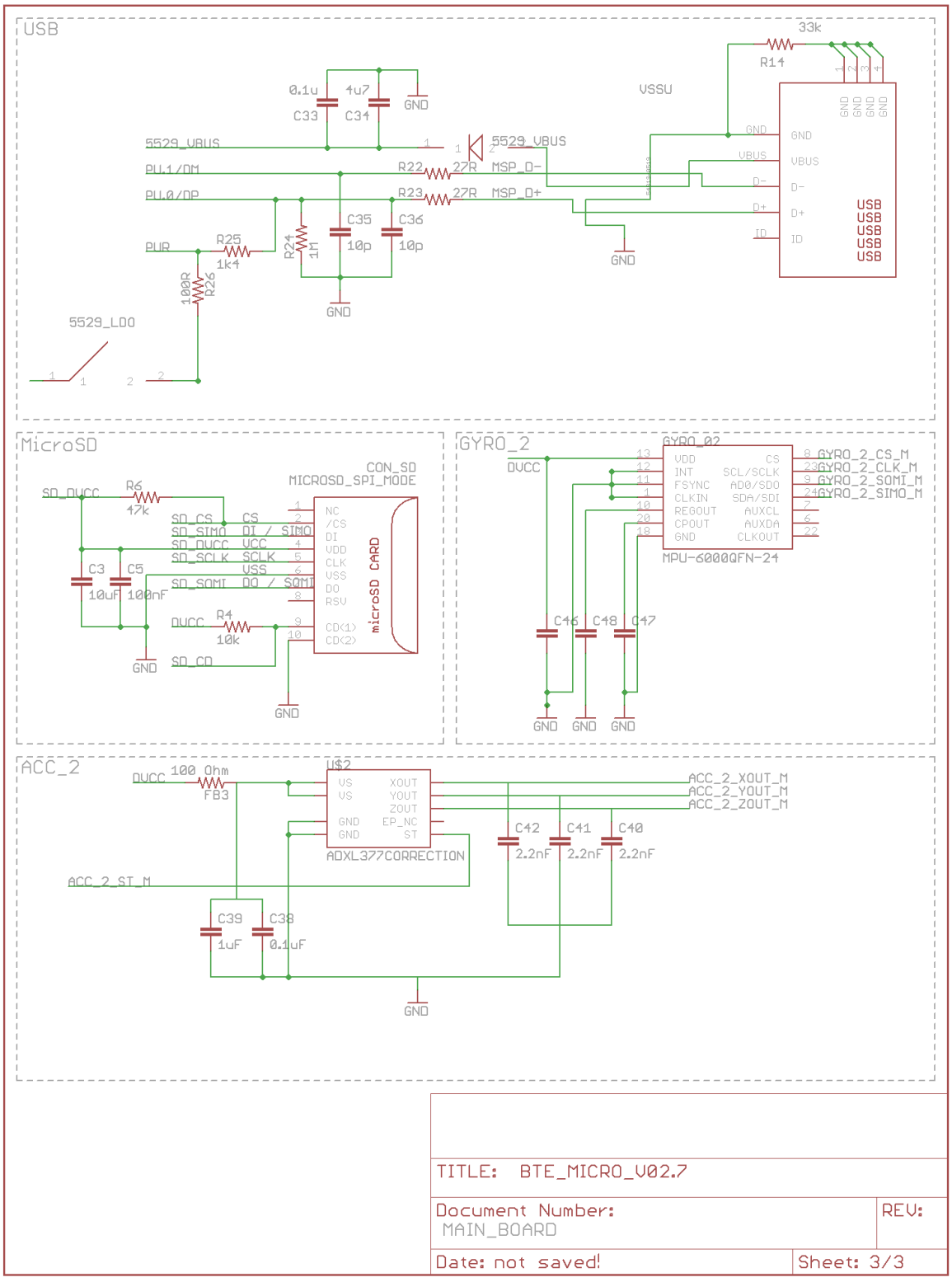

Figure A.10. BTE_MICRO_V2.7 Main PCB

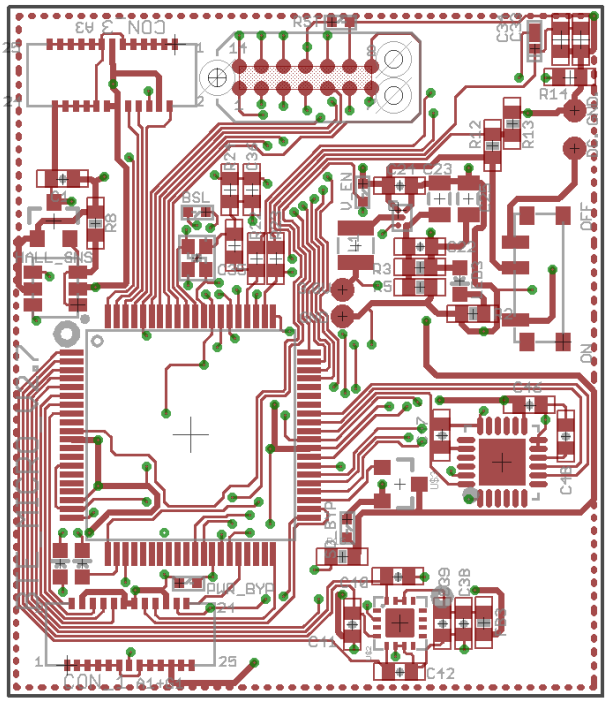

Figure A.11. BTE_MICRO_V2.7 Main PCB top copper

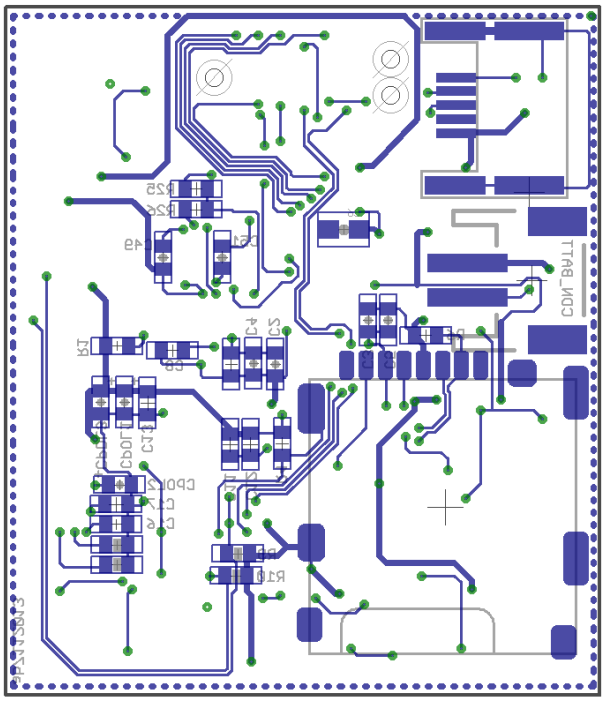

Figure A.12. BTE_MICROV2.7 Main PCB bottom copper

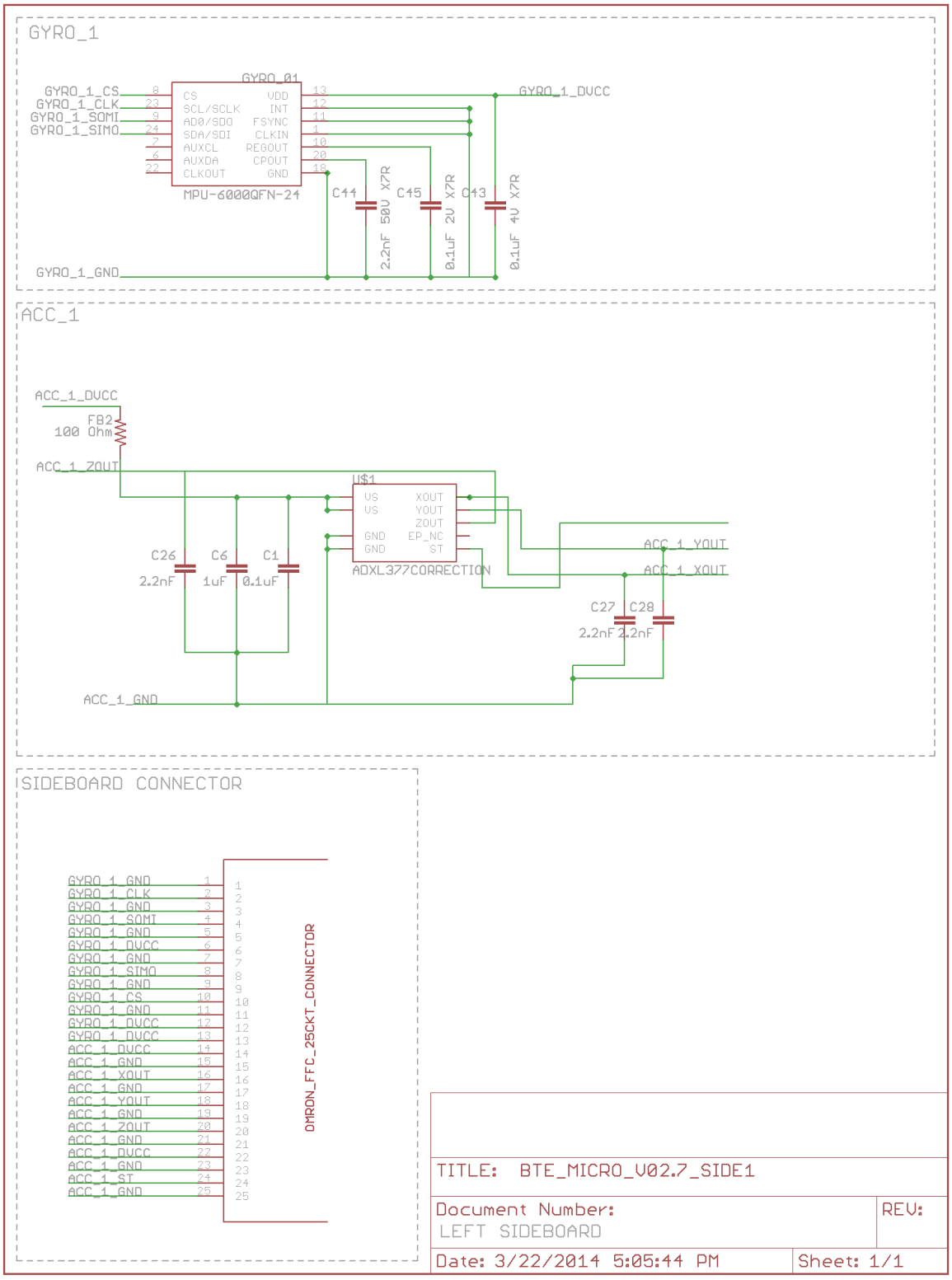

Figure A.13. BTE_MICRO_V2.7 Left Sideboard schematic

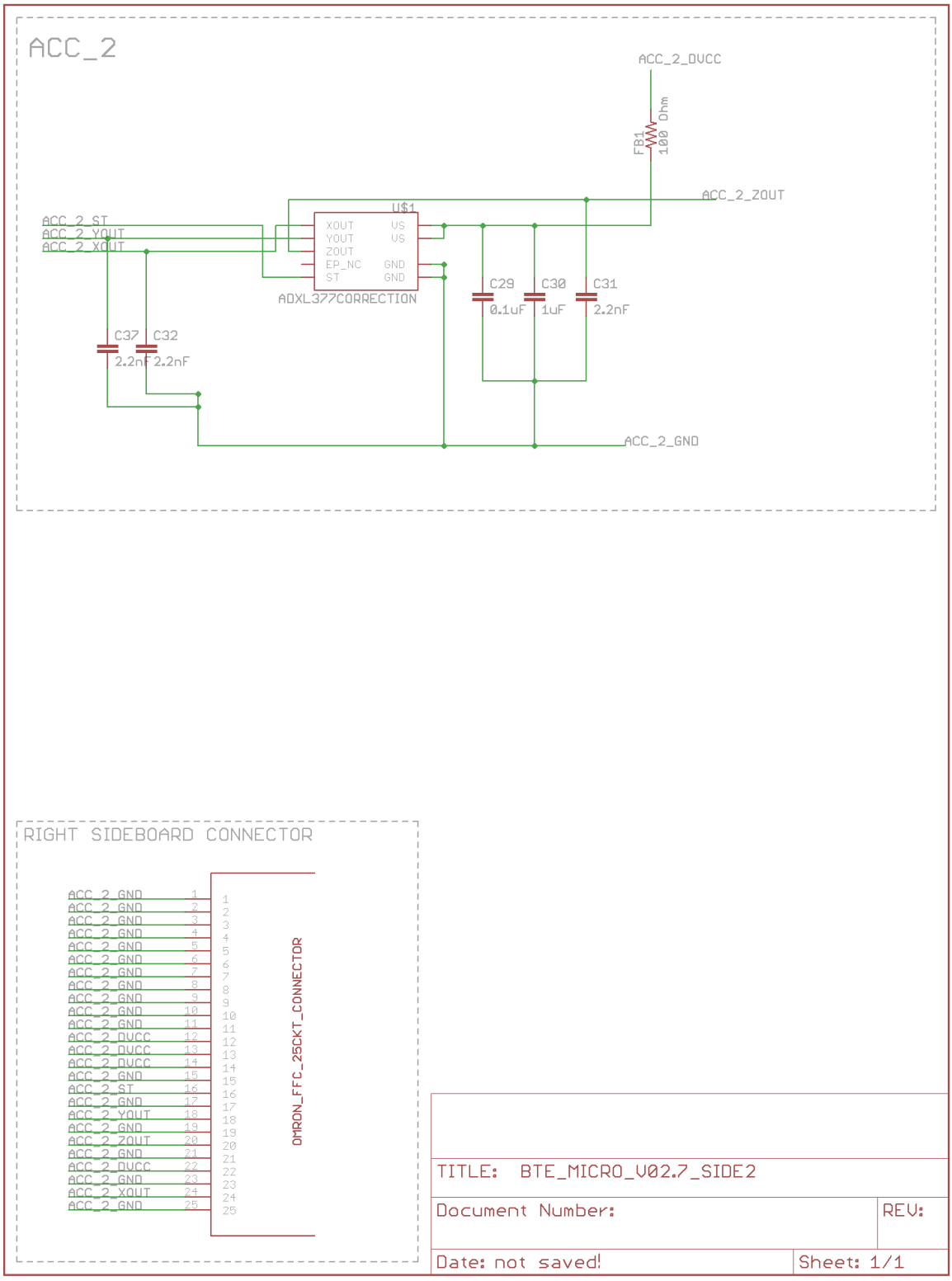

Figure A.14. BTE_MICRO_V2.7 Right Sideboard Schematic

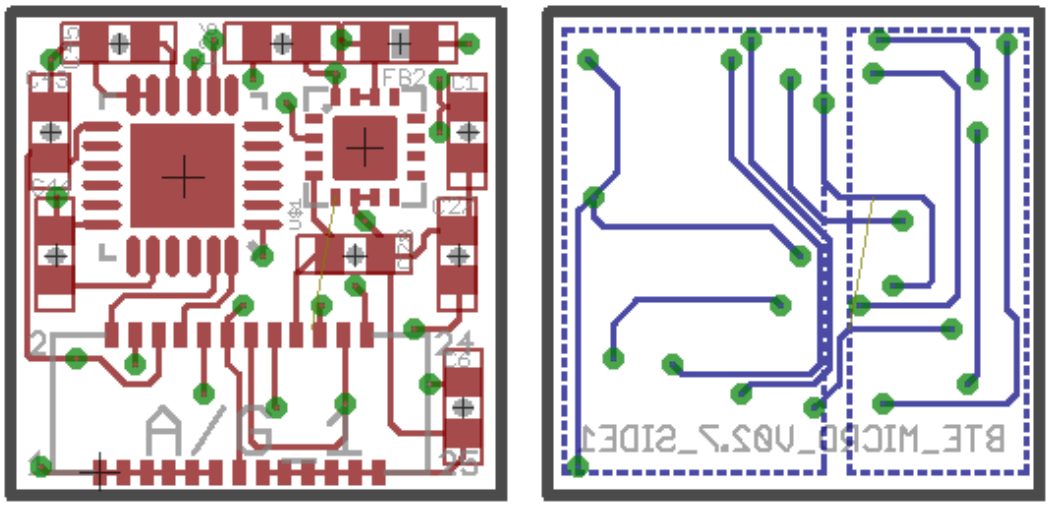

Figure A.15. BTE_MICRO_V2.7 Left Side board Top (red) and bottom (blue) copper

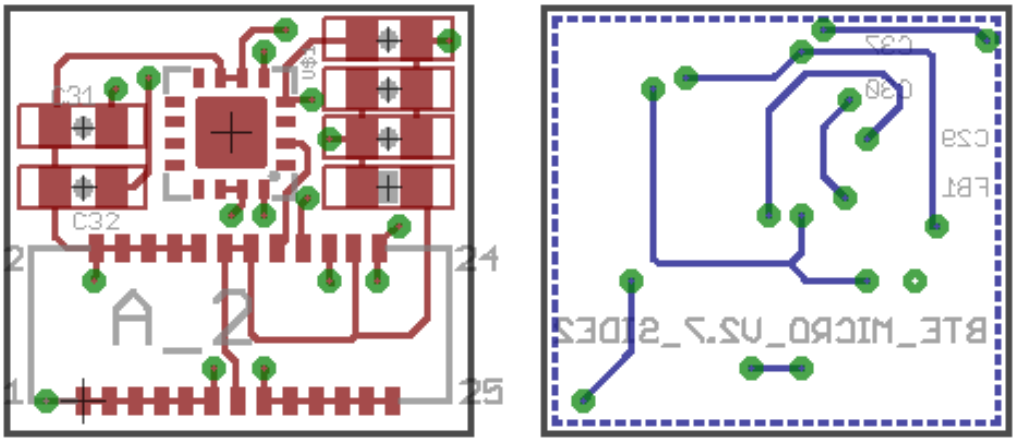

Figure A.16. BTE_MICRO_V2.7 Right Side board Top (red) and bottom (blue) copper

B. SHOCKBOX SAMPLE DATA

This appendix contains sample data generated using the Shockbox by Impakt Protective head impact monitoring system. The device interfaces with the user exclusively through a mobile application. This application allows the user to export all collected data into a spreadsheet, such as the one shown on the next page.

Table B.1. Sample Shockbox export data

Name	#	Shockbox	Age	Gender	State	Helmet	Time:	Direction	Magnitude:	HIC	Rotatio	Assessed	Diagnosed	Concussion
Buster	99	Shockbox-5D60	18	Male	In	Riddell F	Tue Mar 4 2014 at 4:09 pm	Side	Low			FALSE	FALSE	
Buster	99	Shockbox-5D60	18	Male	In	Riddell F	Tue Mar 4 2014 at 4:08 pm	Front	Low			TRUE	FALSE	
Buster	99	Shockbox-5D60	18	Male	In	Riddell F	Tue Mar 4 2014 at 4:08 pm	Front	Low			TRUE	FALSE	
Buster	99	Shockbox-5D60	18	Male	In	Riddell F	Tue Mar 4 2014 at 4:07 pm	Side	Low			TRUE	FALSE	
Buster	99	Shockbox-5D60	18	Male	In	Riddell F	Tue Mar 4 2014 at 4:07 pm	Side	Low			TRUE	FALSE	
Buster	99	Shockbox-5D60	18	Male	In	Riddell F	Tue Mar 4 2014 at 4:07 pm	Side	Low			TRUE	FALSE	
Buster	99	Shockbox-5D60	18	Male	In	Riddell F	Tue Mar 4 2014 at 4:07 pm	Side	High			FALSE	FALSE	
Buster	99	Shockbox-5D60	18	Male	In	Riddell F	Tue Mar 4 2014 at 4:06 pm	Side	High			FALSE	FALSE	
Buster	99	Shockbox-5D60	18	Male	In	Riddell F	Tue Mar 4 2014 at 4:06 pm	Front	Low			TRUE	FALSE	
Buster	99	Shockbox-5D60	18	Male	In	Riddell F	Tue Mar 4 2014 at 4:06 pm	Front	Low			TRUE	FALSE	
Buster	99	Shockbox-5D60	18	Male	In	Riddell F	Tue Mar 4 2014 at 4:06 pm	Front	Low			TRUE	FALSE	
Buster	99	Shockbox-5D60	18	Male	In	Riddell F	Tue Mar 4 2014 at 4:06 pm	Front	Low			TRUE	FALSE	
Buster	99	Shockbox-5D60	18	Male	In	Riddell F	Tue Mar 4 2014 at 4:06 pm	Front	Low			TRUE	FALSE	
Buster	99	Shockbox-5D60	18	Male	In	Riddell F	Tue Mar 4 2014 at 3:58 pm	Side	Low			TRUE	FALSE	
Buster	99	Shockbox-5D60	18	Male	In	Riddell F	Tue Mar 4 2014 at 3:57 pm	Front	Low			TRUE	FALSE	
Buster	99	Shockbox-5D60	18	Male	In	Riddell F	Tue Mar 4 2014 at 3:57 pm	Front	Low			TRUE	FALSE	
Buster	99	Shockbox-5D60	18	Male	In	Riddell F	Tue Mar 4 2014 at 3:56 pm	Side	Low			TRUE	FALSE	
Buster	99	Shockbox-5D60	18	Male	In	Riddell F	Tue Mar 4 2014 at 3:55 pm	Front	Low			TRUE	FALSE	
Buster	99	Shockbox-5D60	18	Male	In	Riddell F	Tue Mar 4 2014 at 3:55 pm	Rear	Low			TRUE	FALSE	
Buster	99	Shockbox-5D60	18	Male	In	Riddell F	Tue Mar 4 2014 at 3:55 pm	Side	Low			TRUE	FALSE	
Buster	99	Shockbox-5D60	18	Male	In	Riddell F	Tue Mar 4 2014 at 3:54 pm	Side	High			TRUE	FALSE	
Buster	99	Shockbox-5D60	18	Male	In	Riddell F	Tue Mar 4 2014 at 3:52 pm	Front	Low			TRUE	FALSE	
Buster	99	Shockbox-5D60	18	Male	In	Riddell F	Tue Mar 4 2014 at 3:52 pm	Front	Low			TRUE	TRUE	FALSE
Buster	99	Shockbox-5D60	18	Male	In	Riddell F	Tue Mar 4 2014 at 3:45 pm	Top	High			TRUE	TRUE	FALSE

C. BILL OF MATERIALS

Table C.1. Complete Bill of Materials for BTE_HITS_V03

Part	Value	Package	Price	Description
BATTERY PACK	1000mAh	Li-Po	$ 11.95	Battery pack
ACC_1	ADXL377	ADXL377	$ 11.62	Accelerometer (x2)
MICRO	MSP430F5659	PZ_S-PQFP-G100	$ 6.18	Microcontroller
GYRO_01	MPU-6000	QFN-24	$ 5.08	MPU-6000
8GB Micro SD card	-	-	$ 5.08	Micro SD card
U$5	MAX1874	TQFN16	$ 2.12	Battery charging IC
BTNCELL	CR1225	CR1225	$ 1.95	Button cell
CON_SD	-	MOLEX 49225-0821	$ 1.78	Micro SD connector
U$4	B2B connector	FP-M02x5	$ 2.68	Fine pitch IDC ribbon cable connector (x2)
OSC_2	24MHz	ABM11-OSC	$ 0.77	Oscillator
BATT0	1000mAh	JST-2-SMD	$ 0.76	Li-Po battery connector
U$10	MOLEX_USB	MOLEX_MINI_USB	$ 0.51	Mini USB receptacle
Ribbon Cable	4"		$ 0.37	Ribbon cable
U$6	32.768kHz	ABS07-OSC	$ 0.34	Oscillator
U$2	LM3671	SOT-23-5	$ 0.33	Switching Regulator
U$1	NDC7003P-SOT	NDC7003P	$ 0.20	Power MOSFET
Q1	FDN302P	SOT23	$ 0.14	Switching MOSFET
Q2	FDN302P	SOT23	$ 0.14	Switching MOSFET
Q3	FDN302P	SOT23	$ 0.14	Switching MOSFET
HALL_SNS	TCS20DLR	SOT23-3	$ 0.13	Hall effect sensor
U$8	NSR10F40NXT5G	USB_DIODE	$ 0.12	Protection Diode
SD_FET	NDS332P	SOT23-3	$ 0.10	Switching MOSFET
3.0V	YG-LED	0603-LED	$ 0.05	LEDs
4.2V	YG-LED	0603-LED	$ 0.05	LEDs
LED2	YG-LED	0603-LED	$ 0.05	LEDs
P4.1	YG-LED	0603-LED	$ 0.05	LEDs
P4.2	YG-LED	0603-LED	$ 0.05	LEDs
P4.3	YG-LED	0603-LED	$ 0.05	LEDs

P4.4	YG-LED	0603-LED	$	0.05	LEDs
D1	MBR0520L	SOD123	$	0.05	Protection Diode
D2	MBR0520L	SOD123	$	0.05	Protection Diode
C1	0.47uF	0402-CAP	$	0.02	Capacitor
C2	10pF	0402-CAP	$	0.02	Capacitor
C3	10uF	0402-CAP	$	0.02	Capacitor
C4	10pF	0402-CAP	$	0.02	Capacitor
C5	100nF	0402-CAP	$	0.02	Capacitor
C7	470n	0402-CAP	$	0.02	Capacitor
C8	4.7nF	0402-CAP	$	0.02	Capacitor
C9	6pF	0402-CAP	$	0.02	Capacitor
C10	100n	0402-CAP	$	0.02	Capacitor
C11	6pF	0402-CAP	$	0.02	Capacitor
C12	1uF	0402-CAP	$	0.02	Capacitor
C13	2.2uF	0402-CAP	$	0.02	Capacitor
C14	100n	0402-CAP	$	0.02	Capacitor
C15	100n	0402-CAP	$	0.02	Capacitor
C16	2.2uF	0402-CAP	$	0.02	Capacitor
C17	4.7uF	0402-CAP	$	0.02	Capacitor
C18	220n	0402-CAP	$	0.02	Capacitor
C19	10uF	0402-CAP	$	0.02	Capacitor
C20	100nF	0402-CAP	$	0.02	Capacitor
C21	220n	0402-CAP	$	0.02	Capacitor
C22	8.2pF	0402-CAP	$	0.02	Capacitor
C24	4.7uF	0402-CAP	$	0.02	Capacitor
C26	0.1uF	0402-CAP	$	0.02	Capacitor
C33	0.1u	0402-CAP	$	0.02	Capacitor
C34	4u7	0402-CAP	$	0.02	Capacitor
C35	10p	0402-CAP	$	0.02	Capacitor
C36	10p	0402-CAP	$	0.02	Capacitor
C38	0.1uF	0402-CAP	$	0.02	Capacitor
C39	1uF	0402-CAP	$	0.02	Capacitor
C40	2.2nF	0402-CAP	$	0.02	Capacitor
C41	2.2nF	0402-CAP	$	0.02	Capacitor
C42	2.2nF	0402-CAP	$	0.02	Capacitor
C46	0.1uF	0402-CAP	$	0.02	Capacitor
C47	2.2nF	0402-CAP	$	0.02	Capacitor
C48	0.1uF	0402-CAP	$	0.02	Capacitor
CPOL4	10uF	0402-CAP	$	0.02	Capacitor
CPOL5	10uF	0402-CAP	$	0.02	Capacitor

CPOL6	10uF	0402-CAP	$	0.02	Capacitor
FB3	100	0402-RES	$	0.02	Resistor
R1	500k	0402-RES	$	0.02	Resistor
R2	100	0402-RES	$	0.02	Resistor
R3	499k	0402-RES	$	0.02	Resistor
R4	10k	0402-RES	$	0.02	Resistor
R5	100k	0402-RES	$	0.02	Resistor
R6	47k	0402-RES	$	0.02	Resistor
R7	500k	0402-RES	$	0.02	Resistor
R8	10k	0402-RES	$	0.02	Resistor
R9	255k	0402-RES	$	0.02	Resistor
R10	500k	0402-RES	$	0.02	Resistor
R11	3k	0402-RES	$	0.02	Resistor
R12	1MOhm	0402-RES	$	0.02	Resistor
R13	1MOhm	0402-RES	$	0.02	Resistor
R14	33k	0402-RES	$	0.02	Resistor
R15	100k++	0402-RES	$	0.02	Resistor
R16	1k	0402-RES	$	0.02	Resistor
R17	10k	0402-RES	$	0.02	Resistor
R18	10k	0402-RES	$	0.02	Varistor
R19	10k	0402-RES	$	0.02	Resistor
R20	100	0402-RES	$	0.02	Resistor
R21	100	0402-RES	$	0.02	Resistor
R22	27R	0402-RES	$	0.02	Resistor
R23	27R	0402-RES	$	0.02	Resistor
R24	1M	0402-RES	$	0.02	Resistor
R25	1k4	0402-RES	$	0.02	Resistor
R26	100R	0402-RES	$	0.02	Resistor
R27	100	0402-RES	$	0.02	Resistor
R28	100k	0402-RES	$	0.02	Resistor
R29	100	0402-RES	$	0.02	Resistor
R30	100	0402-RES	$	0.02	Resistor
R31	301k	0402-RES	$	0.02	Resistor
R33	47k	0402-RES	$	0.02	Resistor
C6	-	0603-CAP	$	0.02	Capacitor
C23	33pF	0805-CAP	$	0.02	Capacitor
C25	10uF	0805-CAP	$	0.02	Capacitor
L1	10uH	1008-IND	$	0.02	Inductors

D. BTE_HITS_V03 SCHEMATIC AND LAYOUT

This appendix contains all schematics and layouts for BTE_HITS_V03. All schematics and layouts were generated using Cadsoft EAGLE 6.4.0 Professional unless otherwise noted. All schematic and layout files are versioned and stored in the PNG BTEv2 PCB repository.

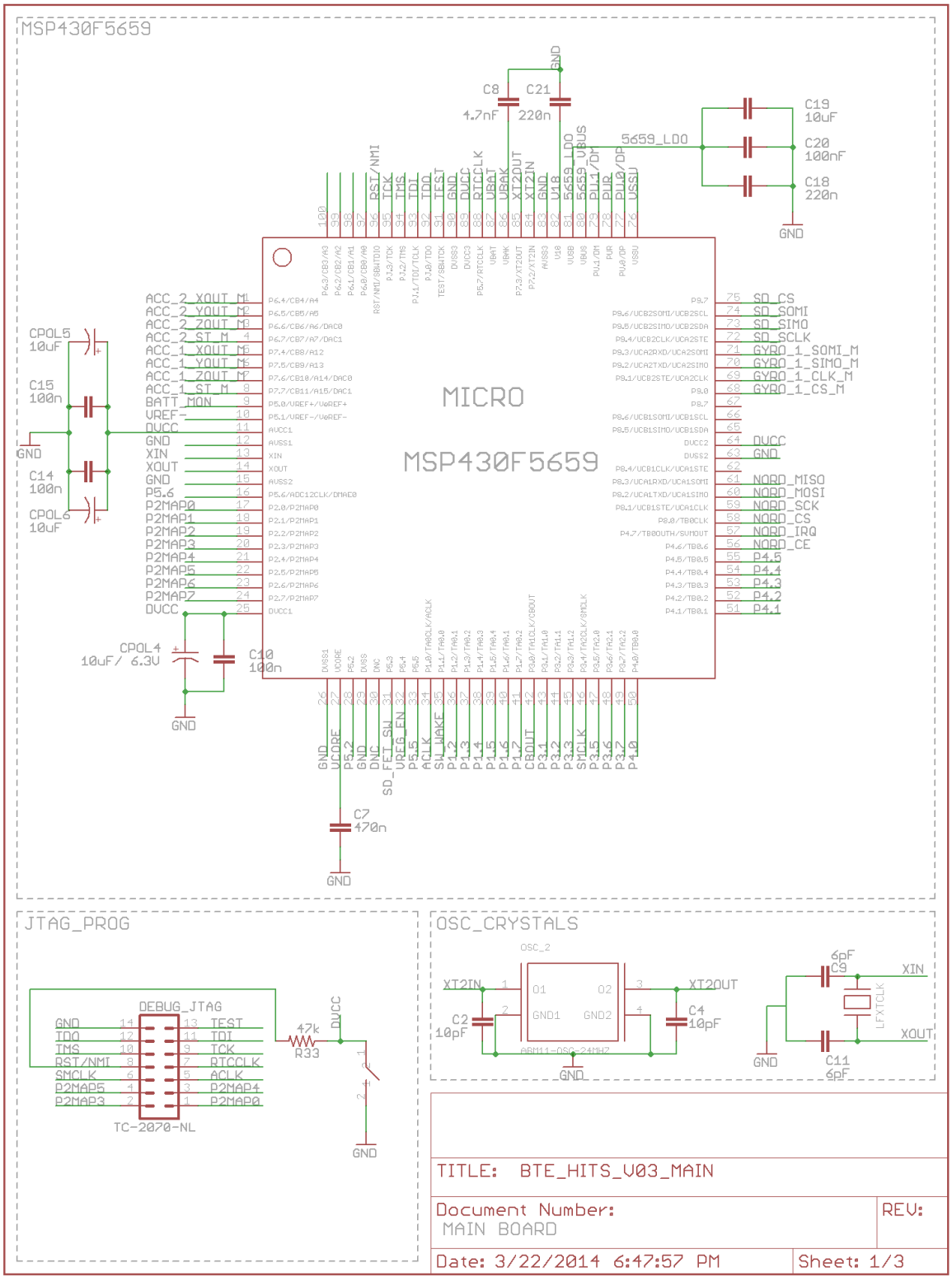

Figure D.1. BTE_HITS_V03 Main Board Schematic

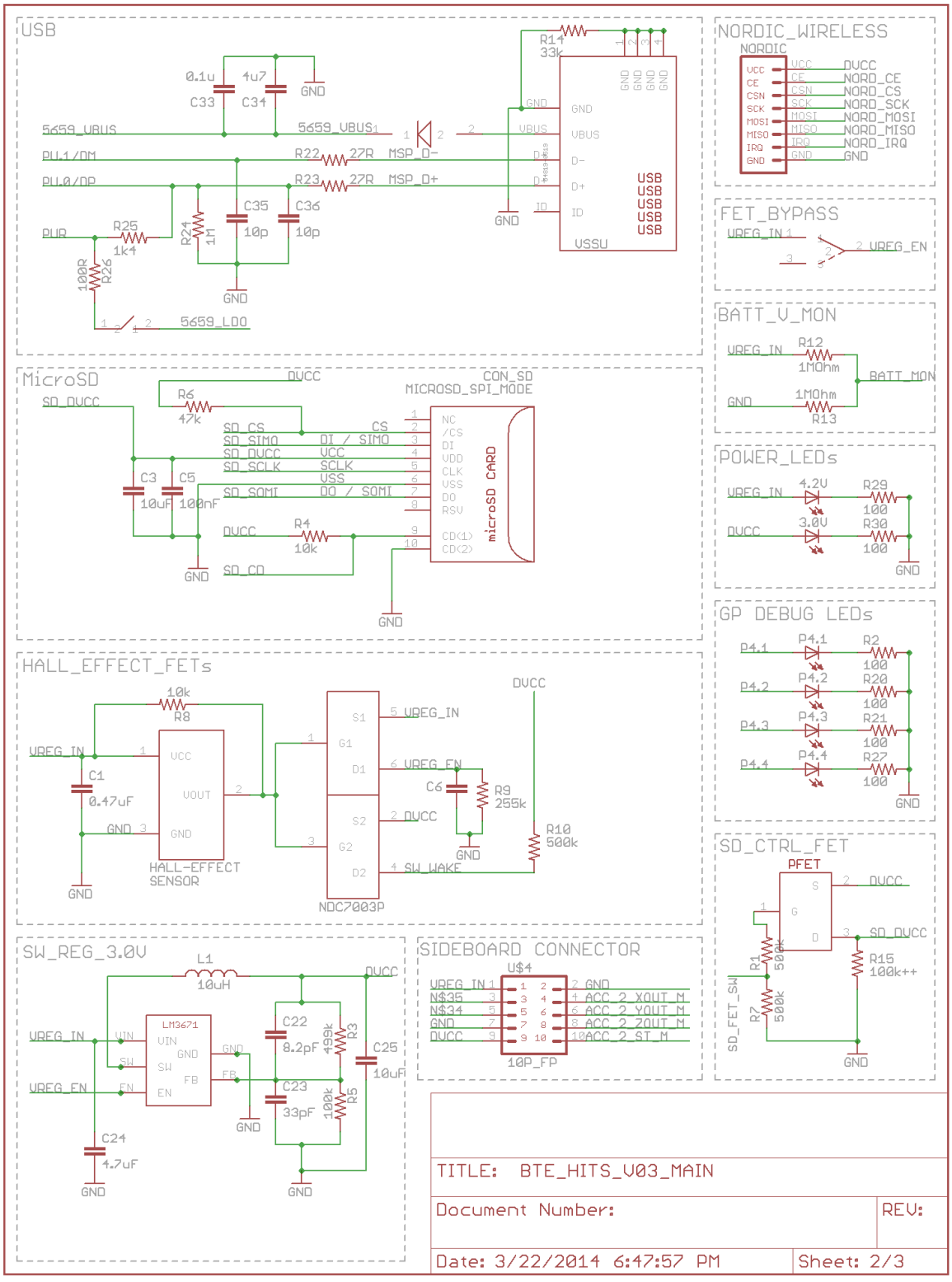

Figure D.2. BTE_HITS_V03 Main Board Schematic

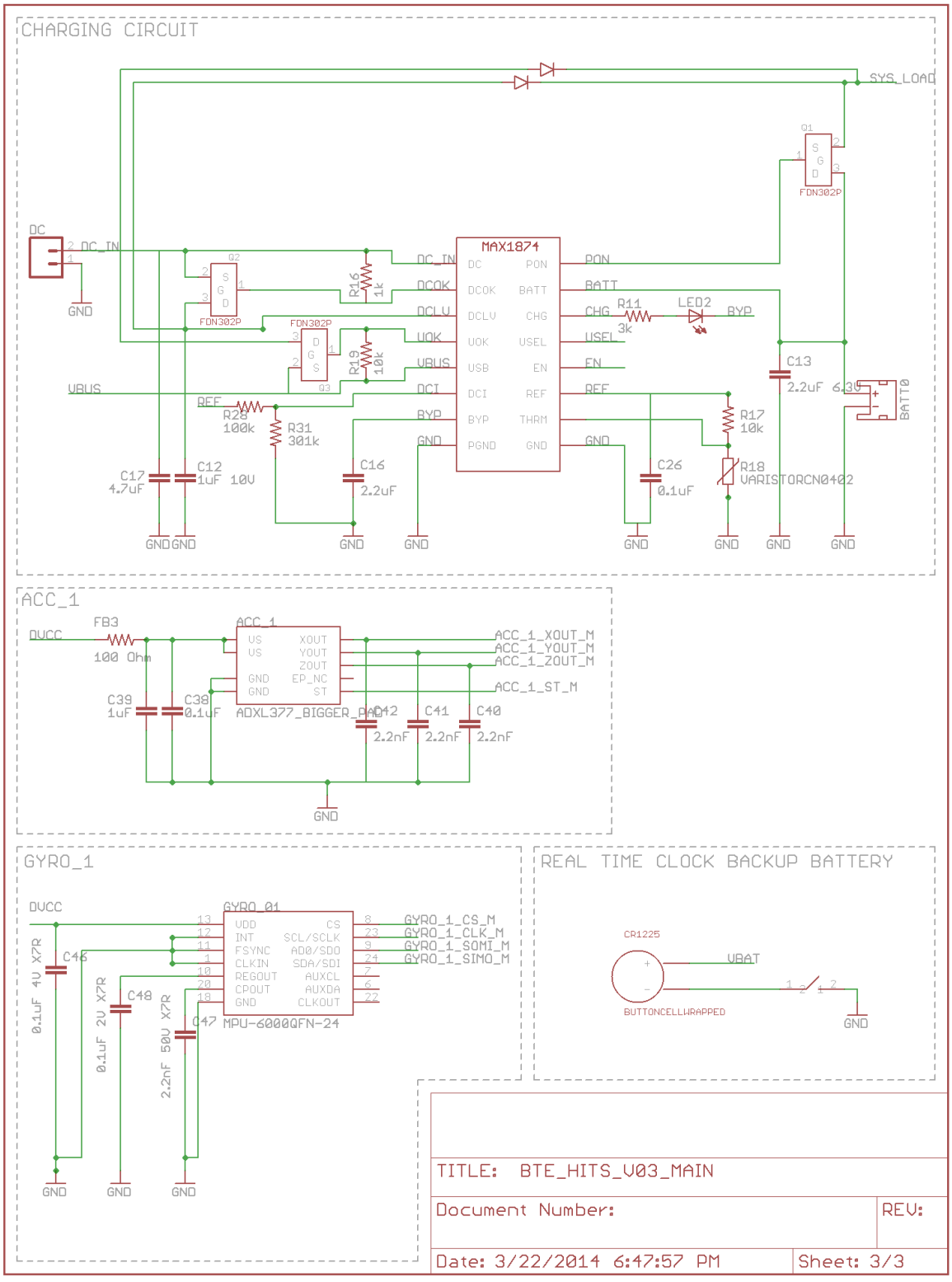

Figure D.3. BTE_HITS_V03 Main Board Schematic

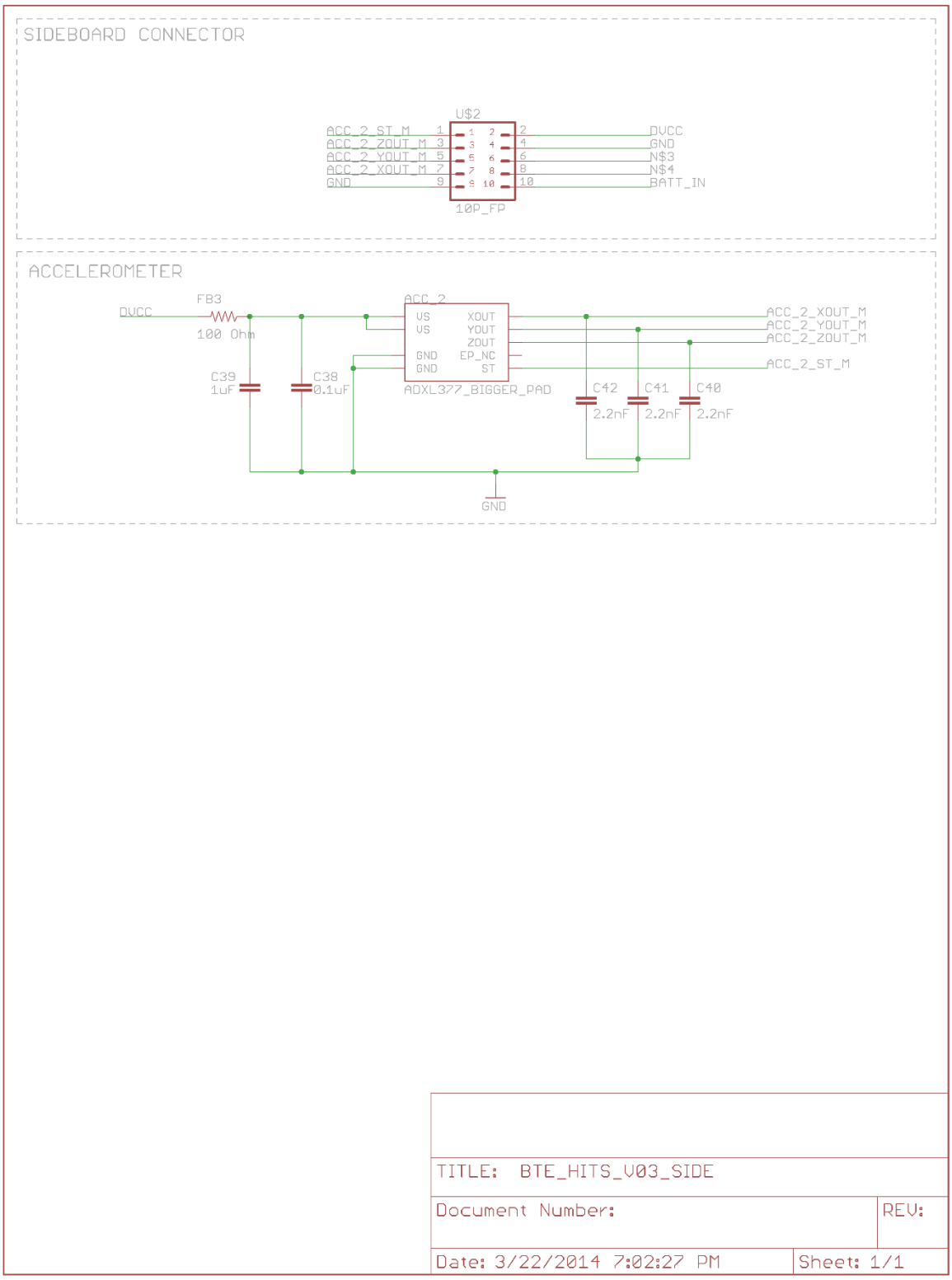

Figure D.4. BTE_HITS_V03 Side Board Schematic

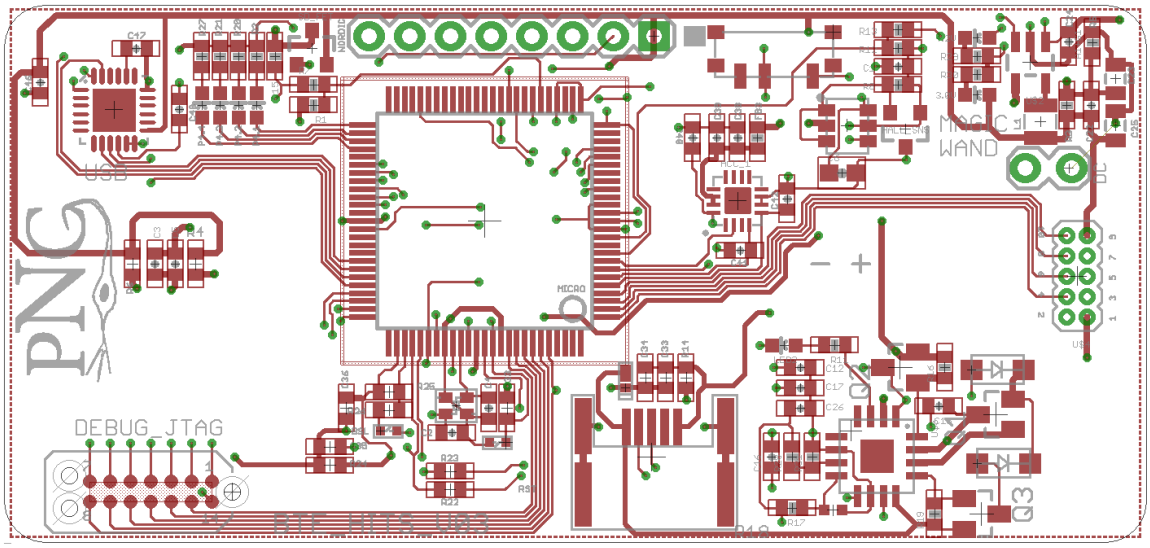

Figure D.5. BTE_HITS_V03 Main Board Top Copper

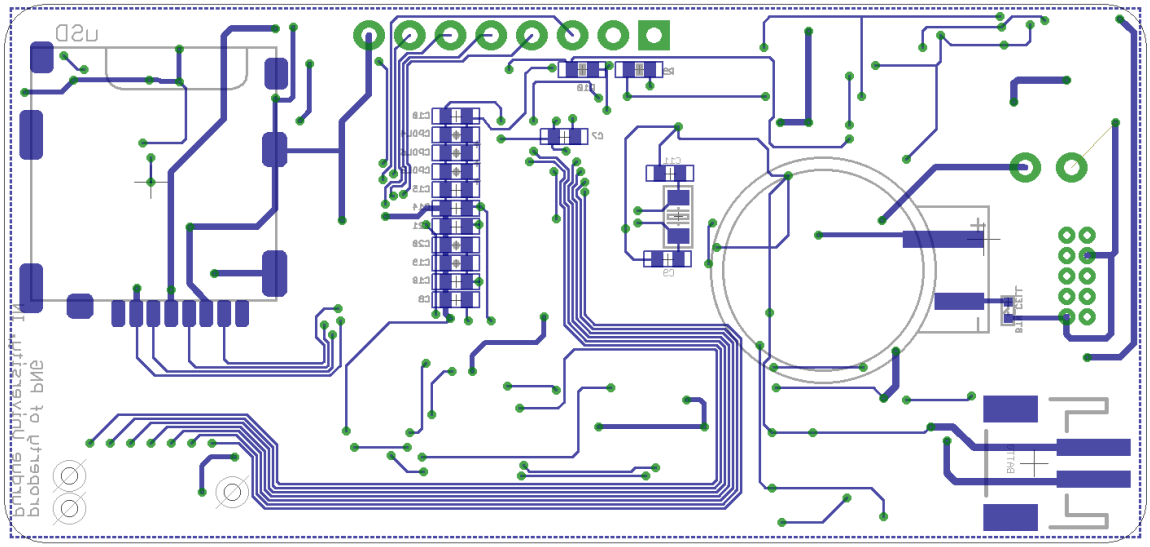

Figure D.6. BTE_HITS_V03 Main Board Bottom Copper

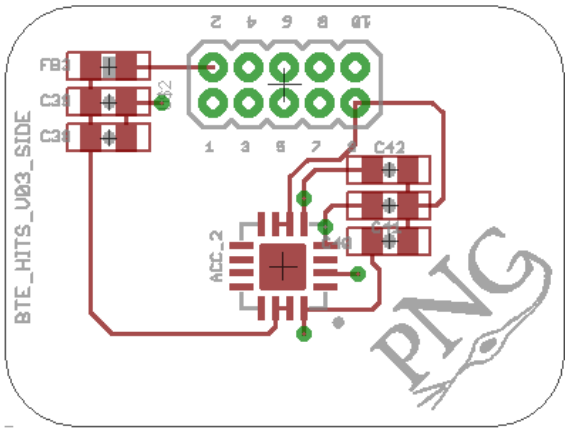

Figure D.7. BTE_HITS_V03 Side Board Top Copper

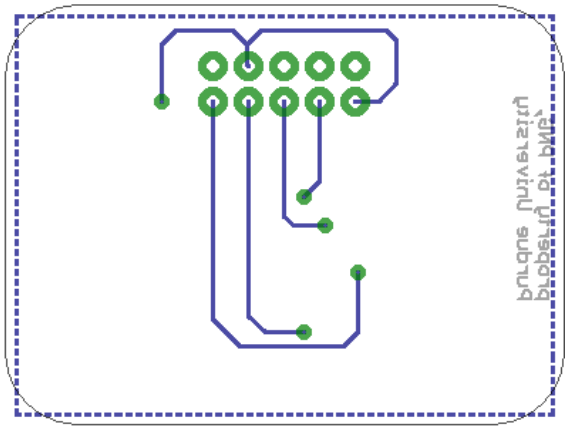

Figure D.8. BTE_HITS_V03 Side Board Bottom Copper